

MINIMISATION AND ABATEMENT OF VOLATILE SULPHUR COMPOUNDS IN SEWAGE SLUDGE PROCESSING

Esther Vega Martínez

Dipòsit legal: Gi. 1805-2014
<http://hdl.handle.net/10803/283655>

ADVERTIMENT. L'accés als continguts d'aquesta tesi doctoral i la seva utilització ha de respectar els drets de la persona autora. Pot ser utilitzada per a consulta o estudi personal, així com en activitats o materials d'investigació i docència en els termes establerts a l'art. 32 del Text Refós de la Llei de Propietat Intel·lectual (RDL 1/1996). Per altres utilitzacions es requereix l'autorització prèvia i expressa de la persona autora. En qualsevol cas, en la utilització dels seus continguts caldrà indicar de forma clara el nom i cognoms de la persona autora i el títol de la tesi doctoral. No s'autoritza la seva reproducció o altres formes d'explotació efectuades amb finalitats de lucre ni la seva comunicació pública des d'un lloc aliè al servei TDX. Tampoc s'autoritza la presentació del seu contingut en una finestra o marc aliè a TDX (framing). Aquesta reserva de drets afecta tant als continguts de la tesi com als seus resums i índexs.

ADVERTENCIA. El acceso a los contenidos de esta tesis doctoral y su utilización debe respetar los derechos de la persona autora. Puede ser utilizada para consulta o estudio personal, así como en actividades o materiales de investigación y docencia en los términos establecidos en el art. 32 del Texto Refundido de la Ley de Propiedad Intelectual (RDL 1/1996). Para otros usos se requiere la autorización previa y expresa de la persona autora. En cualquier caso, en la utilización de sus contenidos se deberá indicar de forma clara el nombre y apellidos de la persona autora y el título de la tesis doctoral. No se autoriza su reproducción u otras formas de explotación efectuadas con fines lucrativos ni su comunicación pública desde un sitio ajeno al servicio TDR. Tampoco se autoriza la presentación de su contenido en una ventana o marco ajeno a TDR (framing). Esta reserva de derechos afecta tanto al contenido de la tesis como a sus resúmenes e índices.

WARNING. Access to the contents of this doctoral thesis and its use must respect the rights of the author. It can be used for reference or private study, as well as research and learning activities or materials in the terms established by the 32nd article of the Spanish Consolidated Copyright Act (RDL 1/1996). Express and previous authorization of the author is required for any other uses. In any case, when using its content, full name of the author and title of the thesis must be clearly indicated. Reproduction or other forms of for profit use or public communication from outside TDX service is not allowed. Presentation of its content in a window or frame external to TDX (framing) is not authorized either. These rights affect both the content of the thesis and its abstracts and indexes.



DOCTORAL THESIS

Minimisation and abatement of volatile sulphur
compounds in sewage sludge processing

Annex included

Esther Vega Martínez

2014

Supervisors: Dr. Maria José Martín Sánchez and Dr. Rafael González Olmos

Thesis submitted in fulfilment of the requirements for the degree of Doctor from the
University of Girona (Experimental Science and Sustainability PhD Programme)

La Dra. Maria José Martín Sánchez, professora del Departament d'Enginyeria Química, Agrària i tecnologia Agroalimentària de la Universitat de Girona i el Dr. Rafael Gonzalez Olmos investigador de la Universitat de Girona

CERTIFIQUEN:

Que la llicenciada en Ciències Ambientals Esther Vega Martínez ha dut a terme, sota la seva direcció, el treball titulat *Minimisation and abatement of volatile sulphur compounds in sewage sludge processing*, que es presenta en aquesta memòria la qual constitueix la seva Tesi per optar al Grau de Doctora per la Universitat de Girona.

I perquè prengueu coneixement i tingui els efectes que correspongui, presentem davant de la Facultat de Ciències de la Universitat de Girona l'esmentada Tesi, signant aquesta certificació a

Girona, 3 de Juliol de 2014

Dr. Maria Jose Martín Sánchez

Dr. Rafael González Olmos

*Als meus,
amics i família.*

AGRAÏMENTS

He pensat milers de cops el dia que m'hauria de posar davant d'aquesta pàgina en blanc i no em crec que la comenci a escriure. El camí ha estat molt llarg i en alguns moments dur però ara si que es l'hora de poder agrair a tota la gent que m'ha acompanyat durant aquest llarg camí.

En primer lloc voldria començar donant les gràcies als meus directors de tesi: Maria i Rafa. Maria moltes gràcies per confiar en mi i donar-me aquesta gran oportunitat i Rafa per tirar del carro en moments en que m'he trobat perduda i donar-me la empenta necessària per tirar endavant tot això. **MOLTES GRÀCIES!**

Agrair també al staff del LEQUIA, en especial a en Jesús i a la Marilós que han tingut sempre paraules d'ànims en aquests últims mesos.

Gràcies a tota la família LEQUIA, en especial als veteranus (Helio, Anna, Sergio, Ramon, Jordi) per els vostres consells en els meus inicis, als dels parc (Sara, Monste, Tico, Jordi, Serni, Patri, Pau, Anna, Narcís, Patricia, Enric) per compartir les estonetes que he estat per el parc i als lequians de ciències (Alexandra i José) per la vostra ajuda. Vull agrair especialment als que ho han viscut de més a prop: Héctor, moltes gràcies per tot el que hem viscut i per la teva ajuda incondicional; Maël, des de la carrera i encara ens trobem per aquí eh? Gràcies per els bons moment; Marta, per les escapadetes i compartir grans estones de xafarderies.. jeje i Sebas, gràcies per els consells que sempre m'has donat.

També volia agrair a en Pepe i a en Jesús l'oportunitat de treballar amb ells i treure resultats molt positius d'aquesta feina. Muchas gracias chicos!

Gràcies a l'Enriqueta, Juanma, Anna i Mònica per tota l'ajuda al laboratori.

A les nenes del laboratori, Ariadna gràcies per l'ajuda que sempre m'heu donat en les tasques del laboratori i Gemma per tota la teva ajuda i per les llargues converses filosofant de la vida al llarg d'aquest temps. Ha estat un plaer!

A les carboneres: Alba C. per compartir part d'aquests darrers anys de la gran aventura. Carla i Alba n'hem viscut de tots els colors i tot i així ens n'hem acabat sortint! Gràcies per els ànims quan a vegades al obrir la porta del despatx es veien les coses negres i sempre heu estat allà! Es un plaer poder haver compartit tants moments amb vosaltres! Mil gràcies carboneres!!

A la Mercè i la Mariana que tot i que no ens veiem tant com voldríem (no hi ha manera de quadrar agendas.. jeje) sempre m'heu estat fent costat en els tots els moments!

A la Susanna, que amb tots aquest anys, m'has acompanyat d'una manera o altre i sempre has tingut les millors paraules de suport. Gràcies guapa!

I no me'n puc estar de donar les gràcies als burrus: Marta, Magan, Marc, Irene, Eli, Jaume, Marisa, Raul, Pau, Sora, Andreu, Erika i Albert; gràcies per formar part dels grans moments que hem viscut, per les vostres paraules d'ànims, per "la copa tonta i tornem a casa", en fi; per ser ELS grans amics! Per cert, ja podeu anar reservant el dia perquè ara si que n'hem de celebrar una de grossa.. jeje

A tu Oriol, perquè sé que no ha estat fàcil aquest camí i has estat allà fent-me veure la part positiva de les coses i donant-me les paraules d'ànims que necessitava per tirar endavant. De segur que acabem trobant el camí amb èxit.. ☺

Finalment li vull donar les gràcies als meus pares i al meu germà. Moltes gràcies pares per aguantar durant aquests anys els mals moments i també els bons que m'ha portat aquesta llarga aventura i per ensenyar-me a tirar endavant sempre. Mama, crec que ja tens resposta a la frase més escoltada a casa de "a ver cuando acabas.." ☺. I gràcies *tete* per els ànims, consells de germà gran i per estar allà sempre quan un ho necessitat!

A tots vosaltres, mil gràcies per ser-hi.

*This research was financially supported by the Spanish MICINN
(Projects PET2008_0261, CTQ2011-24114)*

LIST OF PUBLICATION.....	I
LIST OF TABLES.....	III
LIST OF FIGURES.....	V
LIST OF ACRONYMS.....	IX
RESUM.....	XI
RESUMEN.....	XIII
SUMMARY.....	XV
1 INTRODUCTION.....	1
1.1. <i>Odorous compounds emissions in wastewater treatment plants</i>	3
1.2. <i>Sludge processing and final disposal</i>	4
1.2.1. <i>Odour-causing sulphur compounds formation in sludge processing</i>	10
1.3. <i>End-of-pipe technologies for odour removal</i>	13
1.3.1. <i>Advanced oxidation scrubbers</i>	15
1.3.1.1. <i>UV/H₂O₂ process</i>	17
1.3.1.2. <i>Fenton process (H₂O₂/Fe²⁺)</i>	17
1.3.1.3. <i>Photo-Fenton process (UV/H₂O₂/Fe²⁺)</i>	18
1.3.1.4. <i>Ozonation process</i>	18
1.3.2. <i>Adsorption</i>	18
2 OBJECTIVES.....	23
3 MATERIALS AND METHODS.....	27
3.1 <i>Experimental procedures</i>	29
3.1.1 <i>Sewage sludge drying process</i>	29
3.1.1.1. <i>Lab-scale drying process</i>	29
3.1.1.2. <i>Full-scale drying process</i>	29
3.1.2 <i>Sewage sludge conditioning process</i>	32
3.1.2.1. <i>Chemical conditioning</i>	32
3.1.2.2. <i>Physical conditioning process</i>	34
3.1.3 <i>Advanced oxidation processes</i>	35
3.1.3.1. <i>Cost analysis of AOPs</i>	37
3.1.4 <i>Adsorption tests</i>	38
3.1.4.1. <i>Adsorption capacities</i>	39
3.1.4.2. <i>Computational details: COSMO-RS</i>	40
3.2 <i>Analytical method for determination of VSCs, VOCs and odour concentration</i>	41
3.2.1 <i>VSC analysis in gas samples</i>	41
3.2.2 <i>VSC analysis in liquid samples</i>	42
3.2.3 <i>VOC analysis in gas phase</i>	42
3.2.4 <i>Olfactometric analysis</i>	43
3.3 <i>Sludge characterisation</i>	43
3.3.1 <i>Capillary suction time</i>	43
3.3.2 <i>Extracellular polymeric substances</i>	44
3.4 <i>Liquid phase characterisation</i>	45
3.4.1 <i>Sulphate content</i>	45
3.4.2 <i>Ozone concentration</i>	45
3.4.3 <i>Hydrogen peroxide concentration</i>	45
3.4.4 <i>Dissolved iron content</i>	45
3.5 <i>Activated carbon modifications</i>	46

3.5.1	Oxidative chemical treatments	46
3.5.1.1.	Nitric oxidation	46
3.5.1.2.	Ozone oxidation	46
3.5.2	Gamma irradiation treatment.....	46
3.6	<i>Characterisation of activated carbons</i>	49
3.6.1	Textural characterisation	49
3.6.1.1.	N ₂ adsorption/desorption isotherms	49
3.6.2	Chemical characterisation.....	49
3.6.2.1.	Temperature Programmed Desorption (TPD).....	49
3.6.2.2.	X-Ray Photoelectron Spectroscopy (XPS).....	50
3.6.2.3.	Elemental analysis	51
3.6.2.4.	Measurement of pH _{slurry}	51
RESULTS.....		53
4 IDENTIFICATION OF ODOUR-CAUSING COMPOUNDS IN SEWAGE SLUDGE DRYING PROCESS AT LOW TEMPERATURE		55
4.1	<i>Background and objectives</i>	57
4.2	<i>Methodology</i>	57
4.3	<i>Results and discussion</i>	58
4.3.1	Lab-scale sewage sludge drying process.....	58
4.3.2	Full-scale drying process	62
4.4	<i>Conclusions</i>	67
5 OPTIMISING CHEMICAL CONDITIONING OF UNDIGESTED SEWAGE SLUDGE FOR ODOUR REMOVAL IN DRYING PROCESS.....		69
5.1	<i>Background and objectives</i>	71
5.2	<i>Methodology</i>	71
5.3	<i>Results and discussion</i>	72
5.3.1	Chemical conditioning.....	72
5.3.1.1.	Influence of the individual dosage of conditioners on the dewaterability and odour emission	72
5.3.1.2.	Optimisation of sludge chemical conditioning process using RSM.....	76
5.3.1.3.	Model validation.....	82
5.3.2	Physical conditioning process	83
5.4	<i>Conclusions</i>	85
6 INTEGRATION OF ADVANCED OXIDATION PROCESSES AT MILD CONDITIONS IN WET SCRUBBERS FOR ODOUR SULPHUR COMPOUNDS TREATMENT		87
6.1	<i>Background and objectives</i>	89
6.2	<i>Methodology</i>	89
6.3	<i>Results and discussion</i>	90
6.3.1	Oxidation by UV/H ₂ O ₂ treatment.....	90
6.3.2	Oxidation by H ₂ O ₂ /Fe ²⁺ and UV/H ₂ O ₂ /Fe ²⁺ treatments	92
6.3.3	Oxidation by ozone treatment.....	95
6.3.4	Treatment comparison.....	97
6.4	<i>Conclusions</i>	101
7 ADSORPTION OF VOLATILE SULPHUR COMPOUNDS ONTO MODIFIED ACTIVATED CARBONS: EFFECT OF OXYGEN FUNCTIONAL GROUPS.....		103
7.1	<i>Background and objectives</i>	105
7.2	<i>Methodology</i>	105
7.3	<i>Results and discussion</i>	106

7.3.1	As-received ac adsorption tests	106
7.3.2	Surface characterization of oxidised acs.....	107
7.3.3	Oxidised acs adsorption tests	111
7.4	<i>Conclusions</i>	115
8	REMOVAL OF ODOROUS SULPHUR COMPOUNDS ONTO ACTIVATED CARBON UNDER WET CONDITIONS.....	117
8.1	<i>Background and objectives</i>	119
8.2	<i>Methodology</i>	119
8.3	<i>Results and discussion</i>	120
8.3.1	Surface chemical characterisation of acs.....	120
8.3.2	Adsorption tests	123
8.4	<i>Conclusions</i>	129
9	GENERAL DISCUSSION	131
10	GENERAL CONCLUSIONS	139
11	REFERENCES	145
	ANNEX	167

LIST OF PUBLICATION

The following list contains the *journal publications* resulting from this PhD thesis:

- Vega, E.**, Lemus, J., Anfruns, A., Gonzalez-Olmos, R., Palomar, J., Martin, M.J., 2013. Adsorption of volatile sulphur compounds onto modified activated carbons: effect of oxygen functional groups. *Journal of Hazardous Materials* 258-259, 77-83.
- Vega, E.**, Martin, M.J., Gonzalez-Olmos, R., 2014. Integration of advanced oxidation processes at mild conditions in wet scrubbers for odorous sulphur compounds treatment. *Chemosphere* 109, 113-119.
- Vega, E.**, Monclús, H., Gonzalez-Olmos, R., Martin, M.J., 2014. Optimising chemical conditioning of the undigested sewage sludge for odour removal in drying process. Submitted to *Journal of Environmental Management*.
- Vega, E.**, Gonzalez-Olmos, R., Martin, M.J., 2014. Removal of odorous sulphur compounds onto modified activated carbons under wet conditions. Submitted to *Separation and Purification Technology*.

LIST OF TABLES

Table 1.1 Main odorous compounds associated with WWTPs	3
Table 1.2 Main characteristics of the different types of water contained in sewage sludge	6
Table 1.3 Relevant studies on odorous compounds emissions from conditioned sludge in field applications	12
Table 1.4 Main characteristics of conventional odour abatement technologies	14
Table 1.5 Oxidation potential of common oxidants	16
Table 1.6 Technologies-based AOP for water treatment	16
Table 1.7 Relevant studies about odour removal by wet scrubber using AOSs	17
Table 1.8 Relevant studies on the adsorption of target odorous compounds at low concentration	22
Table 3.1 Range and levels of the three independent variables used in RSM	33
Table 3.2 Experimental design matrix for optimisation sludge conditioning using RSM (X_1 : polyelectrolyte; X_2 : FeCl; X_3 : CaO [g Kg DS ⁻¹])	33
Table 3.3 Main properties of target compounds	35
Table 3.4 Experimental conditions of the studied AOPs	37
Table 3.5 General calculations of capital cost	38
Table 3.6 GC/PFPD analytical conditions	41
Table 3.7 SMPE/GC/MS analytical conditions	42
Table 3.8 Designations of the AC samples obtained	48
Table 3.9 Oxygen functional groups assignment according to the desorption temperatures in TPD curves	50
Table 3.10 Oxygen functional groups assignment according to the binding energies in XPS curves	51
Table 4.1 Environmental conditions and sludge characteristics of each sampling.....	58
Table 4.2 Percentages of the peak area participation (α_i), olfactory threshold participation (τ_i) and odour index (OI) of VOCs analysed from sampling II	60
Table 4.3 Percentages of the peak area participation (α_i), olfactory threshold participation (τ_i) and odour index (OI) of VOCs analysed from sampling III	60
Table 4.4 Percentages of the peak area participation (α_i), olfactory threshold participation (τ_i) and odour index (OI) of VOCs analysed from sampling IV	60
Table 4.5 Percentages of the peak area participation (α_i), olfactory threshold participation (τ_i) and odour index (OI) of VOCs analysed from sampling V.....	61
Table 4.6 Environmental conditions and sludge characteristics of each sampling.....	62

Table 4.7 Percentages of the peak area participation (α_i), olfactory threshold participation (τ_i) and odour index (OI) of VOCs analysed from sampling VI in full-scale.....	63
Table 4.8 Percentages of the peak area participation (α_i), olfactory threshold participation (τ_i) and odour index (OI) of VOCs analysed from sampling VII in full scale	63
Table 4.9 Removal percentages of VSC in the chemical scrubber (S), biofilter (B) and the overall removal (O)	65
Table 4.10 Odour concentration from different sampling points	65
Table 5.1 CST (s), TSC emission (mg S m^{-3}), odour emission (OU_E range) and pH of chemical conditioning samples on the individual assessment	71
Table 5.2 Experimental design and results for overall optimisation.....	75
Table 5.3 Coded regression model equations established by RSM	76
Table 5.4 Statistical parameters obtained from the ANOVA	76
Table 5.5 Verification experiment at optimal conditions	81
Table 6.1 Oxidation percentages of VSC (ETM, DMS, DMDS and TSC), the mineralisation degree achieved and the oxidant consumption percentage of the studied AOPs at 10 minutes	97
Table 6.2 Design parameters (pseudo-first order kinetics (k), the required time for 90% oxidation of TSC (t_{90}) and reactor volume (V_{reactor}) and the total costs of the studied AOPs	97
Table 6.3 Total annual cost of water treatment by the studied AOPs	98
Table 7.1 Henry's constant (bar) for different volatile sulphur compounds (ETM, DMS and DMDS) and the AC models predicted by COSMO-RS at 25 °C.....	105
Table 7.2 Assessment of oxygen surface groups obtained by TPD, CO/CO ₂ ratio and pH _{slurry} for the as-received and oxidised ACs	107
Table 7.3 Surface group distribution (%) obtained XPS of ACs	108
Table 7.4 Textural properties of the as-received and oxidised ACs.....	109
Table 7.5 Saturation times (ST) and adsorption capacities in (x/M) of the as-received and oxidised ACs	111
Table 7.6 Henry's constant (bar) for different volatile sulphur compounds (ETM, DMS and DMDS) and the studied ACs predicted by COSMO-RS at 25 °C.....	112
Table 8.1. Elemental analysis of as-received and irradiated ACs (%w/w)	118
Table 8.2 Assessment of oxygen surface groups obtained by TPD for AC samples.....	119
Table 8.3 Surface groups distribution (%) obtained in XPS for the AC samples	120
Table 8.4 Olfactometric breakthrough times (BT) and removal capacities of ACs samples	123

LIST OF FIGURES

Figure 1.1 Major sources of odour in WWTPs and their contribution	4
Figure 1.2 Diagram of sludge processing in WWTP	5
Figure 1.3 Water distribution in sewage sludge	5
Figure 1.4 Coagulation-flocculation processes	6
Figure 1.5 Diagram of belt drying system	8
Figure 1.6 Distribution of sludge treatment in Catalonia (2005-2012)	8
Figure 1.7 Distribution of sludge disposal in Catalonia (2005-2012)	9
Figure 1.8 Degradation and formation pathways of VSC during sludge processing	10
Figure 1.9 Configuration of odour abatement technologies in WWTPs	13
Figure 1.10 Diagram of chemical scrubber	15
Figure 1.11 Diagram of AC adsorber	19
Figure 1.12 Oxygen functional groups in ACs surface	19
Figure 3.1 Experimental set-up of drying process: a) drying reactor; b) diffuser; c) basket; d) heat gun; e) temperature sensor; f) condenser; g) nalophane bag	29
Figure 3.2 Diagram of sewage sludge treatment plant	31
Figure 3.3 Design of experiment in RSM	34
Figure 3.4 Experimental set-up of AOP test: (a) cooling bath; (b) stirrer; (c) cylindrical quartz reactors; (d) steel container; (e) UV lamp; (f) power supply	35
Figure 3.5 Experimental set-up of dynamic adsorption test: a) syringe pump; b) mass flow controller; c) static mixer; d) adsorption bed reactor	39
Figure 3.6 Individual molecules of sulphur solutes and molecular models for five different oxidative functionalization of ACs	40
Figure 3.7 Picture of gas chromatograph (CP-3800)	42
Figure 3.8 Dynamic olfactometer Bionose 0208: a) sample input; b) front panel; c) smell cup	43
Figure 3.9 Schematic operation of CSTmeter	44
Figure 3.10 Diagram of methodology used in SMP and b-EPS extraction	44
Figure 3.11 Picture of ion chromatography (Metrhom 761-Compact)	45
Figure 3.12 Picture of gamma irradiator	47
Figure 3.13 Picture of Micrometrics apparatus used to obtain nitrogen isotherms	49
Figure 3.14 Picture of infrared adsorption analyser	50
Figure 4.1 Diagram of the methodology used in drying processes	58
Figure 4.2 Distribution of the VOCs emitted in drying process in sampling I	59
Figure 4.3 VSC identified by GC/PFPD from lab-scale drying process	62

Figure 4.4 VSC concentrations in scrubber inflow, scrubber outflow and biofilter outflow: a) sampling VI; b) sampling VII; c) sampling VIII	64
Figure 5.1 Diagram of methodology used in conditioning and drying process	70
Figure 5.2 Individual effect of chemical conditioners doses on the CST of the sewage sludge	71
Figure 5.3 Influence of the individual dosage of chemical conditioners on TSC emissions: (a) polyelectrolyte, (b) iron chloride and (c) calcium oxide	72
Figure 5.4 Three-dimensional response surface plots of CST showing the effect of variables: (a) FeCl ₃ - polyelectrolyte dose, (b) CaO - polyelectrolyte dose, and (c) CaO - FeCl ₃ dose	77
Figure 5.5 Three-dimensional response surface plots of TSC emission showing the effect of variables: (a) FeCl ₃ -polyelectrolyte dose, (b) CaO - polyelectrolyte dose, and (c) CaO - FeCl ₃ dose	78
Figure 5.6 The effect of b-EPS (a) and SMP (b) on sulphur compounds emission from the undigested sewage sludge	79
Figure 5.7 Three-dimensional response surface plots of odour emission showing the effect of variables: (a) FeCl ₃ - polyelectrolyte dose, (b) CaO - polyelectrolyte dose, and (c) CaO - FeCl ₃ dose	80
Figure 5.8 Effect of physical conditioners doses on the CST of the sewage sludge.....	81
Figure 5.9 VSC concentration emitted from physical conditioned sludge during drying process	82
Figure 6.1 Diagram of methodology used in AOPs tests	88
Figure 6.2 Oxidation percentages of ETM (circle), DMS (square), DMDS (triangle) and TSC (line) during UV/H ₂ O ₂ treatment with $C_{0,H_2O_2} = 0.20$ mM	88
Figure 6.3 Effect of the H ₂ O ₂ concentration in the oxidation of TSC during UV/H ₂ O ₂ treatment $C_{0,TSC} = 0.85$ mg L ⁻¹	89
Figure 6.4 UV treatments: (A) oxidation percentages of ETM (circle), DMS (square), DMDS (triangle) and TSC (line) and (B) UV/VIS spectrum of the studied VSCs.....	90
Figure 6.5 Oxidation percentages of ETM (circle), DMS (square), DMDS (triangle) and TSC (line) during Fenton reaction with $C_{0,H_2O_2} = 0.20$ mM, $C_{0,Fe^{2+}} = 0.018$ mM	91
Figure 6.6 Effect of the Fe ²⁺ concentration in the oxidation of TSC during Fenton treatment with $C_{0,H_2O_2} = 0.20$ mM, $C_{0,TSC} = 0.85$ mg L ⁻¹	92
Figure 6.7 Oxidation percentages of ETM (circle), DMS (square), DMDS (triangle) and TSC (line) during photo-Fenton reaction with $C_{0,H_2O_2} = 0.20$ mM and $C_{0,Fe^{2+}} = 0.018$ mM	93
Figure 6.8 Oxidation percentages of ETM (circle), DMS (square), DMDS (triangle) and TSC (line) during ozone treatment with $C_{0,O_3} = 0.20$ mM	94
Figure 6.9 Effect of the O ₃ concentration in the oxidation of TSC during ozone treatment $C_{0,TSC} = 0.85$ mg L ⁻¹	94

Figure 7.1 Diagram of methodology used in dynamic adsorption tests	104
Figure 7.2 Breakthrough curves for ETM, DMS and DMDS on AC-R	104
Figure 7.3 TPD spectra profiles for AC samples: (A) CO evolution; (B) CO ₂ evolution ..	106
Figure 7.4 XPS spectra profiles for carbon samples: (A) C (1s) spectral region; (B) O (1s) spectral region	107
Figure 7.5 N ₂ adsorption/desorption isotherms at -196°C of AC samples	108
Figure 7.6 Breakthrough curves for ETM (A), DMS (B) and DMDS (C) on as-received and oxidised ACs	110
Figure 8.1 Diagram of methodology used in dynamic adsorption tests under wet conditions	117
Figure 8.2 TPD spectra profiles for AC samples: (A) CO evolution; (B) CO ₂ evolution ..	118
Figure 8.3 XPS spectra profiles for carbon samples: (a) C (1s) spectral region; (b) O (1s) spectral region	119
Figure 8.4 Breakthrough curves for DMDS (a), DMS (b) and (ETM) (c) on the ACs.....	121
Figure 8.5 Breakthrough curves for DEEDS on the ACs.....	121
Figure 8.6 Effect of oxygen functional groups content onto ACs samples on the removal capacity for ETM.....	123
Figure 8.7 Effect of ACs samples pH on the ETM oxidation	125

LIST OF ACRONYMS

A	Amortised capital cost
AC	Activated carbon
AC-0	Activated carbon irradiated in the presence of all radicals
AC-A	Activated carbon irradiated in the air (without water)
AC-e	Activated carbon irradiated in the presence of aqueous electrons
AC-H	Activated carbon irradiated in the presence of H [•]
AC-N	Activated carbon oxidised with nitric acid
AC-O	Activated carbon oxidised with ozone in liquid phase
AC-O30	Activated carbon oxidised with ozone in gas phase for 30 min
AC-O60	Activated carbon oxidised with ozone in gas phase for 60 min
AC-OH	Activated carbon irradiated in the presence of hydroxyl radicals
AC-R	As-received activated carbon
A _{ext}	External area
AOP	Advanced oxidation processes
BT	Breakthrough time
b-EPS	Bound extracellular polymeric substance
C	Carbon
CCD	Central composite design
CST	Capillary suction time
DMS	Dimethyl sulphide
DMDS	Dimethyl disulphide
DS	Dry solid
E	Energy consumption
EPS	Extracellular polymeric substances
ETM	Ethyl mercaptan
GC	Gas chromatography
IC	Ion chromatography
k	Pseudo-first order kinetic
K _H	Henry's constant
MTM	Methyl mercaptan
•OH	Hydroxyl radical
OT	Odour threshold
OU _E	European odour unit
P	Power density
PFPD	Pulse flame photometric detector
R	Reactor material cost
RSM	Response surface methodology
SO ₄ ²⁻ -S	Sulphur compounds as sulphate
SMP	Soluble microbial product

ST	Saturation time
t_{90}	time required for 90% oxidation of volatile sulphur compounds
TMA	Trimethylamine
TPD	Temperature programmed desorption
TSC	Total sulphur compounds
UV	Ultraviolet
V_{meso}	Mesopore volume
V_{micro}	Micropore volume
V_{reactor}	Reactor volume
VSC	Volatile sulphur compound
V_t	Total pore volume
WWTP	Waste water treatment plant
x/M	Adsorption capacity
XPS	X-ray photoelectron spectroscopy

RESUM

La contaminació atmosfèrica relacionada amb la emissió de males olors s'ha convertit en els darrers anys en un motiu de preocupació social. La proximitat d'instal·lacions causants de males olors com les estacions depuradores d'aigües residuals (EDAR) a les àrees urbanes, agreuja encara més el problema. Els compostos volàtils de sofre són un dels principals grups de compostos causants de males olors, especialment en el tractament i processament dels fangs generats a les EDARs.

Actualment, existeix una gran varietat d'opcions disponibles per al tractament efectiu de les emissions de compostos de sofre causants de males olors. La minimització o eliminació d'aquests compostos es pot dur a terme durant el procés de tractament de fangs o mitjançant tractaments a final de procés.

En relació als processos de minimització, la present tesi s'ha focalitzat en la investigació del procés de condicionament dels fangs mitjançant l'addició de condicionants químics. A fi de minimitzar les emissions de compostos de sofre i olors durant l'assecat tèrmic de fangs a baixa temperatura, així com millorar la deshidratabilitat dels fangs, s'han realitzat proves amb diferents dosis de clorur de ferro, òxid de calci i polielectròlit. Els resultats obtinguts permeten optimitzar el procés de condicionament i conèixer els efectes sinèrgics existents entre els condicionants químics i les emissions de compostos causants d'olor.

Tot i que les modificacions mitjançant el condicionament millorarien les eficiències de les tecnologies a final de procés, aquestes no són suficients per mitigar les emissions. És per aquest motiu, que s'ha estudiat l'adsorció i els processos de oxidació avançada (POA) com a tractaments a final de procés. Per dur a terme aquests estudis s'han seleccionat tres compostos de sofre representatius de les emissions en les EDARs: etil mercaptà (ETM), sulfur de dimetil (DMS) y disulfur de dimetil (DMDS).

En primer lloc, s'ha estudiat l'eficiència del UV/H₂O₂, Fenton, foto-Fenton i ozó en l'oxidació de una solució aquosa que contenia els compostos objecte d'estudi per tal d'avaluar quin dels esmentats tractaments és l'opció més adequada per ser acoblada a un rentador de gasos. Les altes eficiències obtingudes han demostrat que tots els POA estudiats són adequats per a la oxidació dels compostos causants de olor objectes de l'estudi, essent més rellevant per els tractaments de foto-Fenton i ozó. Per altre banda, la possible aplicació dels POA en sistemes a escala industrial es va avaluar mitjançant l'anàlisi econòmic. S'ha observat que les limitacions del volum dels reactors i la complexitat de remodelació de la planta són un punt important alhora d'establir la opció més viable.

En darrer lloc, s'ha investigat l'adsorció del ETM, DMS i DMDS en carbons activats (CA) modificats. En un primer estudi les modificacions s'han dut a terme utilitzant àcid nítric

i ozó per tal de modificar les propietats, tant texturals com químiques, del CA comercial de partida. Les capacitats d'adsorció obtingudes en les proves en dinàmic i sota condicions inertes han demostrat que l'enriquiment massiu de la superfície del CA amb grups hidroxils, millora els processos d'adsorció del ETM i dels DMS, donat la formació de ponts d'hidrogen. El mètode COSMO-RS de química quàntica s'ha utilitzat en aquesta tesi per simular les interaccions entre els grups superficials del CA i els compostos objecte d'estudi. Coincidint amb les dades experimentals, el model ha predit una major afinitat del DMDS cap al CA, no veient-se afectada la interacció per la presència de grups funcionals oxigenats a la superfície del CA.

Donades les característiques dels efluents en condicions reals, l'efectivitat del procés d'adsorció dels carbons activats en condicions d'humitat i en presència d'oxigen ha estat avaluat. Per aquest cas, les proves d'adsorció s'han portat a terme utilitzant carbons modificats per mitjà de la irradiació gamma. En les condicions estudiades, el eficiències d'eliminació del DMS i el DMDS han estat les més baixes en comparació a les presentades sota condicions inertes. A més, les condicions experimentals han permès conèixer l'efecte de la humitat en el procés d'adsorció així com el procés catalític dels mercaptans.

RESUMEN

La contaminación atmosférica relacionada con la emisión de malos olores se ha convertido en los últimos años en motivo de preocupación social. La proximidad a las áreas urbanas de instalaciones causantes de malos olores como son las estaciones depuradoras de aguas residuales (EDAR), agrava más el problema. Los compuestos volátiles sulfurados son uno de los principales grupos causantes de malos olores, especialmente en el tratamiento y procesamiento de los lodos de depuradora.

Actualmente, existe una gran variedad de opciones disponibles para el tratamiento efectivo de las emisiones de compuestos sulfurados causantes de malos olores. La minimización o eliminación de dichos compuestos se puede llevar a cabo durante el procesamiento de los lodos o bien mediante tratamientos aplicados a final de proceso.

En relación a los procesos de minimización, la presente tesis se ha focalizado en la investigación del proceso de condicionamiento de lodos mediante la adición de condicionantes químicos. Con el fin de minimizar las emisiones de compuestos sulfurados y olores durante el secado térmico a baja temperatura, así como mejorar la deshidratabilidad de los lodos, se han realizado pruebas con diferentes dosis de cloruro de hierro, óxido de calcio y polielectrolito. Los resultados obtenidos permiten optimizar el proceso de acondicionamiento y conocer los efectos sinérgicos existentes entre los condicionantes y las emisiones de compuestos odoríferos.

A pesar que las modificaciones mediante el acondicionamiento mejorarían las eficiencias de las tecnologías aplicadas a final de proceso, estas no son suficientes para mitigar las emisiones. Es por este motivo que se ha estudiado la adsorción y los procesos de oxidación avanzada (POA) como tratamientos a final de proceso. Para llevar a cabo estos estudios se han seleccionado tres compuestos sulfurados representativos de las emisiones en las EDARs: etil mercaptano (ETM) sulfuro de dimetilo (DMS) y disulfuro de dimetilo (DMDS).

En primer lugar se ha estudiado la eficiencia del UV/H₂O₂, Fenton, foto-Fenton y ozono para la oxidación de ETM, DMS y DMDS en solución acuosa con el fin de evaluar cuál de los tratamientos es la opción más adecuada para ser acoplada a un sistema de lavado de gases. Los resultados han demostrado la efectividad de todos los PAO estudiados para la oxidación de los compuestos sulfurados, siendo esta más notoria para el foto-Fenton y el ozono. Por otro lado, la posible aplicación de los PAO en sistemas a escala industrial se evaluó mediante el análisis económico. Se observó que las limitaciones de volumen de los reactores y la complejidad de remodelación de la planta son puntos a tener en cuenta a la hora de establecer la opción más viable.

Por último, se ha investigado la adsorción del ETM, DMS y el DMDS en carbones activados (CA) modificados. En un primer estudio, las modificaciones se han llevado a

cabo usando ácido nítrico y ozono para modificar tanto las propiedades químicas como las texturales del CA comercial de partida. Las capacidades de adsorción obtenidas mediante las pruebas en dinámico y bajo condiciones inertes han mostrado que un enriquecimiento en la superficie del CA con grupos hidroxilo, mejora el proceso de adsorción del ETM i el DMS, debido a la formación de puentes de hidrogeno. El método COSMO-RS de química cuántica se ha usado en esta tesis para simular las interacciones entre los grupos superficiales del CA y los compuestos objetos de estudio. Coincidiendo con los datos experimentales, el modelo fue capaz de predecir una mayor afinidad del DMDS hacia el CA, no encontrándose una capacidad de adsorción mejorada por la presencia de grupos funcionales oxigenados en la superficie.

Dadas las características de los efluentes gaseosos en condiciones reales, la efectividad del proceso de adsorción de los carbones activados en condiciones de humedad y en presencia de oxígeno ha sido evaluada. En este caso, las pruebas de adsorción se han llevado a cabo mediante el uso de carbones modificados mediante radiación gamma. Bajo las condiciones estudiadas, el DMDS i el DMS han presentado eficiencias de eliminación más bajas que las que se obtuvieron en condiciones inertes. A demás, los resultados experimentales permitieron determinar el efecto de la humedad en el proceso de eliminación así como también en el proceso catalítico de los mercaptanos.

SUMMARY

Environmental pollution related to odourous emissions has become in the last years an important public concern. Closeness of odour-causing facilities such as waste water treatment plants (WWTPs) to urban areas further aggravates the problem. Volatile sulphur compounds (VSC) are one of the main groups of odour-causing compounds in WWTPs, especially sludge processing.

Nowadays, there are a several options available for the effective treatment of odorous sulphur compounds emission. The minimisation or abatement of these compounds can be carried out during sludge processing or by applying end-of-pipe treatments.

Regarding to the minimisation processes of odorous sulphur compounds, this thesis has focused on the research of sewage sludge conditioning process using conditioning compounds. Different doses of iron chloride, calcium oxide and polyelectrolyte has been tested in order to assess sulphur and odour emissions during sludge drying process, as well as to improve the sludge dewaterability. The obtained results permitted to optimise the conditioning process and to know the synergistic effects between inorganic conditioners and odorous compounds emissions.

Despite the modification on process would improve the end-of-pipe technologies, these modifications might not be sufficient to mitigate emissions of odorous sulphur compounds in sludge processing. Therefore, end-of-pipe treatments such as adsorption and advanced oxidation processes (AOP) have been assessed in this thesis. In order to carry out these studies, three representative compounds of WWTP emissions have been selected as target compounds: ethyl mercaptan (ETM), dimethyl sulphide (DMS) and dimethyl disulphide (DMDS).

The effectiveness of UV/H₂O, Fenton, photo-Fenton and ozone on the oxidation of a multicomponent aqueous solution containing target compounds was investigated in order to assess which was the most suitable treatment to be coupled with a wet scrubber used in odour treatment facilities. The results revealed that all studied AOP were suitable to oxidise target compounds, especially photo-Fenton and ozone treatments. Furthermore, the possible implementation of AOPs at full-scale was evaluated following an economic analysis. In this sense, it was found that reactor volume limitations or retrofitting complexities might play an important role in establishing the most economical option.

Finally, the adsorption of ETM, DMS and DMDS onto modified activated carbons (AC) was investigated. On first place, nitric acid and ozone were used to modify the chemical and textural properties of commercial AC. The adsorption capacities obtained in dynamic tests under inert conditions have shown a massive enrichment with hydroxyl groups improve the ETM and DMS adsorption process. Quantum-chemical

COSMO-RS method was used to simulate the interactions between AC surface groups and target compounds. In agreement with experimental data, the model was able to predict a greater affinity of DMDS towards AC, unaffected by the incorporation of oxygen functional groups in the surface. Furthermore, the model points out that an increase of the adsorption capacities of AC by the incorporation of hydroxyl groups due to the hydrogen bond interactions between hydroxyl groups and VSC.

Given the characteristics of gaseous effluents at real conditions, the effectiveness of the ACs for VSC removal under wet conditions has been evaluated. In this study, the adsorption tests were carried out using activated carbons modified by gamma irradiation. Under the studied conditions, lower adsorption efficiencies were observed than those obtained at inert conditions for DMS and DMDS. Moreover, the experimental results allowed knowing the effect of the humidity in the VSC removal process, as well as the catalytic process of ETM.

1

INTRODUCTION

1.1. ODOROUS COMPOUNDS EMISSIONS IN WASTEWATER TREATMENT PLANTS

The emission of unpleasant odours produced at some facilities, such as waste water treatment plants (WWTPs), has become in the last years an important public concern since these facilities are located close to residential areas (Frechen, 1994; Karageorgos et al., 2010).

The odorous emissions from WWTPs are composed of a mixture of compounds such as reduced sulphur compounds (sulphides and mercaptans), nitrogenised compounds (ammonia, amines), volatile fatty acids and volatile organic compounds, among others. Despite odorants compounds are emitted from WWTP at trace levels ($\mu\text{g L}^{-1}$ - mg L^{-1}), they can produce important annoyance due to their low odour threshold (OT) which is defined as the minimum concentration perceived by human sense of smell (Leonardos et al., 1969). Table 1.1 lists the main odorous compounds associated with WWTPs. Moreover, the characteristic odour of each compound and their OT are also presented.

Table 1.1 Main odorous compounds associated with WWTPs (Suffet et al., 2004).

Class	Compound	Characteristic odour	OT (ppm _v)
Sulphurous	Hydrogen sulphide	Rotten eggs	0.0005
	Ethyl mercaptan	Decayed cabbage	0.00001
	Methyl mercaptan	Decayed cabbage, garlic	0.00002
	Dimethyl sulphide	Decayed vegetables	0.0006
	Dimethyl disulphide	Putrification	0.0008
Nitrogenous	Ammonia	Sharp, pungent	0.038
	Trimethylamine	Fishy	0.48
	Indole	Faecal, Nauseating	0.0001
	Scatole	Faecal, Nauseating	0.0024
Acids	Acetic	Vinegar	0.0016
	Butyric	Rancid, sweaty	0.09
	Valeric	Sweaty	0.0018
Ketones	Methyl ethyl ketone	Fruit, sweet	1.2
	Acetone	Fruit, sweet	0.25

The emissions of odorous compounds in WWTPs are caused by their stripping from wastewater, the generation of by-products through biochemical reactions in different treatment steps and/or by the use of chemical reagents throughout the process (Vincent, 2001). Frechen (1988), Islam et al. (1998), Dincer and Muezzinoglu (2008) and Zarra et al. (2008) assessed the emissions of odorous compounds from different steps in WWTP. These authors agreed and reinforced the general opinion that the major odour sources are associated with the sludge processing (Figure 1.1).

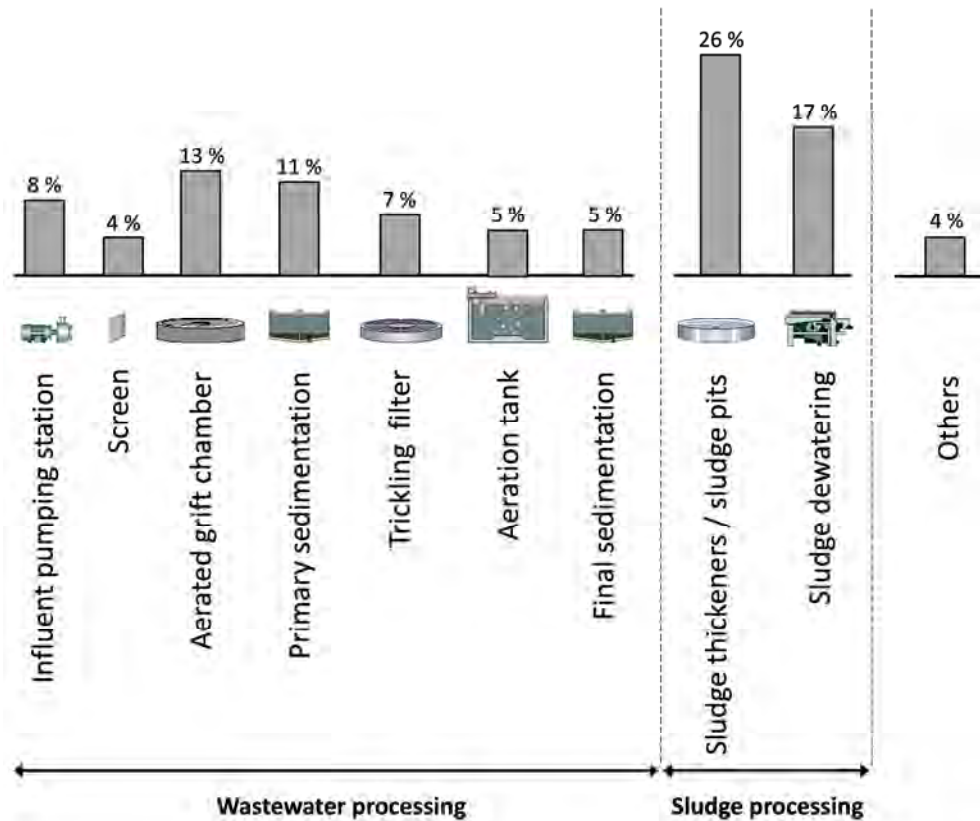


Figure 1.1 Major sources of odour in WWTPs and their contribution (Frechen, 1988).

The odour problems associated with WWTP has led to regulate these odorous emissions. Nowadays, many countries such as Denmark, Germany or Netherlands have specific regulations for odorous emissions from different facilities. In Spain, only the Catalan government adopted the 3/1998 Draft Bylaw odour emissions which established the maximum immision concentration of the odour-causing facilities. All of them have adapted their policies based on the European regulation UNE-EN 13725:2004 "Air quality – Determination of odorous concentration by dynamic olfactometry". This regulation promotes the use of sensory characterisation which provides the real effect of odorous emissions on population and complements the analytical methods.

1.2. SLUDGE PROCESSING AND FINAL DISPOSAL

Sludge from waste water treatment operations and processes contains from 0.25 to 5% dry solids (DS), depending on the operation used. Moreover, this sludge is composed largely of the substances responsible for the offensive, pathogenic and toxic characteristics of the untreated wastewater (Werther and Ogada, 1999). Therefore, sludge processing is focused on reducing the amount of organic solids, pathogen

removal, improving the dewatering characteristics of sludge and reducing the water content. These purposes can be achieved through sludge conditioning, stabilization, dewatering and drying (Figure 1.2)

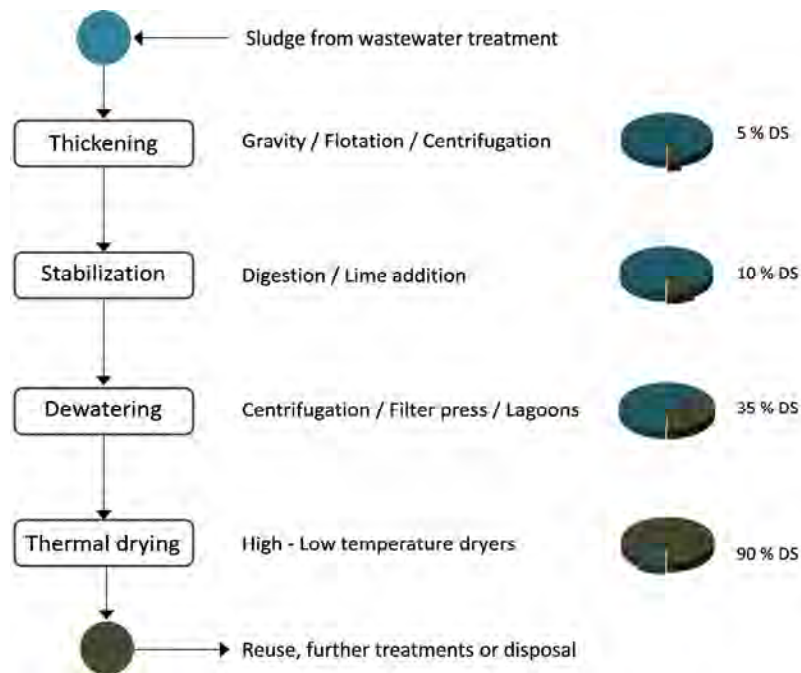


Figure 1.2 Diagram of sludge processing in WWTPS. Adapted from (Werther and Ogada, 1999)

One of the main objectives of sludge processing is the reduction of the water content. In sewage sludge suspension four different types of water can be distinguished according to their physical bonding to the sludge particles: free water, interstitial water, surface water and bound water (Figure 1.3) (Kopp and Dichtl, 2001). The main characteristics of the different types of water contained in sewage sludge are presented in Table 1.2.

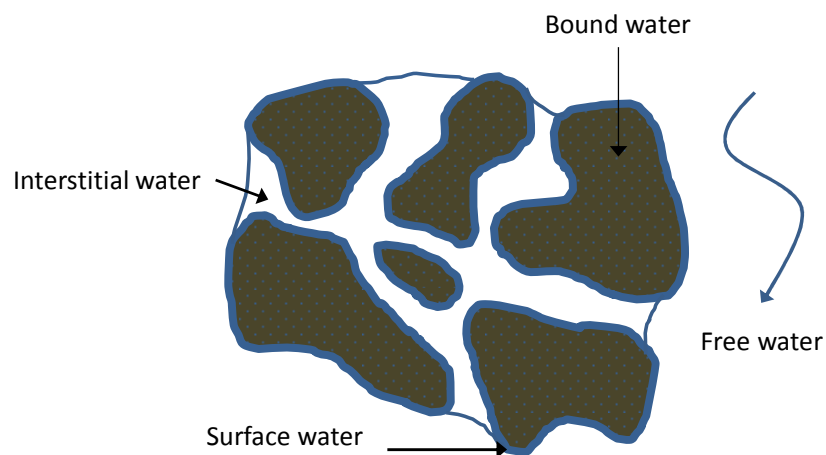
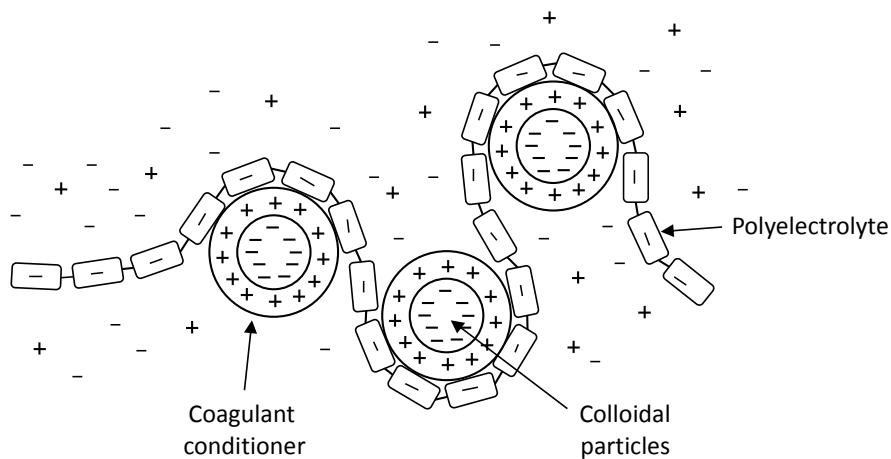


Figure 1.3 Water distribution in sewage sludge.

Table 1.2 Main characteristics of the different types of water contained in sewage sludge

Typology	Characteristics
External water	Free water Water moves freely between the individual sludge particles. Can be separated mechanically (centrifugal forces or filtration).
	Interstitial water Water is kept in the interstice of the sludge particles. Water is bound physically by active capillary forces. Can be separated mechanically (centrifugal forces or filtration).
Internal water	Surface water Water covers the entire surface of the sludge particles in several layers of water molecules. Water is bound by adsorptive and adhesive forces. Can be separated when the sludge particle wall is broken.
	Bound water Water contains the water in cells and water of hydration. Water is physical-chemical bonding to the particles. Can only be removed thermally.

Thus, the first step consists of increasing the solid content by thickening processes, which are carried out by physical methods such as gravity thickening, flotation, centrifugation or belt filters. In the thickening unit, sludge conditioning is necessary to facilitate the free water removal and to increase the processing efficiency of the dewatering device (Zhai et al., 2012). Thus, several efforts have been made to enhance the dewatering process by different techniques such as ultrasonication (Feng et al., 2009; Muller et al., 2009), mechanical processes (Hwang et al., 1997) or electrolysis (Yuan et al., 2010). Nevertheless, the implementation of these techniques is not economically feasible at full-scale, and therefore the combined use of organic and inorganic reagents for the same purpose is preferred (Wu et al., 1997; Lee et al., 2005; Tony et al., 2008; Chen et al., 2010; Zhai et al., 2012). Traditionally, inorganic chemicals such as iron chloride (FeCl_3) or calcium oxide (CaO) and organic chemicals as polyelectrolytes are most commonly used. Polyelectrolyte, which can be cationic or anionic, is used to aggregate sludge particles through charge neutralisation and interparticle binding. On the other hand, iron chloride neutralises the negative surface charges in the sludge solids allowing their aggregation (Figure 1.4), while calcium oxide acts as pH adjuster.

**Figure 1.4** Coagulation-flocculation processes.

In many cases, the further addition of CaO in the same process is considered as a stabilization process which provides high values of pH to destroy pathogenic microorganisms (Werther and Ogada, 1999). However, digestion is widely used in WWTPs as a stabilisation method which involves the partial conversion of the organic matter into a biogas as well as also destroys the pathogen microorganisms.

On the other hand, physical conditioners, often known as skeleton builders or filter aids are also used in order to reduce sludge management cost and reduce the sludge volume to be treated (Qi et al., 2011a). A wide range of carbon-based materials (Albertson and Kopper, 1983; Qi et al., 2011b) and minerals including fly-ashes (Benítez et al. 1994; Chen et al., 2010) or gypsum (Zhao, 2002) have been used as physical conditioners. These conditioners have been applied alone to enhance sludge dewatering. Nevertheless, more often its addition is carried out together with chemical conditioners in order to reduce the consumption of chemicals (Nelson and Brattlof, 1979). Several authors stated the formation of three-dimensional porous lattice due to the bounding of the sludge particles to the surface of physical conditioners particles by chemical and/or electrostatic interactions (Tennery and Cole, 1968; Zall et al. 1987; Zhao, 2002). Moreover, the formation of porous structure may also serve as a draining media for the withdrawal of free water, improving the sludge dewatering (Qi et al. 2011a).

Dewatering and drying process is a prerequisite for the further treatment of sludge, handling, transport and disposal. Dewatering devices use various techniques to further remove water from sludge. These techniques are mainly based on mechanical process such as centrifuges, belt and pressure filter presses which provide a sludge solids concentration around 25%. Finally, the minimum moisture content is practically attainable with thermal drying which also involves a reduction of transportation costs, further pathogen reduction, improvement in storage capability and marketability.

Dryers are commonly classified on the basis of the predominant method of transferring heat to wet solids being dried. These methods are conduction (indirect drying), radiation (infrared drying), convection (direct drying), or a combination of these. In indirect drying, heat transfer is carried out by contact of wet sludge solids with hot surface, while heat transfer is accomplished by radiant energy supplied by electric resistance elements or infrared lamps in infrared drying.

Direct dryers such as flash dryers or direct rotatory dryers are the most common type used in thermal drying of sludge. In this case, heat transfer is accomplished by direct contact between the wet sludge and hot carrier gases (>500°C) which provide the latent heat required for evaporating the liquid fraction from the sludge. Nevertheless, all of these technologies are often considered as an energy demanding, costly and complex process. Moreover, drying systems require careful attention safety aspects such as risks of self-combustion, fires and dust explosions (Tornes and Whipps, 2004).

The combination of combustibles particle, warm temperatures, sufficient oxygen, and high gas velocities make these systems susceptible to fire and explosion. Low temperature drying process such as belt drying systems (Figure 1.5) avoids the mentioned risks. In this system, dewatered sludge is extruded and uniformly distributed on the conveyor belts where the sludge is dried by a stream of dry air at 80°C.

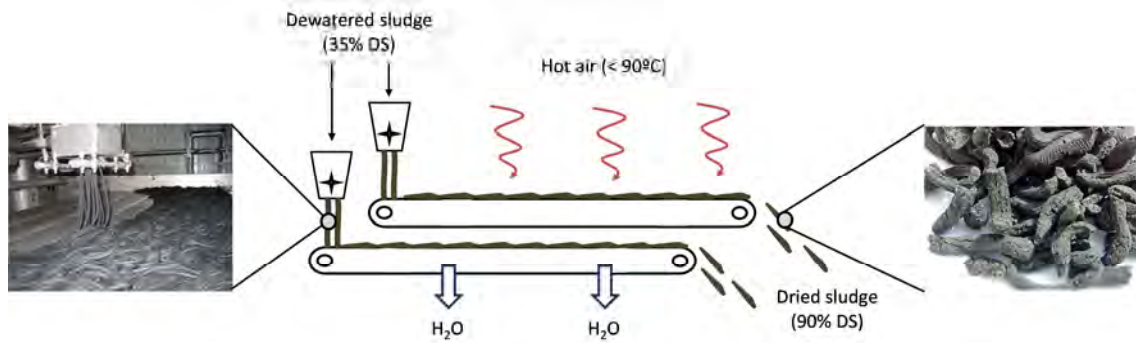


Figure 1.5 Diagram of belt drying system

Not all the sludge produced in WWTPs is treated by thermal drying processes. Digestion without post-treatment and composting processes are alternatives of sludge treatments. Figure 1.6 shows the distribution of different treatment applied to sewage sludge in Catalonia between 2005 and 2012.

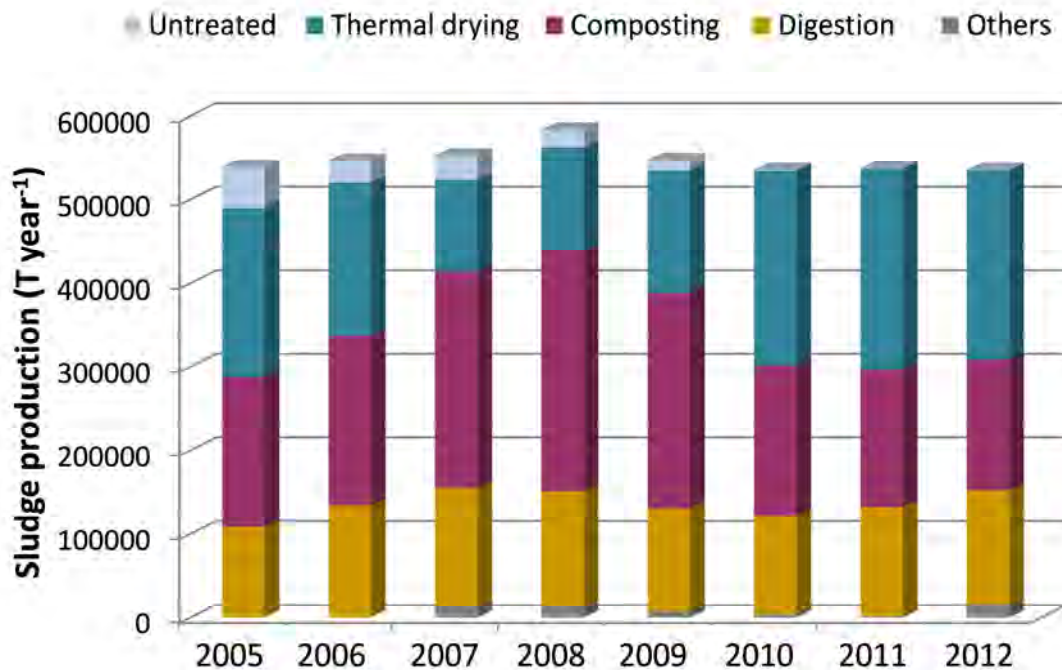


Figure 1.6 Distribution of sludge treatment in Catalonia (2005-2012)

Nowadays, 99.8% of the sewage sludge produced in Catalonia is managed using different treatment, being thermal drying and composting the most commonly used (42% and 29%, respectively).

Generally, the selection of the best disposal route for the dried sludge should start by identifying the most secure and environmentally acceptable final destination for the sludge, and this in turn would dictate the type of treatment required (Werther and Ogada, 1999). Currently, field application, landfill disposal or energy recovery by incineration are the main routes of sludge disposal. Figure 1.7 shows the distribution of sludge disposal in Catalonia between 2005 and 2012.

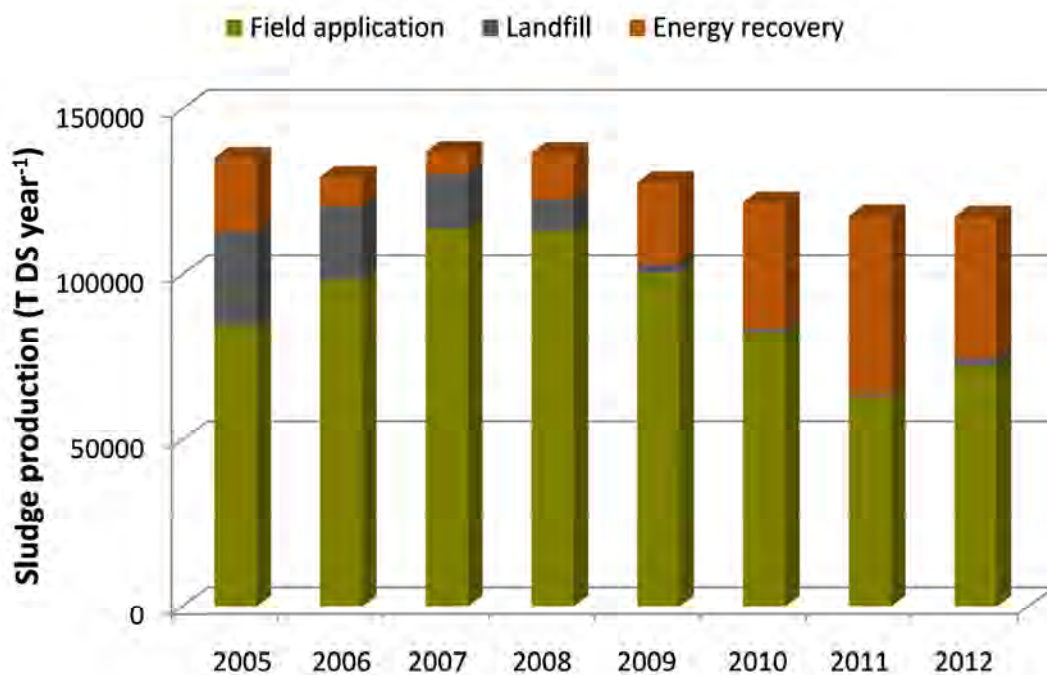


Figure 1.7 Distribution of sludge disposal in Catalonia (2005-2012)

Clearly, the field application as route of sludge disposal is the most commonly used since the high content of nitrogen and phosphorous shows good fertiliser properties. Furthermore, the use of sludge as fertiliser leads the return of the organic materials into the bio-cycle as well as replaces the application of chemical fertilisers whose production also requires a lot of energy (Turovskiy and Mathai, 2006). Moreover, the high calorific value of dry sludge ($3500 \text{ kcal Kg}^{-1}$) lets the energy to be recovered through incineration (Werther and Ogada, 1999). This route of sludge disposal has been an upward trend in recent years.

1.2.1. Formation of odour-causing compounds in sludge processing

During sludge processing, the anaerobic conditions, the high organic matter concentrations and the presence of a well-developed fermentative and sulphate oxidising microbial community, leads to the formation of odorous compounds, especially volatile reduced sulphur compounds (Lebrero et al., 2011) Furthermore, several authors argue that the sulphur compounds emissions are closely linked to the presence of extracellular polymeric substances (EPS) (Higgins et al., 2006; Adams et al., 2008; Higgins et al., 2008).

EPS are different classes of macromolecules such as carbohydrates, proteins, nucleic acids and lipids which are found outside the cell and in the intracellular space of microbial aggregates and represents up to 80% of the mass of activated sludge (Frølund et al., 1996; Flemming and Wingender, 2001). Higgins et al. (2006) corroborated that the degradation of these substances, especially degradation of proteins such as cysteine and methionine to amino acids, can provide a substrate for the production of the odorous sulphur compounds such as sulphides and mercaptans during sludge processing (Figure 1.8). Moreover, Higgins et al. (2006) stated that the iron chloride added in conditioning process could remain attached to the sludge particles hindering the extraction of EPS. Thus, the low availability of these substances would decrease the release of VSC in conditioning process according to the formation pathways of VSC.

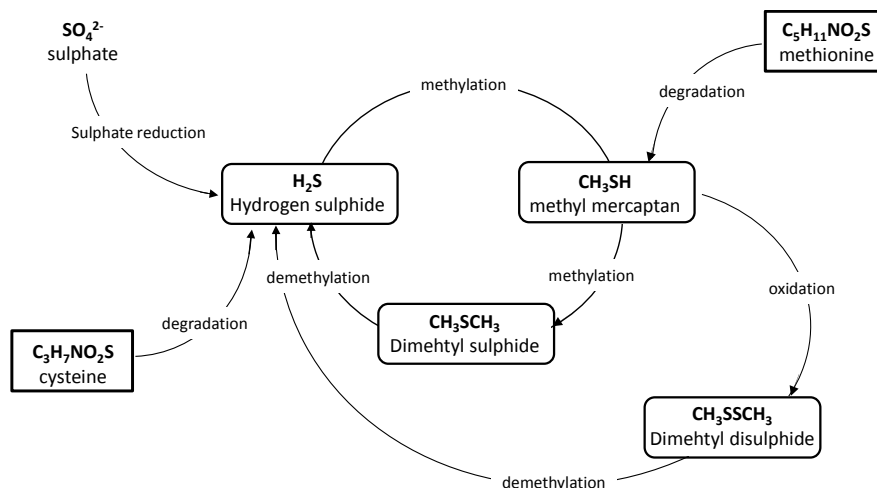


Figure 1.8 Degradation and formation pathways of VSC during sludge processing. Adapted from (Higgins et al., 2006)

Beyond the conditioning effect on odour emission during sludge processing, several authors investigated the effect during the sludge storage for subsequent land application (Chang et al., 2005; Novak et al., 2007; Adams et al., 2008).

Table 1.3 presents the relevant studies on odorous compounds emissions from conditioned sludge in field applications. Similar behaviours were observed in the collected studies despite the different origins of sewage sludge and incubation times. Devai and Delaune (2002) and Liu et al. (2012) agreed on the fact that the iron chloride reduces VSC and odour emissions from undigested sewage sludge, especially hydrogen sulphide. Different behaviour of digested sewage sludge was noted by Novak et al. (2007) who measured increases in the concentration of sulphur compounds as a result of the iron chloride addition. On the other hand, the release of volatile nitrogenised compounds from undigested sewage sludge due to calcium oxide addition and/or polyelectrolyte decomposition was observed by Kim et al. (2002), Kim et al. (2003) Subramanian et al. (2005) and Liu et al. (2012). The literature has focused on the effect of conditioning process on the emission of odorous compounds from sludge in order to study its field application. However, **there is a lack of knowledge about the effect caused by conditioners addition on the odorous compounds emissions in sewage sludge drying process**. Moreover, the mentioned studies put the main objective of conditioners to one side and do not consider the simultaneous effect on the sludge dewaterability. Therefore, both the odorous emissions and the sludge dewaterability would have to be considered as key aspect on conditioning process.

Table 1.3 Relevant studies on odorous compounds emissions from conditioned sludge in field applications (D: digested; UD: undigested; DS: dry solid; PAM: polyacrylamide; NS: not specified; COS: carbonyl sulphide)

Sludge	Conditioner	Conditioner dose	Sampling time	Odorous compounds	Findings	Reference
D	Polymer CaO	P: 9-18 g Kg DS ⁻¹	22 days	TMA	-Release of amines due to the alkaline pH achieved by CaO addition. - Partial degradation of polyelectrolytes can result in generation of amine groups.	(Chang et al., 2005)
D	FeCl ₃	8-50 g Kg DS ⁻¹	20 days	MTM, DMS, DMDS	-The highest iron content in sludge implies the highest emission of sulphur compounds such as mercaptans and sulphides at long periods of storage time	(Novak et al., 2007)
UD	PAM FeCl ₃ CaO	35 g Kg DS ⁻¹ 65 g Kg DS ⁻¹ 100 g Kg DS ⁻¹	40 min	NH ₃ , H ₂ S, COS	-NH ₃ emission is increased by FeCl ₃ /CaO, while SO ₂ and H ₂ S are reduced. - Formation of calcium sulphate	(Liu et al., 2012)
UD	Polymer CaO	30 g L ⁻¹ 50 gL ⁻¹	4 hours	TMA, DMDS	-Polymer/CaO caused amines emission -Protein content of sludge affects amines and sulphides emissions.	(Kim et al., 2002)
UD	FeCl ₃	1000 mg L ⁻¹	1 day	H ₂ S, COS, MTM, DMS, DMDS	-Sulphur compounds emission decreases when FeCl ₃ concentration is increased. -COS concentration is unaffected by FeCl ₃ addition.	(Devai and Delaune, 2002)
UD	Polymer CaO	4500 mg L ⁻¹ 2000 mg L ⁻¹	56 days	TMA, VSC (undefined)	- CaO causes important formation of sulphur and nitrogen compounds at long period storage time. - The formation of amines is correlated with the addition of polymer	(Subramanian et al., 2005)

1.3. END-OF-PIPE TECHNOLOGIES FOR ODOUR REMOVAL

Minimization and abatement of odorous emissions are becoming two major challenges in wastewater treatment utilities worldwide (Lebrero et al., 2011). There are a variety of options available for the effective treatment of odorous compounds emission.

Adsorption (Nguyen-Thanh and Bandosz, 2005; Anfruns et al., 2011), chemical scrubbers (Kastner and Das, 2002; Couvert et al., 2008) or biological treatment such as biofiltration (Pagans et al., 2007; Lebrero et al., 2010) or biotrickling (Gabriel and Deshusses, 2003; Ramírez et al., 2009) have been widely investigated at the end-of-pipe for odorous compounds removal. The selection of the odour abatement techniques depends on the type of contaminant, concentration, gas flow, the desired efficiency and the specific features of the facility (Schlegelmilch et al., 2005). The main characteristics of conventional odour abatement techniques are shown in Table 1.4.

In WWTPs, these technologies are combined in multiple ways for the purpose of polishing air streams according to the needs of each facility. Conventionally, the facilities have a first chemical treatment unit (scrubber) where a majority of odorous compounds are removed. This treatment is followed by a biological treatment either as biofilter, biotrickling, or bioscrubber. However, the variations of the pollutants concentration can be detrimental to the biological unit performance and to the microbial population (Socol et al., 2003). Hence, adsorbers are added as final polishing step (Figure 1.9).

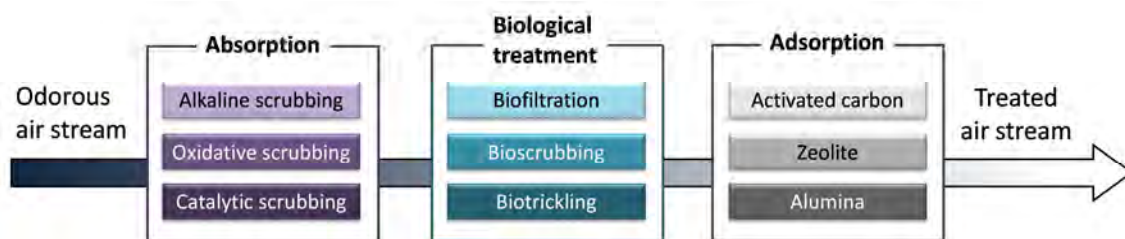


Figure 1.9 Configuration of odour abatement technologies in WWTPs.

This thesis is focused on the removal for odorous compounds by the application of physical/chemical technologies (chemical scrubbers and adsorption) which are explained below.

Table 1.4 Main characteristics of conventional odour abatement technologies (Mills, 1995; Estrada et al. 2011)

Abatement technology	Treated flow (m ³ h ⁻¹)	Capital cost € (m ³ h ⁻¹) ⁻¹	Operation cost € (1000 m ³) ⁻¹	Efficiency %	Advantage	Disadvantage
Thermal oxidation	2000-200000	5-28	0.35	99	<ul style="list-style-type: none"> • Final solution • Accepts variation in flow, concentration and species 	<ul style="list-style-type: none"> • catalytic units costly to replace
Absorption	1000-100000	3-12	0.27	50-99	<ul style="list-style-type: none"> • Collects gases and particles • Gases at or near dew-point can be treated 	<ul style="list-style-type: none"> • Liquid waste effluent is produced • Corrosion resistant materials are required • Multiple stages can be required
Biofilter	200-10000	5-28	0.21	77-99	<ul style="list-style-type: none"> • Media last for approx. 5 years 	<ul style="list-style-type: none"> • Odour formation • Requires steady continuous feed • Sensitive to changes in feed • Large ground area
Bioscrubber	200-10000	10-41	0.13	50-99	<ul style="list-style-type: none"> • Accepts effluents of high concentration • Gases at or near dew-point can be treated 	<ul style="list-style-type: none"> • Acidic effluent liquor
Adsorption	500-50000	4-14	0.45	90-99	<ul style="list-style-type: none"> • Adsorbs majority of compounds 	<ul style="list-style-type: none"> • Large size of equipment • Potential disposal problem of spent carbon

1.3.1. Advanced oxidation scrubbers

Chemical scrubbing technologies are based on the contact of a scrubbing chemical (liquid phase) with the odorous compounds (gas phase), which are absorbed into the liquid solution (Fig. 1.10).

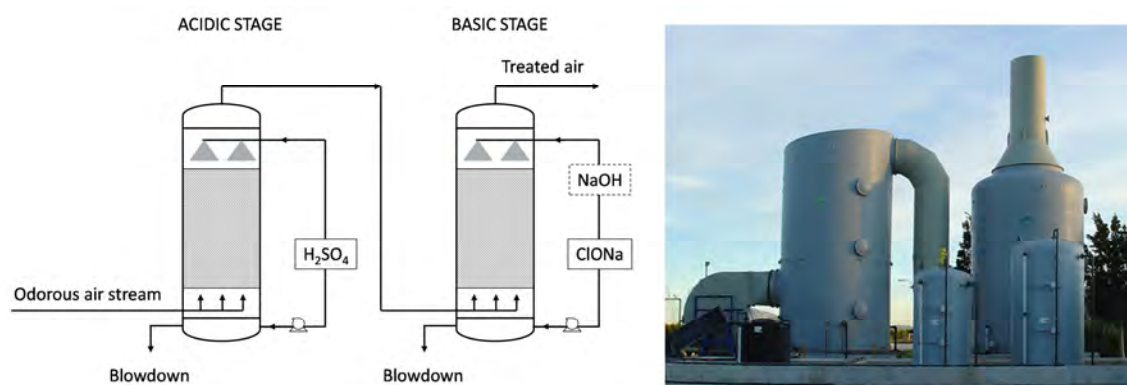


Figure 1.10 Diagram of chemical scrubber

The two-stage packed tower scrubber is the most common configuration for odour treatment. This design is composed by a first acidic stage where nitrogenated compounds are removed and a second basic stage where the neutralisation of sulphur compounds takes place. Moreover, many facilities use an oxidant with a pH control in order to maintain a pH of 8 - 9 and thereby avoiding the formation of odorous by-product (Card 2001). Chlorine, potassium permanganate or hydrogen peroxide are common scrubbing solutions applied for the removal of sulphur compounds in a second stage. Among them, the most widely applied scrubbing chemicals are chlorine in various forms (hypochlorite, chlorite, or even chloride dioxide). Nevertheless, the chlorine-based systems involve the formation of harmful by-products such as chloroform (Myslinski et al., 2000; Lin and Chang, 2005). In order to avoid this drawback, hydroxyl radicals generated via advanced oxidation processes (AOPs) are used as oxidants in advanced oxidation scrubbers (AOSs) instead of traditional oxidants.

The AOPs is a set of chemical reaction which involve the generation of free radicals ($^{\bullet}\text{OH}$, $\text{O}_2^{\bullet-}$, HO_2^{\bullet}), especially hydroxyls radicals ($^{\bullet}\text{OH}$). This radical is the most powerful oxidising species after fluorine (2.8 and 3.0 V, respectively) (Table 1.5), oxidising the most part of organic compounds in aqueous solutions with high reaction rate constants, usually in the order of $10^7 - 10^{10} \text{ M}^{-1} \text{ s}^{-1}$ (Von Gunten, 2003). Chemical oxidation aims at the mineralisation of the organic compounds to carbon dioxide, water and inorganic compounds.

Table 1.5 Oxidation potential of common oxidants (Metcalf, 2003)

Oxidant	Oxidation potential (V)
Fluorine	3.0
Hydroxyl radical	2.8
Ozone	2.1
Hydrogen peroxide	1.8
Potassium permanganate	1.7
Chlorine dioxide	1.5
Chlorine	1.4

Despite the hydroxyl radical is extremely unstable, it must be generated continuously through chemical or photochemical reactions (Esplugas et al., 2002). The wide variety of systems which can generate radicals (Table 1.6) entails to the versatility of these processes (Andreozzi et al., 1999).

Table 1.6 Technologies-based AOPs for water treatment. Adapted from (Prados-Joya, 2010)

Non-photochemical processes	Photochemical processes
<ul style="list-style-type: none"> • Supercritical water oxidation • Fenton reaction ($\text{H}_2\text{O}_2/\text{Fe}^{2+}$) • Electrochemical oxidation • Radiolysis • Non-thermal plasma • Ultrasound • Ozonation 	<ul style="list-style-type: none"> • Photolysis (UV) • UV/H_2O_2 • Photo-Fenton (UV/$\text{H}_2\text{O}_2/\text{Fe}^{2+}$) • UV/$\text{O}_3$ • Heterogeneous catalysis

The odorous compounds removal by means of AOPs has been widely investigated in the field of drinking waters (Peter and Von Gunten, 2007; Matilainen and Sillanpää, 2010; Jo et al., 2011). Nevertheless, the application of these techniques as AOSs for odour compounds removal has been less investigated. Relevant studies about odour removal by AOSs are presented in Table 1.7. All of listed studies are focused on the optimisation of a single AOP to remove target compound. **Nevertheless, a comparative study of different AOPs in order to ascertain the most suitable treatment to be coupled in a wet scrubber has not been carried out yet.**

Table 1.7 Relevant studies about odour compounds removal by wet scrubber using AOPs

Compound	AOP Features	Findings	Reference
DMDS 0.025 mg L ⁻¹	H ₂ O ₂ /Fe ²⁺ [H ₂ O ₂]= 5-50 mg L ⁻¹ [Fe ²⁺]=0.1-1 mg L ⁻¹ T=20-60 °C; pH=3	100% oxidation t=10 min [H ₂ O ₂]= 50 mg L ⁻¹ [Fe ²⁺]=1 mg L ⁻¹ T=60 °C	(Krüger et al., 2009)
Methanethiol (MTM) 50 mL m ⁻³	UV/TiO ₂ UV=365 nm TiO ₂ = 0-4 g L ⁻¹ pH= 6.8-12.5 flow _{MTM} = 5-25 g m ⁻³ h ⁻¹	> 95% oxidation pH=11.5 TiO ₂ =2 g L ⁻¹ flow _{MTM} = 10 g m ⁻³ h ⁻¹ OU _E m ⁻³ reduction By-products= CH ₃ SO ₃ ⁻ , SO ₄ ²⁻	(Liu et al., 2010)
Terpens	H ₂ O ₂ /Fe ³⁺ [H ₂ O ₂]= 100-1000 mg L ⁻¹ [Fe ²⁺]=0-2000 mg L ⁻¹	80% OU _E reduction pH=2.5 [H ₂ O ₂]= 1000 mg L ⁻¹ [Fe ³⁺]= 400 mg L ⁻¹	(Tambosi et al., 2006)
Toluene 930 mL m ⁻³	UV/ H ₂ O ₂ /Fe ²⁺ UV=325 nm [H ₂ O ₂]= 190-2000 mg L ⁻¹ [Fe ²⁺]=0-50 mg L ⁻¹	61% oxidation [H ₂ O ₂]= 630 mg L ⁻¹ [Fe ³⁺]= 20 mg L ⁻¹ By-products not detected	(Tokumura et al., 2012)
DMDS	O ₃ /H ₂ O ₂ [H ₂ O ₂]= 0-1000 mg L ⁻¹ [O ₃]=0-20 mg L ⁻¹ pH=4-11	33% oxidation H ₂ O ₂ /O ₃ ratio = 1.5 pH=8	(Biard et al., 2009)

From all of existing AOPs, UV/H₂O₂, Fenton, photo-Fenton and ozonation were selected to be assessed in this thesis. The fundamentals of each technology are explained below.

1.3.1.1. UV/H₂O₂ process

Photolysis of hydrogen peroxide cleaves the O-O bond to generate two hydroxyl radicals for each H₂O₂ molecule (Eq. 1.1). The concentration of H₂O₂ has to be higher for adequate radical formation due to their low molar extinction coefficient at 254 nm. Nevertheless, it should be emphasised that at high concentrations, hydrogen peroxide can act as scavenger and therefore, reducing the possibility of oxidation (Eq. 1.2) (Andreozzi et al., 1999).



1.3.1.2. Fenton process (H₂O₂/Fe²⁺)

In the Fenton process, the reaction between dissolved Fe²⁺ and H₂O₂ in acidic conditions leads to oxidation of Fe²⁺ to Fe³⁺ and the formation of hydroxyl radicals (Eq. 1.3). This reaction is spontaneous and occurs without the influence of light (Fenton,

1894; Walling, 1975). Moreover, Fe^{3+} is then reduced back to Fe^{2+} by another molecule of H_2O_2 (Eq. 1.4).



1.3.1.3. Photo-Fenton process (UV/ H_2O_2 / Fe^{2+})

Photo-Fenton reaction occurs when Fe^{3+} catalyses the formation of hydroxyl radicals by means of the irradiation of UV light (Eq. 1.3 and 1.5)



Hence, iron becomes cycled between the Fe^{2+} and Fe^{3+} oxidation states and two moles of hydroxyl radicals should be produced per mole of H_2O_2 consumed.

1.3.1.4. Ozonation process

Ozonation process is carried out through two reaction pathways: i) direct reaction with molecular ozone and ii) decomposition of ozone which is favoured by alkaline conditions, and therefore the formation of hydroxyl radicals (Eq 1.6-1.10) (Weiss, 1935; Staehelin and Hoigne, 1985)



1.3.2 Adsorption

In broad terms, adsorption can be defined as a surface phenomenon that consists of the removal of one or more components present in a liquid or gas phase (adsorbates) by concentrating them on the surface of a solid (adsorbent) (Siegell, 1996; Moretti, 2002) (Figure 1.11). Adsorption studies have been conducted on various types of inorganic adsorbents, such as zeolite, alumina, or silica (Cheremisinoff and Ellerbusch, 1980). Nevertheless, the most important adsorbent used for this purpose is activated carbon (AC).

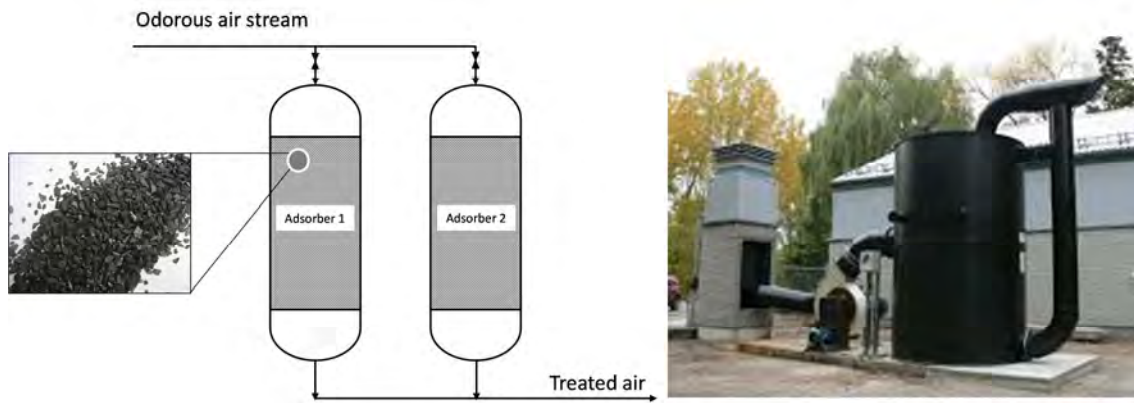


Figure 1.11 Diagram of AC adsorber

One of the main characteristics of AC is its porous structure due to the presence of elementary crystallites of graphite stacked in random orientation, being the porosity the space between these graphitic microcrystallites (Ruthven, 1984). Thus, different sizes of porous can be achieved in the carbonaceous matrix. Micropores, which have diameters less than 2 nm, are responsible for the high surface area and its high adsorption capacity. Mesoporous (2-50 nm) play an important role in the adsorption of large molecules and together with macroporous (> 50 nm), act as access channels to the microporous network (Rodríguez-Reinoso and Linares-Solano, 1989).

Furthermore, the AC structure contains heteroatoms such as oxygen, nitrogen and sulphur which can be bounded to the edges of the graphene layers creating a variety of surface functional groups. The presence of all of these heteroatoms influences the chemical properties of the AC, specially the presence of oxygen groups (Figure 1.12).

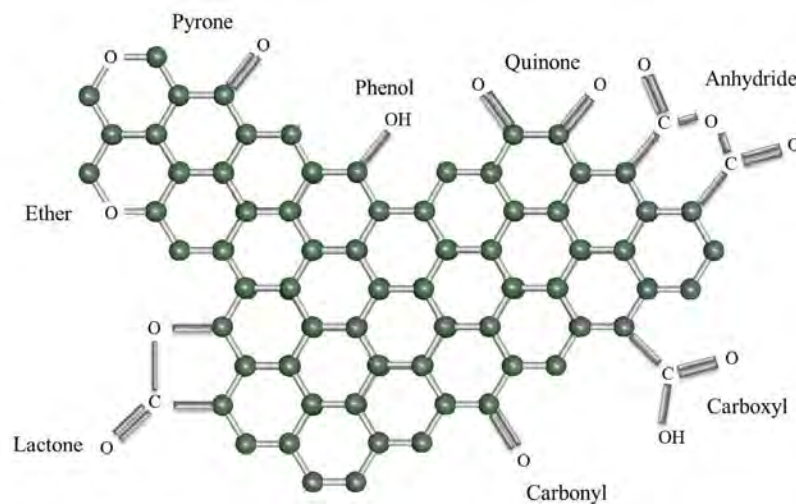


Figure 1.12 Oxygen functional groups in ACs surface.

Structural complexity and chemical composition of AC is developed during the preparation process and is strongly influenced by the type of precursor used. Almost all materials with high carbon content can be used as a precursor for the preparation of AC. However, anthracite, coal, lignite, shells or wood are most commonly used as a precursors. In order to develop the porosity of these materials, chemical or physical activation methods are required (Marsh and Rodríguez-Reinoso, 2006).

Physical activation consists of the carbonisation of the precursor and the subsequently gasification process at high temperatures in the presence of activating agents such as CO_2 or steam. On the other hand, the carbonisation and activation of the precursor takes place simultaneously in the chemical activation. This process consists of mixing the precursor with an activating agent such as ZnCl_2 , H_3PO_4 , KOH or NaOH prior to the thermal treatment.

The characteristics of an adsorption system depend on the chemical nature of the compound to be removed or recovered, on the physical characteristics of the inlet flow (temperature, pressure, and volume), and on the physical and chemical characteristics of the adsorbent. Given the importance of ACs characteristics, several authors have investigated techniques to modify the chemical properties of ACs in order to improve their performance (Bashkova and Bandosz, 2009; Gonçalves et al., 2011, Li et al., 2011).

The most commonly applied methodology for the modification of the AC surface is the use of oxidising agents, either in liquid phase by HNO_3 (Pradhan et al., 1999; Domingo-García et al., 2000), H_2O_2 (Domingo-García et al., 2002; Pereira et al., 2003) or $(\text{NH}_4)_2\text{S}_2\text{O}_8$ (Moreno-Castilla et al., 1997; Lopez-Ramon et al., 1999) or in gas phase with ozone (Mawhinney and Yates Jr, 2001; Valdés et al., 2002; Kohl et al., 2010). Through all of these treatments, acid surface groups such as carboxylic, anhydrides, lactones and phenolic groups are mainly incorporated on the AC surface.

Different comparative studies demonstrated that $(\text{NH}_4)_2\text{S}_2\text{O}_8$ and HNO_3 fix a great amount of acidic oxygen-containing surface groups (Moreno-Castilla et al., 1995; Berenguer et al., 2012). H_2O_2 treatments lead to a slight increase in oxygenated functional groups and these fixations depends on the hydrogen peroxide concentration used in the treatment (Domingo-Garcia et al., 2002).

Regarding to textural properties, all of these treatments affects the porosity of the ACs, being the $(\text{NH}_4)_2\text{S}_2\text{O}_8$ and H_2O_2 treatments which involve less changes on textural properties. Conversely, HNO_3 treatment leads to an important loss of porosity of the materials. This fact is explained by the strong experimental conditions (higher acidic conditions and temperature) which cause the destruction of pore walls (Pereira et al., 2003).

The effect of ozone oxidation on the textural properties of AC has been investigated by several authors. Some of them stated that ozone causes a slight increase on surface area of AC (Tsunoda et al., 1998), whereas other observed noticeable decreases in AC porosity (Valdés et al., 2002; Kawamoto et al., 2005). Different effects are explained by the applied ozone dose: an increase of surface area is promoted by low dose of ozone due to carbon gasification, while high doses of ozone destroy pore walls and fix oxygen functional groups at the entrance of microporous, reducing the surface area (Valdés et al., 2002; Li et al., 2003).

Several authors have investigated alternative methods such as radiation or plasma in order to minimise the modification of physical properties. Tang et al. (2007), Gu et al. (2009) and Velo-Gala et al. (2013) demonstrated that the application of these methods fix oxygen functional groups without modifying significantly the AC textural properties.

Given distinctive features of AC, its application has been extensively investigated to remove a variety of odorous compounds such as nitrogen derivatives (Le Leuch and Badosz, 2007; Canals-Batlle et al., 2008), ketones (Cal et al., 1997; Anfruns et al., 2011) and hydrocarbons (Kawasaki et al., 2004; Lillo-Ródenas et al., 2005). Relevant studies on the adsorption of odorous sulphur compounds are presented in Table 1.8. In all listed studies, the modifications by oxidation or impregnation allow to increase the AC adsorption capacities. **However, the role of oxygen-containing surface groups onto AC in VSC adsorption process has not been investigated in depth.** This knowledge would be helpful for a future design of tailor-made adsorbents.

Table 1.8 Relevant studies on the adsorption of target odorous compounds at low concentration. (NS: not specified; ACF: activated carbon fibers, CNT: carbon nanotubes, GAC: granular activated carbon, ACC: activated carbon cloth, OMC: ordered mesoporous carbons, S_{BET} : BET surface area, $V\text{-DR}_{\text{N}_2}$: volume of micropores obtained by applying the Dubinin-Radushkevich equation to the N_2 adsorption isotherms, VSC: volatile sulfur compound, x/M : adsorption capacity.)

Type of AC	Modification	Test method	S_{BET} ($\text{m}^2 \text{g}^{-1}$)	$V\text{-DR}_{\text{N}_2}$ ($\text{cm}^3 \text{g}^{-1}$)	VSC	[VSC] (ppmv)	Flow (mL min^{-1})	x/M (mg g^{-1})	Reference
AC ACF	None	Static	792-1175	NS	DMS	NS	-	189 - 256	Goyal et al. (2008)
AC	Impregnation (Fe)	Dynamic	1253 - 865	0.481 - 0.601	DMS	1.4	326	0.75 - 0.8	Cui and Turn (2009a)
AC	Impregnation (NaOH, KOH, $\text{Na}_2\text{CO}_3, \text{K}_2\text{CO}_3$)	Dynamic	NS	NS	MTM	20-200	2000-10000	16-53	Tsai and Hsu (1999)
AC	Cu impregnation	Dynamic	624-1230	0.318-0.651	MTM	350	70	NS	Kim and Yie (2005)
OMC	Thermal	Dynamic	1349-1599	0.564-0.604	MTM	350	70	34 - 47	Kim et al. (2005)
GAC ACF	None	Static	1200-1760	0.42 - 0.7	ETM	NS	NS	158-560	Boulinguez and Le Cloirec (2010)
ACF	None	Dynamic	NS	NS	H_2S MTM DMS	3-200	490-1200	NS	Katoh et al (2010)
AC	NaOH, KOH, $\text{Na}_2\text{CO}_3, \text{K}_2\text{CO}_3$ impregnation	Dynamic	NS	NS	H_2S MTM	20-200	2000-10000	50-52	Tsai and Hsu (1999)
GAC	HNO_3 , NaOH oxidation	Dynamic	NS	NS	MTM DMDS	300	100	50-400	Lee et al. (2010)
AC	Oxidation ($\text{HNO}_3, \text{H}_2\text{O}_2$) Impregnation (NaOH, KOH, Fe, Cu, Zn)	Dynamic	NS	NS	H_2S MTM ETM DMS DMDS	0.06-0.4	4000	< 5	Cui et al. (2009b)

2

OBJECTIVES

The main motivation of this thesis is to study the **minimization and abatement of volatile sulphur compounds in sewage sludge processing**. In this light, the main objective is to minimise the volatile sulphur compounds emissions from the beginning of the sludge process and their subsequent abatement through the end-of-pipe technologies. To achieve this, the main objective has been divided into the specific goals:

- To identify the main odour-causing compounds emitted in the sewage sludge drying process at low temperature.
- To ascertain the effect of conditioning process on the reduction of volatile sulphur compounds and odour emissions, as well as the improvement in sludge dewaterability.
- To assess the effectiveness of advanced oxidation process as end-of-pipe treatment for the oxidation of volatile sulphur compounds, as well as to evaluate the economic feasibility of these treatments to be coupled in a wet scrubber.
- To investigate the effect of surface chemical properties and the effectiveness of activated carbons in the adsorption of volatile sulphur compounds at low concentration.
- To assess the effectiveness of activated carbon for volatile sulphur compounds removal under wet conditions and with the presence of oxygen.

MATERIALS & METHODS

3.1 EXPERIMENTAL PROCEDURES

3.1.1 Sewage sludge drying process

3.1.1.1. Lab-scale drying process

Sewage sludge drying process at lab-scale was carried out using the experimental set up shown in Figure 3.1. Dewatered sludge with a dry solid content of 35% was used in drying process. 40 g of dewatered sludge was extruded and placed in the drying reactor which was equipped with a steel basket inside it. In order to carry out the drying process, a heat gun supplied a hot air flow of 445 mL min^{-1} at 90°C to the reactor through the diffusers for 1 hour. The reactor outflow was conducted by condensers to the nalophane bags where the gas sample was collected for odour and VSC analysis. Thus, the sample was analysed both combining analytical and olfactometry methods.

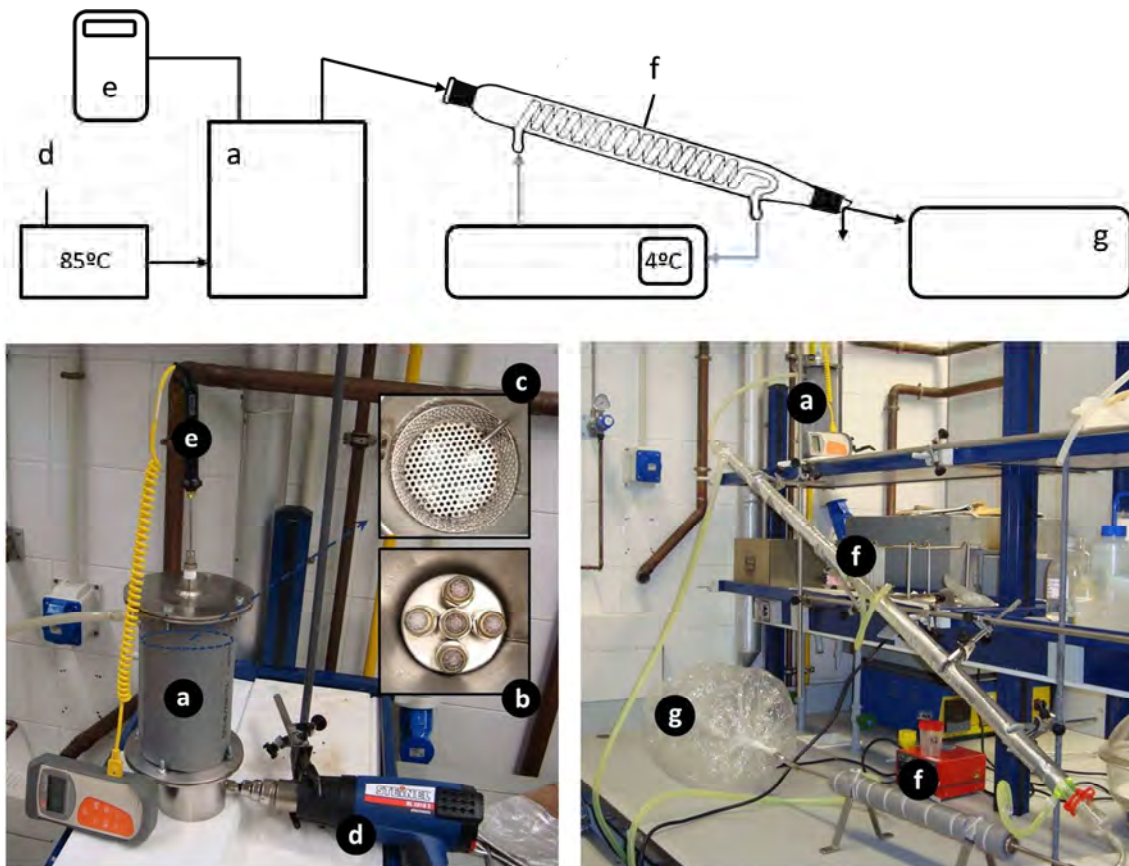


Figure 3.1 Experimental set-up of drying process: a) drying reactor; b) diffuser; c) basket; d) heat gun; e) temperature sensor; f) condenser; g) nalophane bag

3.1.1.2. Full-scale drying process

Three sampling campaigns were performed in a real sewage sludge drying plant in order to check the reproducibility of the results and study the presence of VSC in the

line of gas treatment. A diagram of the sludge drying process and the odour abatement technologies in the studied facility are presented in Figure 3.2.

Dewatered sludge with a dry solid content of 35% is conducted to the belt drying system. Sludge is extruded and placed in a system of conveyor belts where the sludge is dried by hot air until it reaches a 90% of dry solid content. The extracted air from the belt drying system is drawn into a system of chemical scrubbers which have acid, alkaline and neutral stages. Afterwards, the chemical scrubber outflow is treated by a biofilter packed with oyster shells and finally, the outflow is emitted to the atmosphere. All samples were collected with nalophane bags which were maintained closed until its subsequent analysis.

The inflow of chemical scrubbers (1) and biofilters (2) and the outflow of biofilters (3) were established as sampling point. Collected samples were analysed by chromatography methods as well as olfactometric methods. The sampling points are marked in Figure 3.2 with coloured stars.

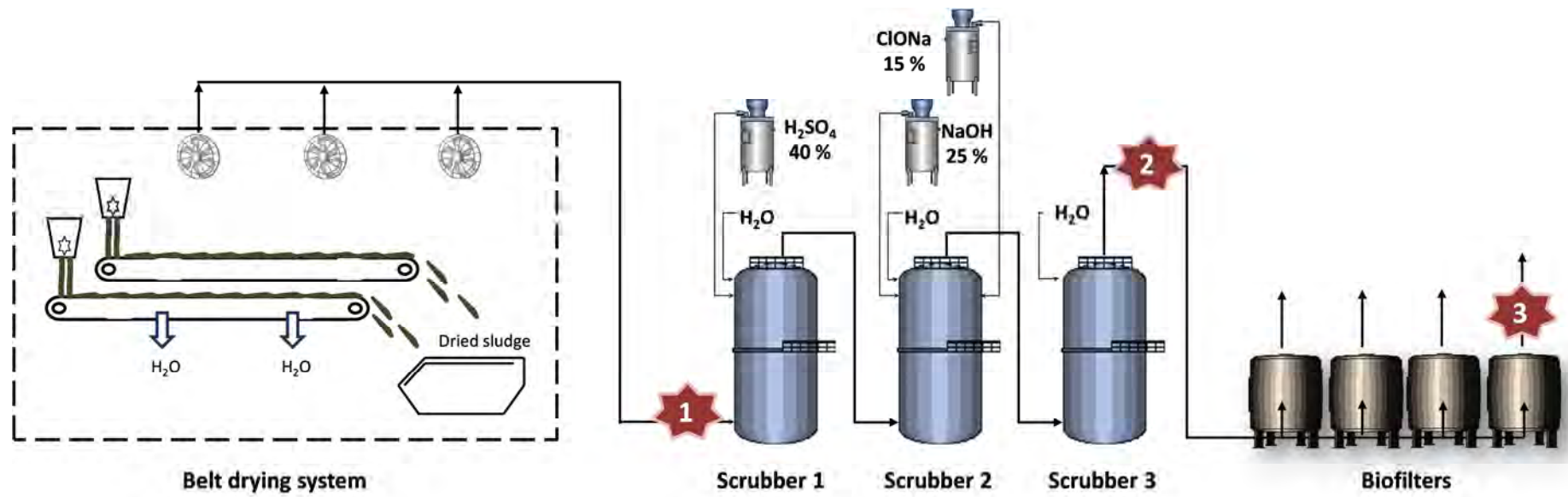


Figure 3.2 Diagram of sewage sludge treatment plant

3.1.2 Sewage sludge conditioning process

3.1.2.1. Chemical conditioning

A mixture of sludge (pH= 6.1, TSS = 39800 mg L⁻¹, VSS = 10090 mg L⁻¹) collected from primary and secondary thickener tanks from a WWTP (Girona, Spain) was used in conditioning process studies. For sludge conditioning, a commercial cationic polyelectrolyte solution of 1% (w/w) purchased from Snf Floerger Ibérica, iron chloride solution (FeCl₃) of 30% (w/w) and calcium oxide (CaO) supplied by Sharlau (Spain) were used.

Chemical conditioning was conducted at room temperature by means of the addition of the studied conditioner at different doses. The chemical dosage was expressed as gram of chemical per kilogram of dry solids (g Kg DS⁻¹). The ranges of conditioners used in the conditioning tests were selected based on preliminary experiments and the literature: polyelectrolyte dose 0-10 g Kg DS⁻¹, iron chloride 0-60 g Kg DS⁻¹ and calcium oxide 0-100 g Kg DS⁻¹ (Turovskiy and Mathai, 2006).

Once the different doses were established, designed experiments were carried out. 300 mL of sludge sample was homogenised using a jar test at 150 rpm for 5 min. The iron chloride and calcium oxide doses were added separately prior to polyelectrolyte according to the methodology proposed by Higgins (2010). Once the iron chloride and calcium oxide were added, the sample was mixed for 30 seconds at 200 rpm. Afterwards, the polyelectrolyte was slowly added and mixed for 30 seconds at 200 rpm and then 90 seconds at 50 rpm.

The dewatering process was carried out using 50 mL of the conditioned sludge, which were placed into plastics cells and were centrifuged (R380, Hettich Instrument) at 3000 xg during 30 minutes. 30 gr of the sludge cake sample, which contains 18% of DS, were extruded (6 mm) and placed in a glass bottle (1L) and were capped with a rubber septum. Then, the sludge cake sample was heated at 85°C for 1 hour in order to reproduce the temperature conditions in the sludge drying process at low temperature. The gas phase obtained in the heating process was analysed, both combining analytical and olfactometry methods.

The addition of chemical conditioners in sludge conditioning were carried out according to the response surface methodology (RSM) which is a set of mathematical and statistical techniques that are suitable for the modelling and analysis of problems in which a response of interest is influenced by several variables and optimise this response (Montgomery, 1996). The most common design under RSM is central composite design (CCD) which fit a model by least squares techniques. Thus, CCD was used to evaluate the combined effects of the three studied independent variables (polyelectrolyte, iron chloride and calcium oxide doses). Table 3.1 lists the range and

levels of the three studied independent variables which were converted to dimensionless ones (X_1 , X_2 , X_3).

Table 3.1 Range and levels of the three independent variables used in RSM.

Variable	Code	Coded levels of variables		
		Low level (-1)	Center (0)	High level (+1)
Polyelectrolyte (g Kg DS ⁻¹)	X_1	0	5	10
FeCl ₃ (g Kg DS ⁻¹)	X_2	0	30	60
CaO (g Kg DS ⁻¹)	X_3	0	50	100

Moreover, the low, center and high levels of each variable are denoted according to the face centered CCD as -1, 0, and +1, respectively. For statistical analysis, the independent variables are codified and converted into dimensionless values in order to compare variables with different units and decrease the error in the polynomial fit according to Eq. 3.1.

$$x_i = \frac{X_i - X_0}{\Delta X} \quad (3.1)$$

where x_i is the dimensionless coded value of the i^{th} independent value, X_0 is the value of X_i at center point and ΔX is the step change value (Mohajeri et al., 2010). Twenty experiments, including five replicates at center point to get a good estimate of the experimental error (Wan and Hameed, 2011), were required for a complete set of the experimental design. The experimental design matrix is presented in Table 3.2.

Table 3.2 Experimental design matrix for optimisation sludge conditioning using RSM (X_1 : polyelectrolyte; X_2 : FeCl; X_3 : CaO [g Kg DS⁻¹])

Trial	Variable		
	X_1	X_2	X_3
1	5	30	50
2	10	60	100
3	5	30	50
4	5	30	0
5	0	60	0
6	5	30	100
7	0	0	0
8	5	60	50
9	10	60	0
10	5	30	50
11	0	0	100
12	5	30	50
13	5	30	50
14	10	0	0
15	5	30	50
16	0	30	50
17	5	0	50
18	10	0	100
19	0	60	100
20	10	30	50

A multiple regression analysis of experimental data was carried out to calculate the coefficients of the second order polynomial equation (Eq. 3.2) proposed to correlate the response of three variables (polyelectrolyte, iron chloride and calcium oxide doses) (Montgomery, 1996):

$$Y = \beta_0 + \sum \beta_i x_i + \sum \beta_{ii} x_i^2 + \sum \sum \beta_{ij} x_i x_j \quad (3.2)$$

where Y is the predicted response (sulphur emission, odour emission and CST), $\beta_0, \beta_i, \beta_{ii}$ and β_{ij} are the constant, linear quadratic and interaction coefficients, respectively, and x_i and x_j are the coded independent variables. The response surfaces were developed by the fitted quadratic polynomial equation. Analysis of variance (ANOVA) and regression analysis were carried out using Design-Expert software version 6.0.7 (Stat-Ease Inc., Minneapolis, USA). Figure 3.3 shows the design of experiments in RSM.

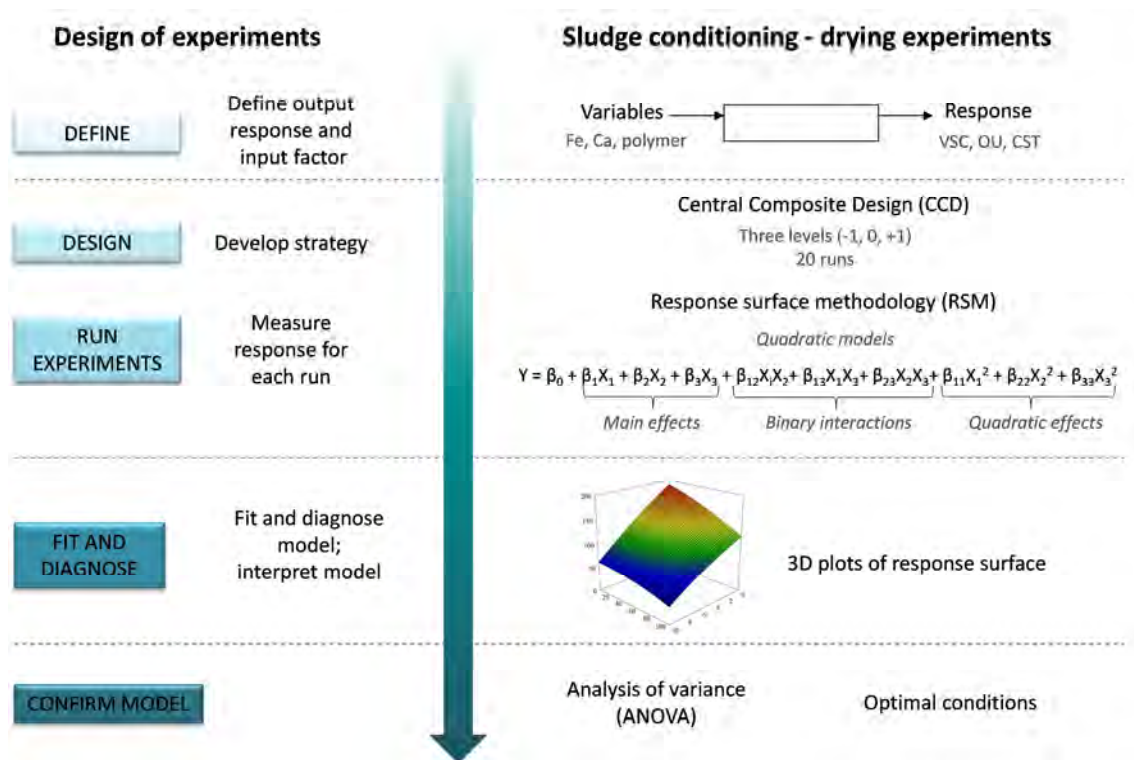


Figure 3.3 Design of experiment in RSM. Adapted from (Witek-Krowiak et al., 2014)

3.1.2.2. Physical conditioning process

Sewage sludge physical conditioning was carried out with the same thickened sludge used in chemical conditioning. For physical conditioning, a commercial activated carbon (AC) W35 supplied by Norit (USA) and fly ash from the combustion of coal and biomass power station in Tilbury (UK) were used as conditioners.

Physical conditioning was conducted at room temperature by the individual addition of fly ash and AC. The dosage of conditioners was expressed as gram of conditioner per

kilogram of dry solids (g Kg DS^{-1}). The tested ranges were 100 and 300 g Kg DS^{-1} for both conditioners. As performed in chemical conditioning, 300 mL of sludge sample was homogenised using a jar test at 150 rpm for 5 min. AC or fly ash were added and the sample was mixed for 30 seconds at 200 rpm and then 90 seconds at 50 rpm. Dewatering process was carried out in the same way as chemical conditioning which has been detailed in section 3.1.2.1.

3.1.3 Advanced oxidation processes

Ethyl mercaptan (ETM), dimethyl sulphide (DMS) and dimethyl disulphide (DMDS) were selected as target compounds in order to perform the dynamic adsorption test. All liquid compounds with purities higher than 99% were supplied by Acros Organics (Belgium). The main properties of target compounds are listed in Table 3.3.

Table 3.3 Main properties of target compounds

	ETM	DMS	DMDS
Formula	$\text{C}_2\text{H}_6\text{S}$	$\text{C}_2\text{H}_6\text{S}$	$\text{C}_2\text{H}_6\text{S}_2$
Molecular weight	62.13	62.13	94.20
Melting point ($^{\circ}\text{C}$)	-148	-98	-85
Boiling point ($^{\circ}\text{C}$)	35	38	110
Solubility in water at 20 $^{\circ}\text{C}$ (g L^{-1})	15.5	20.8	3
Dipole moment (D)	1.5	1.5	NS

The experimental set-up used in advanced oxidation process is described in Figure 3.4.

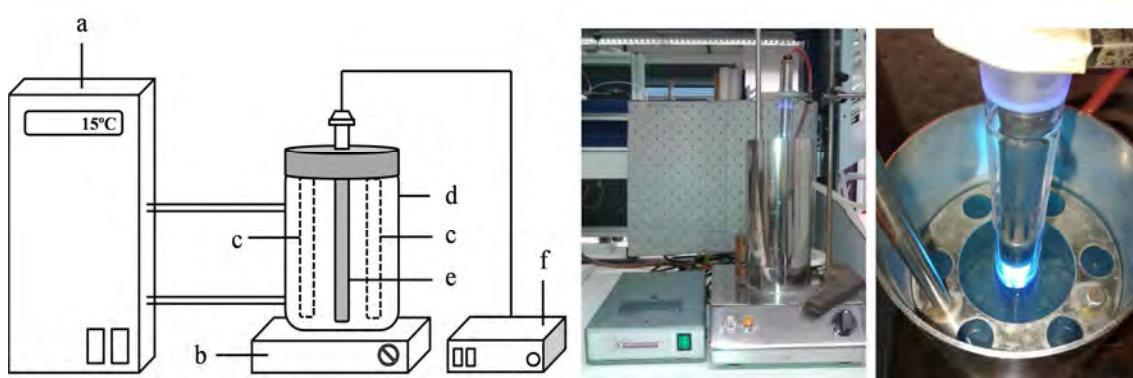


Figure 3.4 Experimental set-up of AOP test: (a) cooling bath; (b) stirrer; (c) cylindrical quartz reactors; (d) steel container; (e) UV lamp; (f) power supply

The steel container can hold up to 6 cylindrical quartz reactors (diameter = 1.8 cm; height = 17.5 cm) which are magnetically stirred and is equipped with a thermostatic bath. The device can also be fitted with a UV lamp in the centre when required. After adding 25 mL of a synthetic multicomponent solution containing 0.5 mg L^{-1} of each VSC (ETM, DMS and DMDS) in distilled water, the cylindrical quartz reactors were capped

with a rubber septum, leaving a headspace volume (HSV) of 5 mL. The gas tightness of the cylindrical reactors was checked. Neither leakage nor permeation were detected since the concentration of the VSC in the HSV remained constant for 30 min. Since the ratio gas-to-liquid volume is low and the solution is stirred, the partition of the VSC among the liquid and gas phases was fast, achieving steady concentration in the HSV is less than 2 min. Furthermore, the analysis of HSV sample revealed that only a small fraction of the VSC initially in solution was transferred to the gas phase (0.4% for ETM and DMDS and 0.3% for DMS). In all oxidation experiments, the oxidant was injected through the rubber septum once the partitioning between liquid and gas phase had reached the steady state.

Photoirradiation experiments (UV/H₂O₂ and UV/H₂O₂/Fe²⁺) were carried out using a low-pressure Hg lamp TNN 15/32 Heraeus (15 W) with a wavelength emission at 254 nm and an irradiation intensity of 0.07 W cm⁻². The filled reactors were distributed equidistant around the UV lamp (at 4 cm) and the reactor area belonging to gas phase was covered with aluminium foil in order to avoid the UV oxidation of the VSC in gas phase during the experiments.

A reactor was taken off from the container every two minutes and the concentration of VSC was determined as explained in analytical procedures. Triplicate experiments were carried out at 15 °C and at free pH (6.7 ± 0.2). In order to compare the oxidative efficiency of the studied treatments, the same molar concentration of both hydrogen peroxide and ozone (0.20 mM) was used. This corresponds to the stoichiometric amount of hydrogen peroxide needed for the complete oxidation of the synthetic multicomponent solution.

The influence of hydrogen peroxide concentration (0.2-4 mM) in the VSC oxidation was tested with UV/H₂O₂ treatment. In the Fenton treatment (H₂O₂/Fe²⁺), the effect of Fe²⁺ concentration (0.004-0.018 mM) was also studied. In the Fenton treatment, the reactors were covered with aluminium foil to avoid the incidence of the natural light during the reaction. Photo-Fenton treatment was performed in a similar way as Fenton treatment but in the presence of UV light and without aluminium foil covering the liquid phase.

The ozone treatment was carried out using the ozone stream, which was generated by ozone generator (Anseros COM-AD-02, Actualia) coupled with Actualia HCM 2003 oxygen concentrator. An ozone flow of 10 g O₃ h⁻¹ was bubbled in water during a certain time until the amount of ozone in solution, which was measured by the colorimetric indigo method, was 9.8 mg L⁻¹ (0.20 mM). After that, the ozone solutions were immediately used in order to avoid the decomposition of the ozone (Lovato et al., 2009). The experimental conditions used for each treatment are summarised in Table 3.4.

Table 3.4 Experimental conditions of the studied AOPs

Treatment	UV	Fe ²⁺ (mM)	H ₂ O ₂ (mM)	O ₃ (mM)
UV/H ₂ O ₂	On	-	0.2-4	-
H ₂ O ₂ /Fe ²⁺	Off	0.004-0.018	0.2	-
UV/H ₂ O ₂ /Fe ²⁺	On	0.018	0.2	-
O ₃	Off	-	-	0.2

3.1.3.1. Cost analysis of AOPs

A cost estimation of different AOPs was calculated taking into account both capital cost (amortised annual capital cost) and operating cost (reagents and electrical cost) according to the methodology proposed by Mahamuni and Adewuyi (2010).

First, pseudo-first order kinetics (k) were estimating using the half-life ($t_{0.5}$, min) of the total sulphur compounds during each reaction according to Eq. 3.3:

$$k = \frac{\ln 2}{t_{0.5}} \quad (3.3)$$

Using k , t_{90} which is defined as the time required for 90% oxidation of VSC was calculated by following Eq. 3.4:

$$t_{90} = \frac{0.9 C_0}{k} \quad (3.4)$$

Volume reactor was calculated from the design flow rate of 3000 L min⁻¹ and considering t_{90} of each treatment. Thus, volume AOP reactor was estimated by multiplying the flow rate with t_{90} .

The energy consumption (E) was considered as energy dissipated per unit volume and was given by Eq. 3.5.

$$E = \text{flow rate} * t_{90} * P \quad (3.5)$$

where P is power density of device, expressed in W L⁻¹. Thus, it was necessary to know the number of such standard commercial units required. The number of device (n device) was calculated by dividing the energy consumption with energy supplied by a single unit of AOP. By these data, the capital cost of AOP reactor was estimated by Eq. 3.6.

$$\text{AOP}_{\text{reactor}} = n \text{ device} * \text{device cost} * R \quad (3.6)$$

where R is the reactor material cost which was calculated using SuperPro Designer 8. From this data, the general calculation of capital cost is presented in Table 3.5.

Table 3.5 General calculations of capital cost. Adapted from (Mahamuni and Adewuyi, 2010)

Item	Cost
AOP reactor	P
Piping, valves, electrical (30%)	0.3 P
Site work (10%)	0.1 P
Subtotal	1.4 P = Q
Contractor (15%)	0.15 Q
Subtotal	1.15 Q = R
Engineering (15%)	0.15 R
Subtotal	1.15 R = S
Contingency (20%)	0.2 S
Total capital	1.2 S

The capital cost is amortised over a span of years at given amortisation rate. Thus, amortised capital cost (A) is given by following Eq. 3.7.

$$A = \frac{1.2S*r}{1 - \left(\frac{1}{1+r}\right)^n} \quad (3.7)$$

Considering the total capital cost is amortised at a rate of 7% (r) over a period of 20 years (n) to arrive at total amortised annual capital cost.

For operating cost estimations, only chemical and electrical costs were taken into account, while labour and analytical costs were underestimated. Annual electrical cost was calculated for each treatment by multiplying E with annual work time and the electricity price. For this calculation, it has been considered that the plant is running 8760 h year⁻¹ and 0.07 € KWh⁻¹ (October, 2013) as the electricity price in Spain. On the other hand, annual chemical cost was estimated by multiplying the volume of treated water in a year with the price of chemical reagents used in the same time. Therefore, the annual operating cost is defined as the sum of annual electrical and chemical cost. Finally, the sum of capital and operating cost and taking into account the volume of treated water in a year, the total annual cost of each AOP was calculated.

3.1.4 Adsorption tests

Figure 3.5 shows the experimental set-up used to carry out the dynamic adsorption test and to determine the adsorption capacities of the studied materials. The stream used in the adsorption test was generated by means of the injection of liquid VSC to a nitrogen stream generated by a compressor (Pintuc, MDR2-EA/11). An adequate amount of liquid VSC (ETM, DMS or DMDS) was injected into nitrogen or oxygen stream using a syringe pump (Harvard Apparatus-PHD 22/2000) equipped with 500 µL, 3.26 mm internal diameter syringe (Gas Tight Series, Hamilton). Moreover, three static mixers were placed before the bed reactor, in order to obtain an adequate mixing of the VSC in stream. The adsorption tests were conducted in a fix-bed reactor, with an

internal diameter of 7 mm. The adsorption bed consisted in 250 mg of AC with bed heights ranging from 0.5-0.6 cm, depending on the tested adsorbent material. The inlet flow was set to 250 mL min⁻¹ using a mass flow controller (Alicat Scientific model: MC-500SCCMM-D).

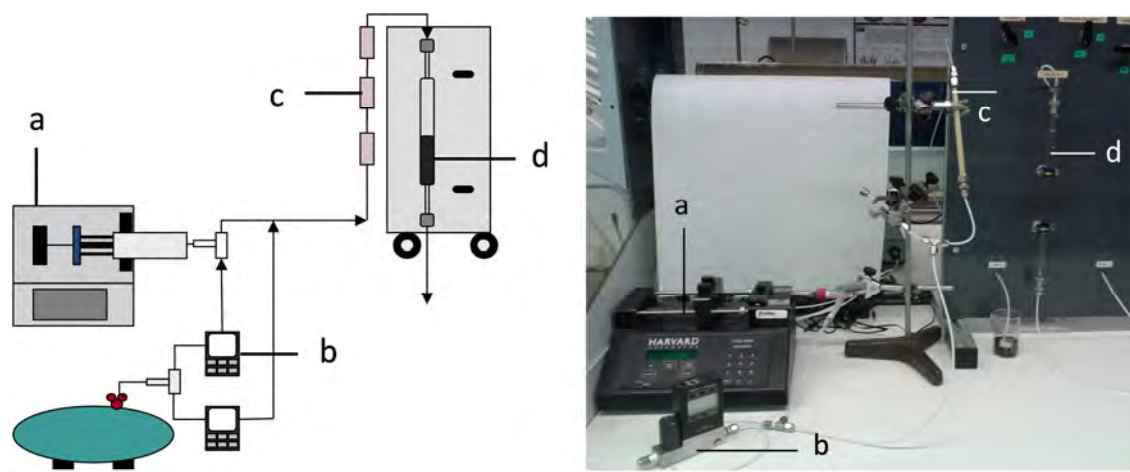


Figure 3.5 Experimental set-up of dynamic adsorption test: a) syringe pump; b) mass flow controller; c) static mixer; d) adsorption bed reactor

3.1.4.1. Adsorption capacities

The adsorption tests of oxidised chemical ACs were carried out at 20 ± 2 °C until the studied sulphur compound outlet concentration matched the inlet concentration. As a result of plotting the concentration of VSCs vs. time, the breakthrough curves were obtained. The adsorption capacity (x/M , mg of VSC g⁻¹ of adsorbent) for each VSC/adsorbent system was calculated using Eq. 3.8:

$$\frac{x}{M} = \frac{QM_W}{\omega V_M} \left(c_{in}ST - \int_0^{ts} c_{out}(t)dt \right) \quad (3.8)$$

where Q is the inlet flow (m³ s⁻¹), M_w is the VSC molecular weight (mg mmol⁻¹), ω is the adsorbent weight (g), V_M is the ideal molar gas volume (ml mmol⁻¹), c_{in} is the VSC inlet concentration (ppm, v/v), ST is the bed exhaustion time (s) and $c_{out}(t)$ is the VSC outlet concentration (ppm, v/v) at a given time. Moreover, the breakthrough time (BT) which is defined as the time when the ratio of C_{out}/C_{in} is higher than 0.05, was also calculated. Experiments were carried out by triplicate and typical errors were below 10% of the reported mean values.

Unlike the previous tests, the adsorption capacities of irradiated ACs were calculated until the olfactometric breakthrough time which is defined as the time at which the breakthrough concentration (C_B) is reached. C_B was calculated according to the Eq. 3.9 (CEN, 2003):

$$C_B = D \cdot OT_{VSC} \quad (3.9)$$

where D is the maximum odour concentration of a mixture (dimensionless odour units (OU m⁻³)). According to the German regulation for WWTPs on air pollution control (TA Luft, 2002), the established value for D was 500 OU m⁻³. OT_{VSC} is the odour thresholds of each VSC (0.001, 0.0025 and 0.00033 mg m⁻³ for DMDS, DMS and ETM, respectively) (Van Gemmert, 2003).

3.1.4.2. Computational details: COSMO-RS

The molecular geometry of all compounds (ETM, DMS, DMDS and AC models) was optimised at the B3LYP/6-31++G** computational level in the ideal gas phase using the quantum chemical Gaussian03 package (Frisch et al., 2004). Vibrational frequency calculations were performed in each case to confirm the presence of minimum energy. Once the molecular models were optimised, Gaussian03 was used to compute the COSMO files. The ideal screening charges on the molecular surface for each species were calculated by the continuum solvation COSMO model using BVP86/TZVP/DGA1 level of theory. Subsequently, COSMO files were used as an input in COSMOthermX (2001) code to calculate the Henry's laws constant of VSCs for different AC models. According to the chosen quantum method, the functional and the basis set, the corresponding parameterisation (BP TZVP C21 0108) was used for COSMO-RS calculations in COSMOtherm code. The three VSCs and different molecular models of simulated AC with a wide variety of functional groups are depicted in Figure 3.6. ACs functionalised with hydrogen bond (HB)-acceptor surface oxygen groups, such as carboxylic anhydride and carbonyl groups, and HB-donor groups, such as hydroxyl and carboxylic acids, were simulated.

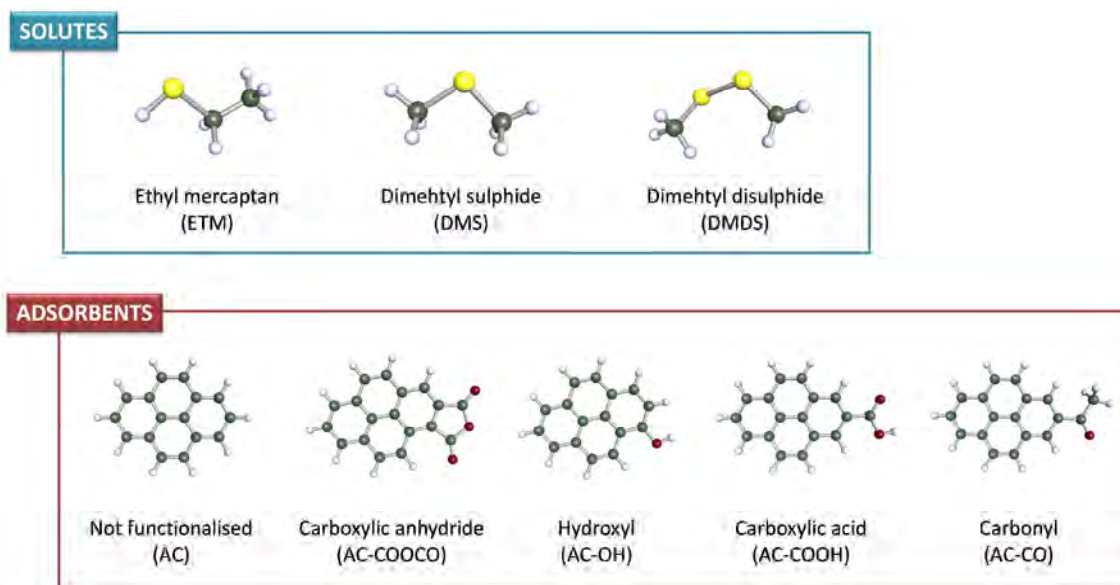


Figure 3.6 Individual molecules of sulphur solutes and molecular models for five different oxidative functionalization of ACs.

Henry's constants of these solutes were used as reference parameter for affinity predictions. The numerical value of Henry's constant is reversely proportional to the predicted concentration of VSC retained in the AC phase, following the Eq. 3.10:

$$K_H = \frac{P_{eq_{Gas}}^{VSC}}{x_{AC}^{VSC}} \quad (3.10)$$

where K_H is the Henry's constant, x_{AC}^{VSC} is the mole fraction of the VSC solute in the AC phase and $P_{eq_{Gas}}^{VSC}$ is the partial pressure of VSC compound in the gas phase. Therefore, a lower value of K_H means higher affinity of the adsorbent for VSC.

3.2 ANALYTICAL METHOD FOR DETERMINATION OF VSCs, VOCs AND ODOUR CONCENTRATION

3.2.1 VSC analysis in gas samples

The concentration of VSC in gas phase was determined by gas chromatography (GC) (CP-3800 Varian) equipped with a pulse flame photometric detector (PFPD) using a GS-GasPro column (J&W Scientific) (Figure 3.7). Moreover, the GC is equipped with valves system which fills the sample loop (1 mL) and allows an automatic sampling every 25 min. The experimental conditions of GC/PFPD used to determine the VSC concentration in gas phase are presented in Table 3.6.

Table 3.6 GC/PFPD analytical conditions

Oven Temperature	50°C (1 min), to 230 °C at 20 °C min ⁻¹ , hold for 5 min, to 250 °C at 20 °C min ⁻¹ .	
Column	GS-Gas Pro, 0.32 mm x 30 m (J&W Scientific)	
Carrier gas	Helium, constant flow, 4 mL min ⁻¹	
PFPD Settings	Temperature	200 °C
	H ₂ flow	13 mL min ⁻¹
	Air (1)	17 mL min ⁻¹
	Air (2)	10 mL min ⁻¹
	CMT	650V, trigger level: 200 mV

For the calibration, two certified cylinder (1000 ppmv of H₂S and 50 ppmv sulphur mix (SO₂, MTM, ETM, DMS and DMDS)) were used to prepare the standards in gas phase. The dilution standards were prepared with air as well as nitrogen using a gas mixing system (Envionics, S4000). The obtained calibration curves by plotting the GC/PFPD response against the standard concentration in gas phase are presented in Figure 1A of Annex A.



Figure 3.7 Picture of gas chromatograph (CP-3800)

3.2.2 VSC analysis in liquid samples

The amount of ETM, DMDS and DMS contained in liquid phase was determined by the analysis of headspace using gas chromatography. For the calibration, the same AOP experimental set-up was used. 25 mL of standard solutions with a known concentration of the VSCs were placed in the cylindrical quartz reactors, under the same temperature and stirring conditions used during oxidation experiments. Once the partition equilibrium was achieved (2 min), a sample (100 μL) of the headspace volume was injected in the GC/PFPD. The calibration curves were obtained by plotting the GC/PFPD response against the standard solution concentration in liquid phase (Figure 2A of Annex A). The analytical conditions were the same as used in the gas phase analysis.

3.2.3 VOC analysis in gas phase

In order to identify the volatile organic compounds (VOC) in odorous matrix, the samples were collected using a Carboxen/Polydimethylsiloxane (CAR/PDMS) 75 μm SPME fibre which was exposed to gas sample for 1 hour at 22 $^{\circ}\text{C}$.

The identification of VOC was carried by gas chromatographic analysis with a Trace GC 2000 coupled to PolarisQ ion trap mass spectrometer detector (Thermo Scientific) using a TRB-5 MS capillary column. The split/splitless injection port was equipped with a 0.75 mm ID SMPE liner which operated at 250 $^{\circ}\text{C}$. The experimental conditions of SMPE/GC/MS used to determine the VSC concentration in gas phase are presented in Table 3.7.

Table 3.7 SMPE/GC/MS analytical conditions

Oven Temperature	35 $^{\circ}\text{C}$ (10 min), to 150 $^{\circ}\text{C}$ at 5 $^{\circ}\text{C min}^{-1}$, to 250 $^{\circ}\text{C}$ at 15 $^{\circ}\text{C min}^{-1}$, hold for 2 min,
Column	TRB-5 MS, 0.25 mm x 30 m (Teknokroma)
Carrier gas	Helium, constant flow, 1 mL min^{-1}

3.2.4 Olfactometric analysis

The odour concentration was measured by olfactometric analysis according to the European regulation (CEN, 2003). The dynamic olfactometry is based on a dilution system in which a mixture of odours is diluted with neutral air to be judged by panel composed by four members. Prior to analysis, the calibration of each panel members against a reference gas is required. 123 μg of n-butanol (reference gas) evaporated in 1 m^3 of neutral gas are equivalent to 1 European odour unit (OU_E). This equivalence is the basis for the traceability of odour units for any odorous sample to the reference gas. Thus, 1 $\text{OU}_E \text{ m}^{-3}$ is defined as the odour concentration in the detection threshold, i.e. the odour concentration of odorous sample is measured determining the dilution factor required to reach the detection threshold.

The olfactometric analysis was conducted by dynamic olfactometer BioNose 0208 (Odournet, Barcelona). The odorous sample contained in the nalophane gas was attached to olfactometer which was connected to a cylinder of synthetic air with a pressure of 3 bar. The front panel was positioned at value 5 which provides the highest sample dilution. The value of the front panel was decreasing until the odour was detected by the panel (Figure 3.8). It has to be highlighted that the panel members were calibrated according to CEN (2003) and the individual's average threshold measurement of n-butanol was in the range of 20 – 80 ppbv.

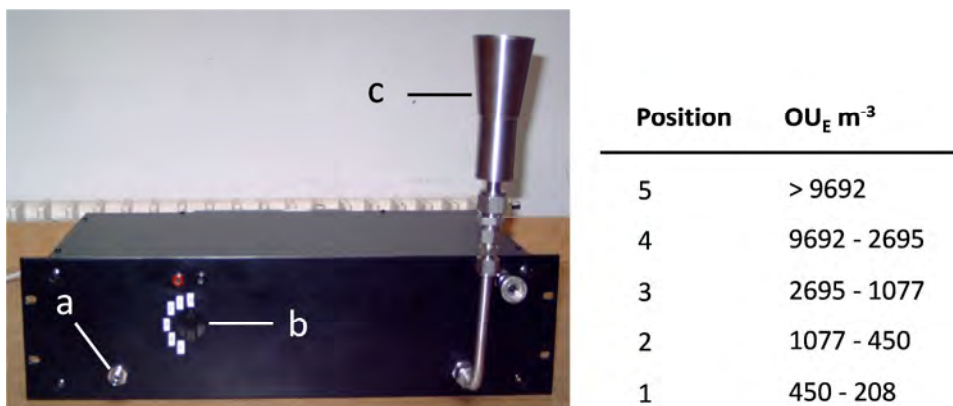


Figure 3.8 Dynamic olfactometer Bionose 0208: a) sample input; b) front panel; c) smell cup

3.3 SLUDGE CHARACTERISATION

3.3.1 Capillary suction time

Capillary suction time (CST) of sewage sludge was measured by CST meter (Triton electronics Ltd, Type 304 B) which consisted in a stainless-steel tube with an inner radius of 1 cm and absorbed papers. 6 mL of sludge were poured into the tube to

guarantee that filtrate would not be exhausted during measurement. CST is defined as the time required to wet the filter paper between radius of 1 and 3 cm (Figure 3.9).

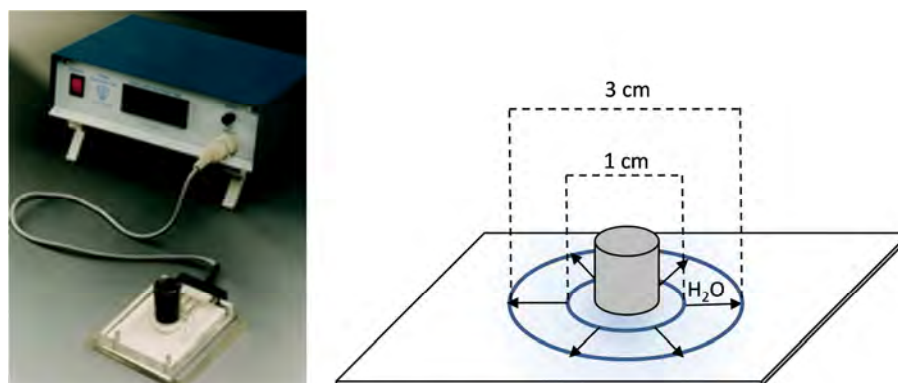


Figure 3.9 Schematic operation of CSTmeter

3.3.2 Extracellular polymeric substances

Extracellular polymeric substances are defined as the set of macromolecules such as carbohydrates, proteins, nucleic acids, lipids and other polymeric compounds which have been found outside the cell surface and in the intercellular space of microbial aggregates (Flemming and Wingender, 2001).

Extraction of extracellular polymeric substances (EPS) was carried out using the thermal methodology established by Forster (1971). According to this method, the samples were separated into two parts: the bound EPS (b-EPS) and the soluble microbial products (SMP). First, 100 mL of sample was centrifuged at 12000 xg during 20 minutes at 4°C (RC 5B PLUS, SORVALL®). The obtained supernatant which contains the SMP was subsequently analysed. The b-EPS was extracted by the pellet resuspension with a NaCl 0.9% solution. The mixture was digested at 100°C during 1 hour (Chang and Lee, 1998) and was centrifuged at 6000 rpm during 30 min. The obtained supernatant, which contains the b-EPS, is subsequently analysed. Figure 3.10 shows the diagram of methodology used in SMP and b-EPS extraction.

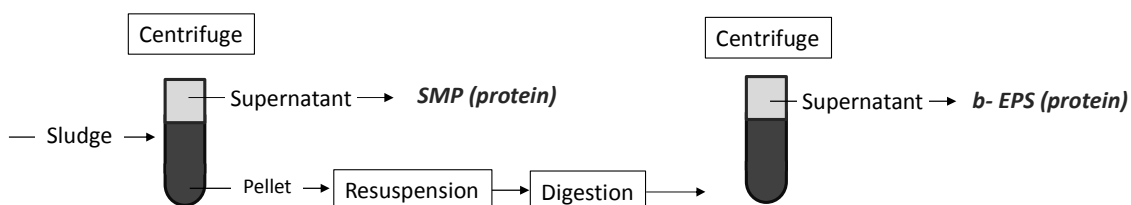


Figure 3.10 Diagram of methodology used in SMP and b-EPS extraction

The protein content of both fractions was carried out measuring the concentration of protein by colorimetric method at 740nm. The protein content was quantified using a Total Protein Kit (TP03000, Sigma-Aldrich), according to the method proposed by Lowry et al. (1951) and modified by Peterson (1977). Standard calibration curve of protein content is presented in Figure 3A of Annex A.

3.4 LIQUID PHASE CHARACTERISATION

3.4.1 Sulphate content

The sulphur content as sulphate (SO_4^{2-} -S) of the liquid samples was analysed at the end of the reaction according to the Standard Methods for the Examination of Water and Wastewater (APHA, 2005) using ion chromatography (IC) (Metrohm 761-Compact) (Figure 3.11). The detection limit of the method is 0.1 mg L^{-1} of SO_4^{2-} -S.



Figure 3.11 Picture of ion chromatography (Metrohm 761-Compact)

3.4.2 Ozone concentration

The concentration of ozone dissolved in water was determined by the colorimetric indigo method developed by Bader and Hoigne (1981). Indigo reagent was prepared by the addition of 20 mL indigo stock solution, 10 g sodium dihydrogen phosphate (NaH_2PO_4) and 7 mL concentrated phosphoric acid in 1L volumetric flask. 1 mL of indigo reagent was added to 9 mL of sample and the absorbance was measured immediately using a spectrophotometer (Thermo Scientific, Genesys 10S UV-VIS).

3.4.3 Hydrogen peroxide concentration

Hydrogen peroxide concentration was determined by colorimetric measurements using a solution of Ti(IV) oxysulfate at 410 nm (Mendham et al., 2000). 0.5 mL of solution of Ti(IV) oxysulfate were added to 10 mL sample and the absorbance was measured immediately using a spectrophotometer (Thermo Scientific, Genesys 10S UV-VIS). Standard calibration curve is presented in Figure 4A of Annex A.

3.4.4 Dissolved iron content

Dissolved iron concentration was determined by photometric measurements at 540 nm using the Spectroquant Iron test (Merck). 3 drops of the reagent were added to 5 mL of sample and the absorbance was measured after 5 minutes of reaction using a spectrophotometer (Thermo Scientific, Genesys 10S UV-VIS). Standard calibration curve is presented in Figure 5A of Annex A.

3.5 ACTIVATED CARBON MODIFICATIONS

Steam activated extruded RB3 carbon supplied by Norit was used as raw material (AC-R) in all adsorption tests. The AC-R was grounded and sieved in order to achieve a particle size lower than 212 μm . All AC samples were dried overnight at 105 $^{\circ}\text{C}$ before being used.

3.5.1 Oxidative chemical treatments

3.5.1.1. Nitric oxidation

Nitric oxidation of AC was carried out by boiling 1 g of AC in 10 mL of a 6 N nitric acid solution during 20 minutes (Calvo et al., 2006). Afterwards, the sample was washed with distilled water until neutral pH and dried overnight at 105 $^{\circ}\text{C}$. The AC sample oxidised with nitric acid was denoted as AC-N.

3.5.1.2. Ozone oxidation

Two different ozone treatments were studied. An oxidation with ozone in gas phase was carried out in which only the ozone was the oxidising species in the AC oxidation. Moreover, an oxidation with ozone in aqueous phase was performed in alkaline conditions. Under alkaline conditions, the OH^- accelerates the ozone decomposition and the consequent production of hydroxyl radicals (Staehelin and Hoigne, 1985; Sotelo et al., 1987; Langlais et al., 1991).

The gas phase oxidation was carried out in a fixed bed reactor loaded with 0.25 g of AC-R. The ozone was produced from pure oxygen (Anseros COM-AD-02, Actualia) with a reaction yield of 95%. A constant flow of 20 $\text{mg O}_3 \text{ min}^{-1}$ was passed through the bed for two different periods of time, 30 and 60 minutes. The samples were denoted as AC-O30 and AC-O60, respectively. Afterwards the samples were dried for 1h at 60 $^{\circ}\text{C}$, 1h at 100 $^{\circ}\text{C}$, 1h at 150 $^{\circ}\text{C}$ and 24 h at 170 $^{\circ}\text{C}$ (Valdes et al., 2003). The gradual was necessary in order to desorb any oxygen molecules adsorbed during the oxidation process.

In order to carry out the ozone oxidation in aqueous phase, 0.25 g of AC-R were mixed with 150 mL of distilled water at pH 10 using NaOH (0.1 M) and a constant flow of 140 $\text{mg O}_3 \text{ min}^{-1}$ was bubbled for 2h. The ozonised sample was washed with distilled water until neutral pH and was dried overnight at 105 $^{\circ}\text{C}$. The final AC sample was denoted as AC-O.

3.5.2 Gamma irradiation treatment

Irradiation studies were performed using a MARK-I gamma irradiator model 30 J (Shepherd & Associates) in the Experimental Radiology Unit of the Scientific Instrumentation Center (CIC) of the University of Granada (Spain) (Figure 3.12). The

equipment includes four ^{137}Cs sources with a total combined activity of 3.70×10^{13} Bq (1000 Ci) and has three irradiation positions for different dose rates: position 1 (3.83 Gy min^{-1}); position 2 (1.66 Gy min^{-1}); and position 3 (1.06 Gy min^{-1}).



Figure 3.12 Picture of gamma irradiator

All irradiations were conducted at a dose rate of 3.83 Gy min^{-1} , administering a total dose of 25 kGy (Velo-Gala et al., 2013). The as-received material (AC-R) was irradiated in the air (in absence of water) by placing 5.0 g of previously dried AC into 15 mL plastic tubes. Irradiation in aqueous solution was conducted by introducing 5.0 g AC into 50 mL plastic tubes and filling them with ultrapure water previously bubbled with N_2 for 1 h. Before the irradiation, samples were bubbled with N_2 to avoid the presence of dissolved O_2 , and the tubes were sealed to prevent entry of air. The interaction of gamma irradiation with water molecules gives rise to multiple highly reactive radical species (Reaction 3.11).



The predominance of specific radiolytic species in the media was obtained by irradiating 5.0 g samples of the ACs in 50 mL plastic tubes under different experimental conditions: i) $1000 \text{ mg L}^{-1} \text{Cl}^-$ and $\text{pH} = 1.0$, because the chloride ion acts as HO^\bullet and e_{aq}^- radical scavenger (Atinault et al., 2008) (Reactions 3.12-3.19) and Reaction 3.20 is favored at this pH (Buxton et al., 1988), producing the predominance of H^\bullet species in the medium; ii) $1000 \text{ mg L}^{-1} \text{Br}^-$ and $\text{pH} = 7.5$, because the bromide ion acts as HO^\bullet radical scavenger, giving rise to Reactions 3.21-3.24 (Ershov et al., 2002; LaVerne et al., 2009; Roth and Laverne, 2011), and Reaction 3.25 is favored at this pH (Buxton et al., 1988), producing the predominance of e_{aq}^- species; iii) $1000 \text{ mg L}^{-1} \text{NO}_3^-$ and $\text{pH} = 12.5$, because Reactions 3.25-3.27 take place under these conditions (Buxton et al., 1988;

Mezyk and Bartels, 1997; Roth and Laverne, 2011), and the nitrate anion acts as H^\bullet and e_{aq}^- scavenger, producing the predominance of HO^\bullet radicals in the medium. Table 3.8 lists the designations of the irradiated ACs.

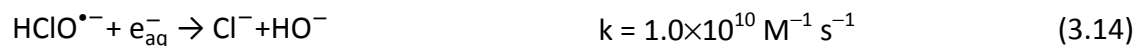


Table 3.8 Designations of the AC samples obtained.

AC designation	Irradiation
AC-R	As-received activated carbon
AC-H	Activated carbon irradiated in the presence of H^\bullet
AC-e	Activated carbon irradiated in the presence of e_{aq}^-
AC-OH	Activated carbon irradiated in the presence of HO^\bullet
AC-0	Activated carbon irradiated in the presence of all radicals
AC-A	Activated carbon irradiated in the air (without water)

3.6 CHARACTERISATION OF ACTIVATED CARBONS

3.6.1 Textural characterisation

3.6.1.1. N₂ adsorption/desorption isotherms

The amount of gas adsorbed on a solid material at different relative gas pressures and constant temperature is defined as the adsorption isotherm. Each point on the isotherm represents the equilibrium between the volume of gas adsorbed and relative gas pressure (P/P_0).

Nitrogen isotherms of adsorbent materials were obtained using a Micrometrics apparatus (Tristar II 3020 model) at $-196\text{ }^\circ\text{C}$ (Figure 3.13). Previously, the samples were outgassed at $150\text{ }^\circ\text{C}$ for 8 h under a vacuum of 10^{-5} Torr. The determination of apparent surface area (A_{BET}) was carried out according to the methodology developed by (Brunauer et al., 1938) and the textural parameters of microporus were estimated according to Dubinin (1979). The difference between the N₂ adsorbed volume at 0.95 relative pressures and the micropore volume was considered as mesopore volume ($V_{\text{mesop.}}$).



Figure 3.13 Picture of Micrometrics apparatus used to obtain nitrogen isotherms

3.6.2 Chemical characterisation

3.6.2.1. Temperature Programmed Desorption (TPD)

Oxygen surface groups were determined by Temperature Programmed desorption (TPD). This technique is based on the thermal decomposition of oxygenated groups on the surface of AC. The oxygenated groups decompose giving rise to CO and CO₂ by means of the effect of the temperature in an atmosphere of an inert gas. The desorption of oxygenated functional groups at different temperatures allows determining the chemical nature of groups in the obtained curves (Figueiredo et al., 1999; Moreno-Castilla et al., 2000).

0.1 g of adsorbent were heated up to 1100°C in a vertical quartz tube with a N₂ flow of 1 L min⁻¹ at a heating rate of 10°C min⁻¹. Evolved amounts of CO and CO₂ were determined by means of a non-dispersive infrared adsorption analyser (Siemens, model Ultramat 22) (Figure 3.14).



Figure 3.14 Picture of infrared adsorption analyser

The deconvolution of the peaks was performed by fitting Gaussian functions using the software OriginPro v5.8, according to the literature (Figueiredo et al., 2007; Figueiredo and Pereira, 2010). The oxygenated groups and their corresponding temperatures are shown in Table 3.9.

Table 3.9 Oxygen functional groups assignment according to the desorption temperatures in TPD curves.

Desorbed species	Oxygenated groups	Temperature (°C)
CO	Anhydride	400-600
	Phenol	600-700
	Carbonyl / Quinone	700-900
	Ether / Chromene	≈ 800
	Pyrone	800-1000
CO ₂	Carboxylic	100-400
	Anhydride	400-600
	Lactones	500-700

3.6.2.2. X-Ray Photoelectron Spectroscopy (XPS)

X-Ray Photoelectron spectroscopy XPS was used to identify the functional stated of carbon existing on the surface of the ACs. The X-ray radiation interacts with the sample and results in electrons being ejected from core orbitals of the atoms presents on the surface. Thus, the atoms are detached from the sample with a kinetic energy equal to the energy difference between the photon and the binding energy of the electron (Burke et al., 1992). Unlike the TPD analysis, the XPS technique provides information on the chemical composition of the few uppermost layers of the ACs due to only the electrons generated a few nanometres of the surface are detached. The spectrum

XPS, which is defined as the plot of the number of electrons detected in a range of energies against its nuclear binding energy, is obtained in XPS analysis.

X-ray photoelectron spectra (XPS) in C (1s) and O (1s) spectral regions were obtained with a VG ESCALAB 220i-XL spectrometer, using unmonochromatized Al K_{α} X-Ray source (1486.6 eV). The vacuum in the analysis chamber was at a pressure of 4×10^{-9} mbar. The survey scan spectra were collected with pass energy of 50 eV, whereas the high-energy resolution spectra were performed with the pass energy of 25 eV. The deconvolution of peaks was carried out adjusting Gaussian functions. The assessment of different functional groups was performed taking into account the literature (Moreno-Castilla et al., 2000; Figueiredo and Pereira, 2010). The groups and their corresponding binding energies are shown in Table 3.10.

Table 3.10 Oxygen functional groups assignment according to the binding energies in XPS curves.

Region	Binding energy (eV)	Assignment
C1s	284.6 ± 0.3	Graphite (C=C)
	285.2 ± 0.2	Aliphatic defects (C)
	284.6 ± 0.3	Phenol (C-O)
	287.6 ± 0.3	Carbonyl / quinonen / ketone (-C=O)
	289.1 ± 0.3	Carboxylic acids (COOC)
	290.6 ± 0.2	$\pi \rightarrow \pi^*$ transition in C
O1s	531.1 ± 0.3	Quinones / carbonyl (C=O)
	532.3 ± 0.2	Hydroxyl / ether / anhydride (C-OH / C=O)
	533.3 ± 0.3	Ester / anhydride (COOCO)
	534.2 ± 0.3	Carboxyl (-COOH)
	536.1 ± 0.3	Adsorbed water

3.6.2.3. Elemental analysis

The elemental analysis consists in determining the C, H, N, S and O content of a sample. This technique is based on the combustion (1000 °C) in pure oxygen of the test sample. Combustion converts the organic molecules in single gas such as CO₂, N₂, H₂O and SO₂. The gases are pressurised and separated to be measured and quantified.

Elemental analysis were conducted with an 2400 Series II CHNS/O System (Perkin Elmer), which determine the C, H and N, allowing the O content to be determined by difference.

3.6.2.4. Measurement of pH_{slurry}

The pH_{slurry} of ACs was measured by mixing 0.5 of AC with 25 mL of miliQ water. The mixture was equilibrated for 24 h. Afterthat, the pH of the solutions was determined with a Crison microPH 2000 pHmeter.

RESULTS

**IDENTIFICATION OF ODOUR-CAUSING
COMPOUNDS IN THE DRYING PROCESS OF
SEWAGE SLUDGE AT LOW TEMPERATURE**

4.1 BACKGROUND AND OBJECTIVES

Odorous emissions from WWTPs are composed of a complex mixture of volatile compounds (VOCs) such as ketones and aldehydes, nitrogen compounds, volatile sulphur compounds (VSC), organic acids, among other. The major odour sources are associated with the sludge processing, especially in drying processes where volatilisation of odorous compounds is favoured by temperature conditions. The main problem associated with odorous emissions is the low odour threshold of these compounds despite their low emitted concentrations in WWTPs. Furthermore, the synergistic and antagonistic effects between odorous compounds further aggravate the problem and complicate the identification of odorous-causing compounds. Therefore, both analytical and olfactometric methods are required to characterise the odorous emissions.

Thus, the main objective of this chapter is to identify and quantify the main VOCs and VSCs emitted in the drying processes of sewage sludge at low temperature, as well as to validate the drying methodology used at lab-scale. Furthermore, the effectiveness of odour abatement technologies for VSC removal is assessed at full-scale.

4.2 METHODOLOGY

Dewatered sludge from a full-scale centrifuge was dried in the laboratory at low temperature (80°C). VOCs and VSCs emitted in drying processes were analysed by chromatographic techniques as well as olfactometric techniques. Moreover, the assessment of the efficiencies of the odour abatement technologies for VSCs removal at full-scale was carried out. Figure 4.1 shows the diagram of the methodology used in this chapter. For further details about experimental and analytical procedures used, please refer to the materials and methods section indicated between brackets.

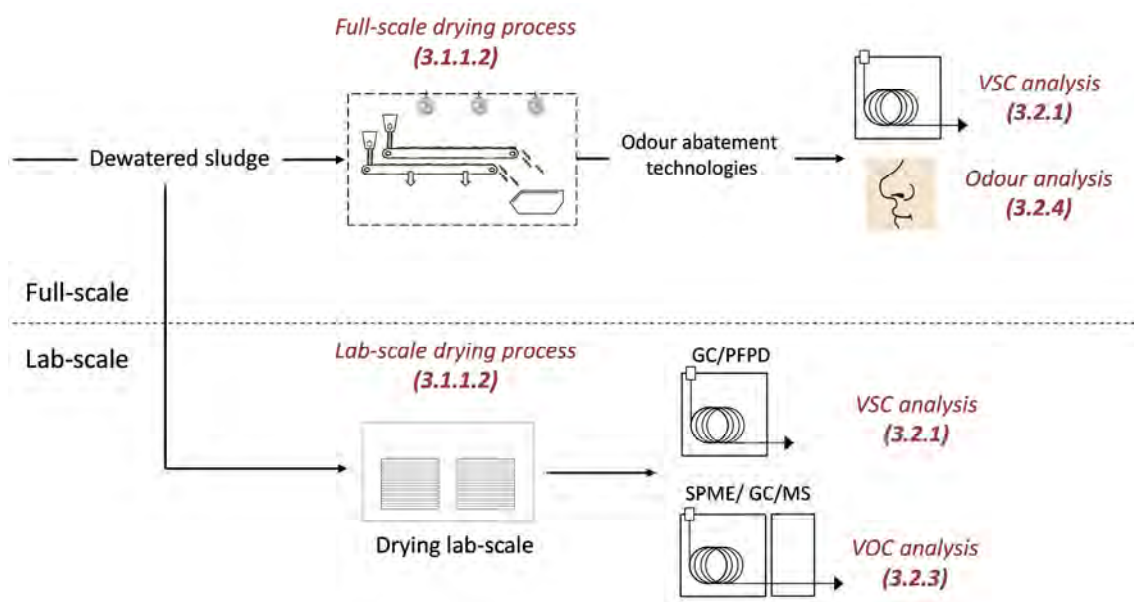


Figure 4.1 Diagram of the methodology used for identifying odour-causing compounds in sewage sludge drying process at low temperature.

4.3 RESULTS AND DISCUSSION

4.3.1 Lab-scale drying process of sewage sludge

Dewatered sludge from a plant located in Barcelona (Catalonia, Spain) was collected in five different campaigns. The environmental conditions of the different sampling periods and the main sludge characteristics are listed in Table 4.1.

Table 4.1 Environmental conditions and sludge characteristics of each sampling

	Sampling				
	I	II	III	IV	V
Month	January	February	March	May	July
Environmental conditions					
Average temperature (°C)	7.2	8.7	11.2	18.8	24.4
Average rainfall (mm)	67.6	42.7	67.3	17.4	45.0
Sludge characteristics					
Total suspended solids (mg L ⁻¹)	42651	41060	40391	39219	41224
Volatile suspended solids (mg L ⁻¹)	31427	28742	30293	30490	33209

No significant differences in the main sludge characteristics were found despite the differences in the environmental conditions in which the samplings were carried out. The sludge sample I was subjected to a lab-scale drying process in order to identify the emitted volatile compounds by SPME/GC-MS method. The non-condensable outflow of sewage sludge drying process at lab-scale was sampled. The distribution of these compounds according to their typology is shown in Figure 4.2.

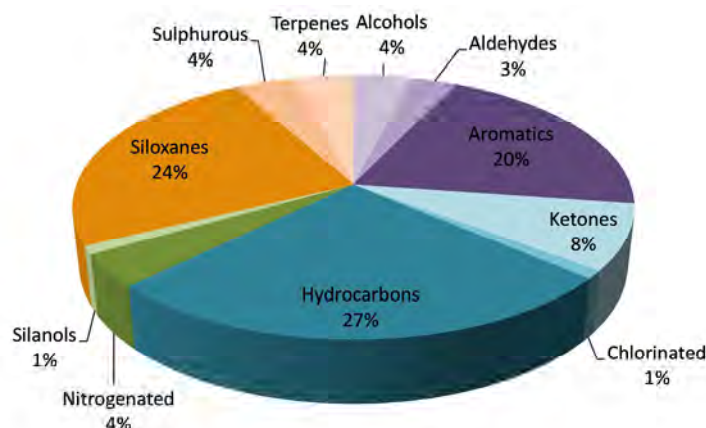


Figure 4.2 Distribution of the VOCs emitted in drying process in sampling I

The SPME/GC-MS results reveal that linear hydrocarbons, siloxanes and aromatic compounds are the main compounds emitted during the sewage sludge drying process. To understand the weight of each analysed group on odorous sample, the odour index (OI) was estimated. Thus, four drying tests (sampling II-V) between February and July 2009 were carried out and, as a result, the emission of VOCs were analysed.

The contribution of each analysed compounds in overall odorous emissions was identified according to the methodology established by Freudenthal et al. (2005). To demonstrate the separate influence of the two factors, concentration and olfactometry threshold, the percentage of peak area participation (α_i) and the percentage of olfactometry threshold participation (τ_i) of each compound in overall odorous sample, were calculated according to Eqs 4.1-4.3.

$$\alpha_i(\%) = \frac{a_i}{\sum_{j=1}^n a_j} \cdot 100 \quad (4.1)$$

$$\tau_i = \frac{\sum_{j=1}^n OT_j}{OT_i} \quad (4.2)$$

$$\tau_i(\%) = \frac{\tau_i}{\sum_{j=1}^n \tau_j} \cdot 100 \quad (4.3)$$

where a_i is the peak area within the total ion chromatogram (TIC) of the compound and OT_i is the olfactometry threshold of the compound i . It has to be highlighted that this approach assumes that the detected peak areas correlate with the concentration of the compounds. The odour index (OI) of each sample was estimated by the peak area participation and the olfactometry threshold participation. OI describes the potential contribution of each single compound to the cumulative odour sample (Eq. 4.4)

$$OI_i(\%) = \frac{\alpha_i(\%)}{\tau_i(\%)} \quad (4.4)$$

Tables 4.2 - 4.5 shows the peak area (a_i) within the TIC of each compound, the percentage of peak area participation α_i (%), the olfactometry threshold participation τ_i (%), and the odour index (OI) of the main compounds identified in each sampling. The overall area of the listed compounds represented 48% of the total area of the identified peaks in the chromatogram.

Table 4.2 Peak area (a_i) within the TIC, percentages of the peak area participation (α_i), olfactometry threshold participation (τ_i) and odour index (OI) of the main volatile compounds identified in sampling II.

Compounds	a_i	α_i (%)	OT_i (mg m^{-3}) ^a	τ_i (%)	OI (%)
Methylene Chloride	87322068	45.59	730	0.00	0.02
2-Butanone	63932263	33.38	0.21	2.06	29.93
Chloroform	ND	0	20	0	0.0
Dimethyl disulphide	3441759	1.80	0.005	86.70	67.66
Toluene	10431037	5.45	3.5	0.12	0.29
Tetrachloroethylene	484271	0.25	12	0.04	0.00
Ethylbenzene	928957	0.48	78.3	0.01	0.00
m-p-xylene	3317933	1.73	9.1	0.83	0.63
o-xylene	1016881	0.53	23.6	0.56	0.13
Phenol	76610	0.04	0.22	9.42	0.16
Limonene	20599518	10.75	1.7	0.25	1.19

^a (Van Gemert, 2003)

Table 4.3 Peak area (a_i) within the TIC, percentages of the peak area participation (α_i), olfactometry threshold participation (τ_i) and odour index (OI) of the main volatile compounds identified in sampling III.

Compounds	a_i	α_i (%)	OT_i (mg m^{-3}) ^a	τ_i (%)	OI (%)
Methylene Chloride	294493526	82.60	730	0.00	0.51
2-Butanone	ND	0.00	0.21	0.00	0.00
Chloroform	17266790	4.84	20	0.02	1.09
Dimethyl disulphide	284474	0.08	0.005	97.22	72.07
Toluene	24724392	6.93	3.5	0.14	8.95
Tetrachloroethylene	714792	0.20	12	0.04	0.08
Ethylbenzene	2033026	0.57	78.3	0.01	0.03
m-p-xylene	8096322	2.27	9.1	0.05	1.13
o-xylene	2383344	0.67	23.6	0.02	0.13
Phenol	2327998	0.65	0.22	2.21	13.40
Limonene	4192218	1.18	1.7	0.29	3.12

Table 4.4 Peak area (a_i) within the TIC, percentages of the peak area participation (α_i), olfactometry threshold participation (τ_i) and odour index (OI) of the main volatile compounds identified in sampling IV.

Compounds	a_i	α_i (%)	OT_i (mg m^{-3}) ^a	τ_i (%)	OI (%)
Methylene Chloride	350428420	30.90	730	0.00	0.01
2-Butanone	704709613	62.14	0.21	2.27	62.47
Chloroform	11707553	1.03	20	0.02	0.01
Dimethyl disulphide	9667405	0.85	0.005	95.29	35.99
Toluene	35481578	3.13	3.5	0.14	0.19
Tetrachloroethylene	714792	0.06	12	0.04	0.00
Ethylbenzene	1008535	0.09	78.3	0.01	0.00
m-p-xylene	3514136	0.31	9.1	0.05	0.01
o-xylene	1304128	0.11	23.6	0.02	0.00
Phenol	15563079	1.37	0.22	2.17	1.32
Limonene	ND	0.00	1.7	0.00	0.00

Table 4.5 Peak area (a_i) within the TIC, percentages of the peak area participation (α_i), olfactometry threshold participation (τ_i) and odour index (OI) of the main volatile compounds identified in sampling V.

Compounds	a_i	α_i (%)	OT_i (mg m^{-3}) ^a	τ_i (%)	OI (%)
Methylene Chloride	2962970097	12.21	730	0.00	0.01
2-Butanone	4650383592	19.17	0.21	2.31	51.17
Chloroform	13170312086	54.28	20	0.02	1.52
Dimethyl disulphide	98682539	0.41	0.005	97.12	45.61
Toluene	2189125284	9.02	3.5	0.14	1.45
Tetrachloroethylene	126667643	0.52	12	0.04	0.02
Ethylbenzene	168979532	0.70	78.3	0.01	0.00
m-p-xylene	633340722	2.61	9.1	0.05	0.16
o-xylene	237214145	0.98	23.6	0.02	0.02
Phenol	ND	0.00	0.22	0.00	0.00
Limonene	25486897	0.11	1.7	0.29	0.03

Although the same VOCs have been identified in all samples, only slight differences in gas composition from different drying test were found. The results indicated that, as expected, the abundance of certain VOCs is not correlated with the odour index. Thus, chlorinated compounds such as methylene chloride or chloroform have high peak area but these compounds have negligible contribution in the odour index (OI). Conversely, compounds with lower peak area such as dimethyl disulphide have a significant contribution to the overall odour sample due to their low odour threshold. Therefore, these results demonstrated the significant effect of odorous compounds with a low odour threshold although these compounds are in a minority in the odorous sample. Moreover, as expected, the absence or reduction of a compound force the increase of odour index contribution of the others compounds in the sample, e.g., the absence of 2-butanone which has an important weight on OI causes that other compounds such as phenol take over the contribution in the OI in sampling II.

Some compounds could not be identified because of the selectivity of the analytical method and the complexity of the odorous sample. Hence, a selective chromatographic analysis for compounds with a low odour threshold such as sulphurs was carried out. Sample II-VI were also analysed by GC-PFPD and VSCs such as hydrogen sulphide (H_2S), ethyl mercaptan (ETM), methyl mercaptan (MTM), dimethyl sulphide (DMS) and dimethyl disulphide (DMDS) were identified (Figure 4.3).

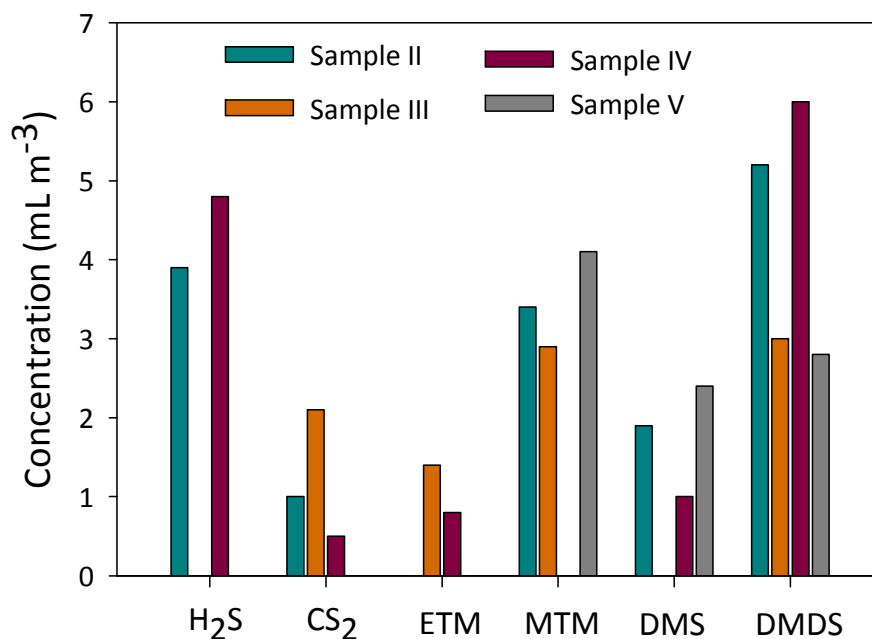


Figure 4.3 VSCs identified by GC/PFPD from lab-scale drying process

Despite the presence of the sulphur compounds was variable for different samples, the same sulphur compounds were identified. Moreover, in agreement with the results reported by Sekyiamah et al. (2008), significant changes in VSC concentrations during sampling periods were not noted. These authors investigated the seasonal variation in VSC formation in WWTP and stated that neither VSC formation nor odour concentration were correlated with the sampling season.

4.3.2 Full-scale drying process of sewage sludge

Identification of VOCs and VSCs emitted in a low temperature drying process at full-scale was also carried out. For this purpose, the non-condensable outflow of sewage sludge drying process was sampled in three campaigns between January and April. The environmental conditions of sampling periods and the main sludge characteristics at each sampling are listed in Table 4.6.

Table 4.6 Environmental conditions and sludge characteristics of each sampling

	Sampling		
	VI	VII	VIII
Month	January	February	April
Environmental conditions			
Average temperature (°C)	6.6	8.0	14.1
Average rainfall (mm)	62.2	96.1	23.4
Sludge characteristics			
Total suspended solids (mg L ⁻¹)	39652	39411	40132
Volatile suspended solids (mg L ⁻¹)	30532	31007	31569

Samples collected from drying system outflow were analysed by SPME/GC-MS. The results obtained from sampling VI and VII are shown in Table 4.7 and 4.8, respectively.

Table 4.7 Peak area (a_i) within the TIC, percentages of the peak area participation (α_i), olfactometry threshold participation (τ_i) and odour index (OI) of the main volatile compounds from sampling VI at full-scale

Compounds	a_i	α_i (%)	OT_i (mg m ⁻³) ^a	τ_i (%)	OI (%)
Methylene Chloride	1685935455	30.40	730	0.00	0.03
2-Butanone	328884326	5.93	0.21	2.31	21.75
Chloroform	2688253	0.05	20	0.02	0.00
Dimethyl disulphide	22958432	0.41	0.005	97.12	63.76
Toluene	456432698	8.23	3.5	0.14	1.81
Tetrachloroethylene	945456425	17.05	12	0.04	1.09
Ethylbenzene	158579854	2.86	78.3	0.01	0.03
m-p-xylene	594258436	10.72	9.1	0.05	0.91
o-xylene	54545445	0.98	23.6	0.02	0.03
Phenol	ND	0.00	0.22	0.00	0.00
Limonene	1295545254	23.36	1.7	0.29	10.58

Table 4.8 Peak area (a_i) within the TIC, percentages of the peak area participation (α_i), olfactometry threshold participation (τ_i) and odour index (OI) of the main volatile compounds from sampling VII at full scale.

Compounds	a_i	α_i (%)	OT_i (mg m ⁻³)	τ_i (%)	OI (%)
Methylene Chloride	297414654	9.84	730	0.00	0.02
2-Butanone	158987414	5.26	0.21	2.31	28.99
Chloroform	6255366	0.21	20	0.02	0.01
Dimethyl disulphide	6389352	0.21	0.005	97.12	48.93
Toluene	689820016	22.82	3.5	0.14	7.55
Tetrachloroethylene	1288567483	42.62	12	0.04	4.11
Ethylbenzene	51351350	1.70	78.3	0.01	0.03
m-p-xylene	7843964	0.26	9.1	0.05	0.03
o-xylene	62315821	2.06	23.6	0.02	0.10
Phenol	ND	0.00	0.22	0.00	0.00
Limonene	454521852	15.03	1.7	0.29	10.24

As it has been noted in lab-scale experiments, 2-butanone or DMDS play an important role in the OI of overall odorous sample. However, limonene was determined in full-

scale drying process causing an increase in the OI. The comparison between lab-scale and full-scale reveals that the methodology used at lab-scale is an accurate and representative tool to characterise the emissions from a drying process at full-scale.

VSCs were monitored through the odour abatement technologies (chemical scrubbers and biofilter) at the full-scale facilities. Figure 4.4 shows the VSC concentration in the scrubber inflow, scrubber outflow and biofilter outflow of the three samples. The total sulphur compounds (TSC) which is defined as the sum of H₂S, MTM, ETM, DMS plus DMDS (mg S m⁻³) are also presented. Furthermore, the removal percentages of VSC in the chemical scrubber, biofilter and at the end-of-pipe technologies are presented in Table 4.9.

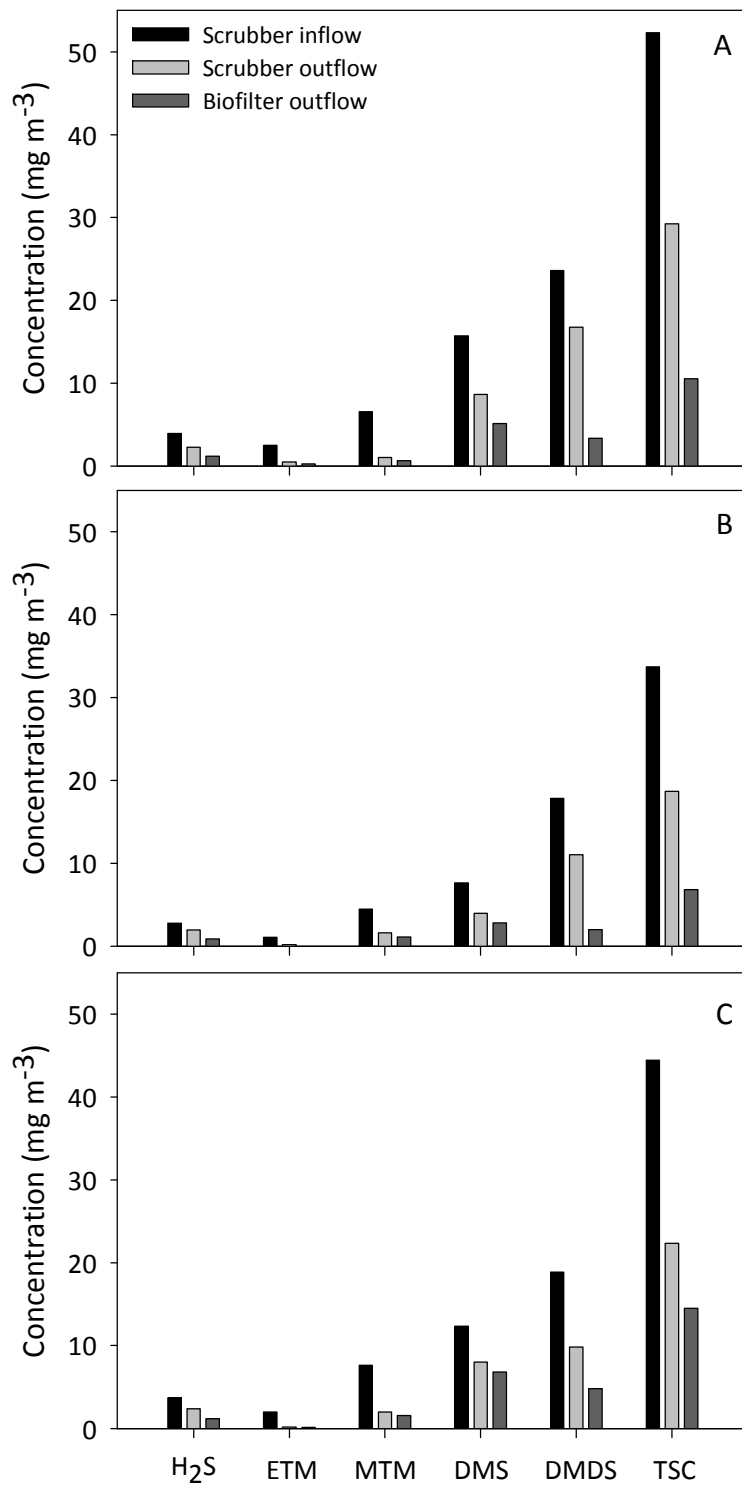


Figure 4.4 VSC concentrations in scrubber inflow, scrubber outflow and biofilter outflow: a) sampling VI; b) sampling VII; c) sampling VIII.

Table 4.9 Removal percentages of VSC in the chemical scrubber (S), the biofilter (B) and overall removal (O).

	Sampling VI			Sampling VII			Sampling VIII		
	S	B	O	S	B	O	S	B	O
H ₂ S	42	48	80	30	54	68	35	51	51
ETM	80	50	90	86	58	94	92	22	92
MTM	84	38	90	64	32	76	74	21	79
DMS	45	41	67	48	30	63	35	15	45
DMDS	29	80	86	38	82	89	48	51	74

The VSC emissions follow the same trend in all samples, being DMDS the most abundant compound and ETM the least. Three-stage packed tower scrubbers provide high removal efficiencies according to the following order: ETM \geq MTM>DMS \geq H₂S>DMDS, being the mercaptans (ETM and MTM) the sulphur compounds with the highest percentage removal through the oxidative scrubber.

In the biofiltration process, the degradation sequence of VSC was opposite to the results obtained in chemical scrubber (DMDS>ETM \geq H₂S>MTM>DMS). The highest percentage removal was obtained for DMDS (82%) while the lowest efficiency removal was obtained for DMS (15%). Different degradation sequence (H₂S>MTM>DMDS>DMS) was observed by Myung cha et al. (1999) during the treatment of an odour gas mixture of volatile sulphur compounds at high concentration (200 ppmv of H₂S and 50 ppmv of MTM, DMS and DMDS). This result demonstrate that the degradation sequence can not be generalised because of the selective use of microbial population can change the sequence of VSC degradation rates (Smet et al., 1998). However, several authors agreed that DMS is often difficult to degrade because of the DMS degraders are strongly inhibited by the presence of other VSC (Myung cha et al., 1999; Cho et al., 1991; Ho et al., 2008).

The removal efficiencies of the biofilter in the third sampling were lower for all VSC removal comparing to the previous samplings. The replacement of the biofilter packing few weeks before of sampling VIII could explain the lower removal efficiency.

In order to complement the analytical methods, the measurement of odour concentration by means of olfactometric methods was carried out. Table 4.10 show the odour concentration (OU m⁻³) and TSC emission (mg S m⁻³) of each sample at the different points of sampling campaigns.

Table 4.10 Odour concentration ($\text{OU}_E \text{ m}^{-3}$) and TSC (mg m^{-3}) from different sampling points.

	Sampling					
	VI		VII		VIII	
	$\text{OU}_E \text{ m}^{-3}$	TSC	$\text{OU}_E \text{ m}^{-3}$	TSC	$\text{OU}_E \text{ m}^{-3}$	TSC
Inlet chemical scrubber	> 9692	52	> 9692	33	> 9692	44
Inlet biofilter	2695-9692	29	2695-9692	18	2695-9692	22
Outlet biofilter	208-450	10	208-450	7	1077-2695	15

The same olfactometric results were obtained from sampling VI and VII where the odorous emissions were reduced below $450 \text{ OU}_E \text{ m}^{-3}$ by the odour abatement technologies. The odour concentration of the third sample was reduced by chemical scrubbers, as in the previous cases. Nevertheless, the outlet concentration of biofilter is higher in the third sample, in which odour concentrations between 1077 and 2695 $\text{OU}_E \text{ m}^{-3}$ were determined. This increase of odour concentration is correlated with the loss of efficiency in the biofilter in the third sampling. Therefore, the high concentration of TSC emitted in sampling VIII implied an important increase of odour concentration.

These results are in agreement with those of Adams et al (2003) who analysed the odorous compounds emissions from digested biosolids during dewatering process using analytical and olfactometric methods. Adams et al (2003) stated that most of the odour samples analysed showed a positive correlation between olfactometry measurements and the VSC concentration. Conversely, no discernible relationships between odour concentration and volatile nitrogen compounds or volatile fatty acids were found.

Despite the low concentrations emitted at the assessed end-of-pipe treatments, this has not been enough to reduce the odour concentration. These results demonstrate the importance of olfactometric analysis as a complementary tool to the analytical methods and the need to investigate other polishing treatments

4.4 CONCLUSIONS

VOCs and VSCs emitted in the drying process were analysed by different chromatographic techniques at lab and full-scale. A significant variability in the composition of VOCs in the odorous matrix is not observed in spite of the season variation between the collected samples. Nevertheless, slight variations in the composition of the gaseous matrix cause significant changes in the OI. Moreover, the results indicated that VSC are the main responsible for odorous emissions in the sewage sludge drying process.

The comparison between full and lab scale reveals that the methodology used at lab-scale is a useful and representative enough tool to characterise the emissions from

drying process at full-scale. Furthermore, the olfactometric measurements reflect the obtained analytical results and qualitatively complement the characterisation of odorous emissions.

OPTIMISING CHEMICAL CONDITIONING OF UNDIGESTED SEWAGE SLUDGE FOR ODOUR REMOVAL IN DRYING PROCESSES

Adapted from:

Vega, E., Gonzalez-Olmos, R., Martin, M.J., 2014. *Optimising chemical conditioning of the undigested sewage sludge for odour removal in drying processes. Submitted to Journal of Environmental Management.*

5.1 BACKGROUND AND OBJECTIVES

The chemical conditioning sludge is required to improve the processing efficiency of dewatering devices and thereby to reduce the sludge volume and disposal cost. Inorganic and organic conditioners have been widely used in this process as the most economical solution.

The sludge management in this process implies the emission of odorous compounds, especially volatile sulphur compounds (VSC). The effect of the addition chemical conditioners on odorous emissions has been focused in field applications. However, the use of conditioners to minimise the odours within the process has not been considered significant. Moreover, the research to date has tended to focus on the conditioning process in order to improve the sludge dewaterability or to reduce the odorous compounds. Nevertheless, both targets have not been simultaneously studied.

For this reason, the main objective of this chapter is to assess the combined effects of the addition of chemical conditioners to undigested sewage sludge over dewaterability and odour emissions, paying attention to sulphur compounds emissions, during the drying process. The design of the experiments, the model prediction and the determination of the optimum conditions to achieve better dewatering results and less odour emissions in the conditioning process were carried out by means of response surface methodology (Montgomery, 1996). Moreover, the effectiveness of physical conditioners was also assessed.

5.2 METHODOLOGY

A thickened sludge was conditioned using iron chloride, calcium oxide and polyelectrolyte at different concentrations in the 20 experiments established by central composite design (CCD). Capillary suction time of conditioned samples was measured to ascertain the effect on sludge dewaterability. Moreover, these samples were centrifuged to obtain dewatered sludge which was subjected to the drying process at low temperature. The gas phase resulting from drying process was analysed by chromatographic and olfactometric analysis. Figure 5.1 shows the diagram of methodology used in this chapter. For further details about experimental and analytical procedures used, please refer to the materials and methods section indicated between brackets.

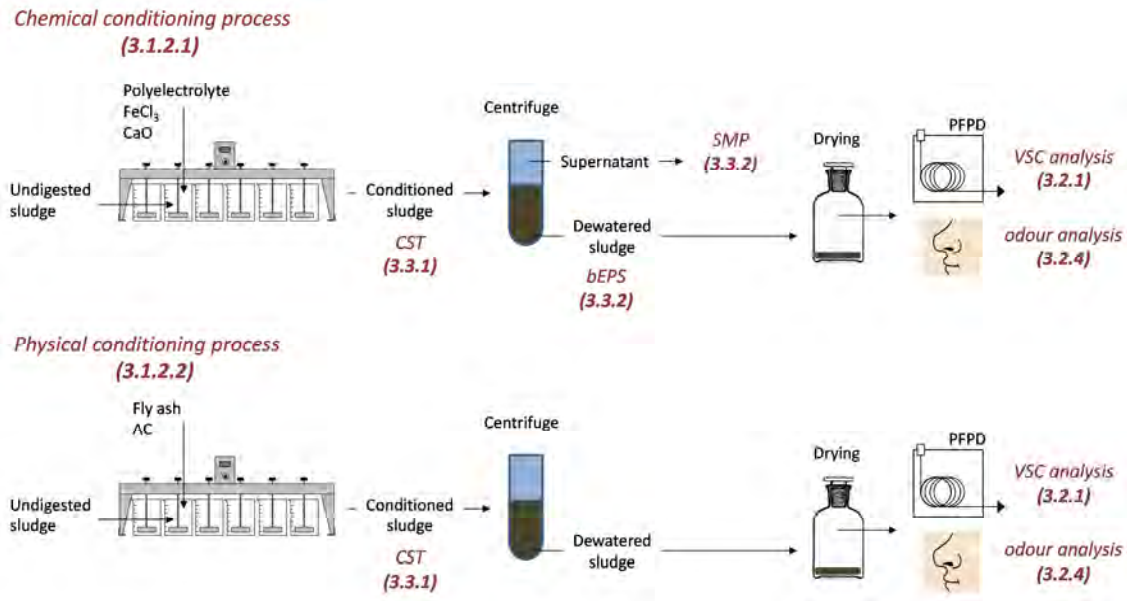


Figure 5.1 Diagram of methodology used in conditioning and drying process.

5.3 RESULTS AND DISCUSSION

5.3.1 Chemical conditioning

5.3.1.1. Influence of the individual dosage of conditioners on the dewaterability and odour emission

Prior to the optimisation process of sludge chemical conditioning, the influence of the individual dosage of chemical conditioners on the dewaterability and sulphur and odour emission was investigated.

The assessment of dewaterability was carried out by the measurement of capillary suction time (CST) since it is a well-established technique to characterise the dewaterability of sludge samples (Chen et al., 1996). A lower CST is correlated with high sludge dewaterability. As it was expected, the CST decreased when conditioners were added. The CST measured at different doses is presented in Figure 5.2. As mentioned before, the inorganic (iron chloride) and organic (polyelectrolyte) chemical conditioners play a different role in the conditioning process. Nevertheless, both conditioners are able to reduce the amount of free moisture retained in conditioned sludge, thereby enhancing the dewatering process (Tsang and Vesilind, 1990).

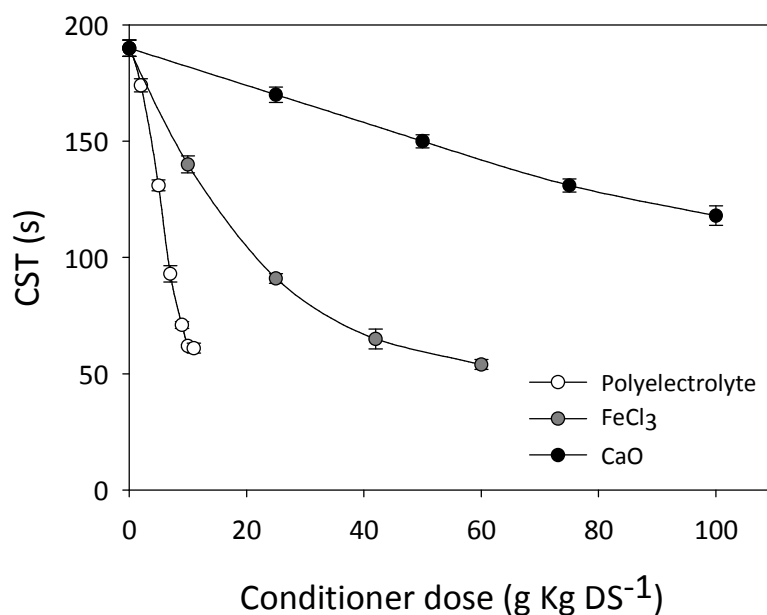


Figure 5.2 Individual effect of chemical conditioners doses on the CST of the sewage sludge

The CST results obtained using the maximum dose of chemical conditioners are presented in Table 5.1. Moreover, the influence of these conditioners on sulphur and odour emission with the same dose is also presented.

Table 5.1 CST (s), TSC emission (mg S m^{-3}), odour emission (OU_E range) and pH of chemical conditioned samples on individual assessment using 10 g Kg DS^{-1} of polyelectrolyte, 60 g Kg DS^{-1} of iron chloride and 100 g Kg DS^{-1} of calcium oxide

	Chemical conditioners			
	Blank	Polyelectrolyte	FeCl ₃	CaO
CST (s)	190.1	61.4	54.2	117.6
TSC emission (mg S m^{-3})	29.4	26.3	21.3	25.0
Odour emission (OU_E range) ^a	3.0	3.0	4.0	4.0
pH	6.1	6.6	3.8	11.1

^a OU_E range: (1) $208\text{-}450 \text{ OU}_E \text{ m}^{-3}$; (2) $450\text{-}1077 \text{ OU}_E \text{ m}^{-3}$; (3) $1077\text{-}2695 \text{ OU}_E \text{ m}^{-3}$; (4) $2695\text{-}9692 \text{ OU}_E \text{ m}^{-3}$; (5) $>9692 \text{ OU}_E \text{ m}^{-3}$

The following VSCs were detected during the drying process: Hydrogen sulphide (H_2S), carbon disulphide (CS_2), methyl mercaptan (MTM), dimethyl sulphide (DMS) and dimethyl disulphide (DMDS). Total sulphur compounds (TSC) emission is defined as the sum of sulphur emitted by all detected VSCs (mg S m^{-3}). The VSC and TSC emissions at different tested doses during the individual assessment are presented in Figure 5.3.

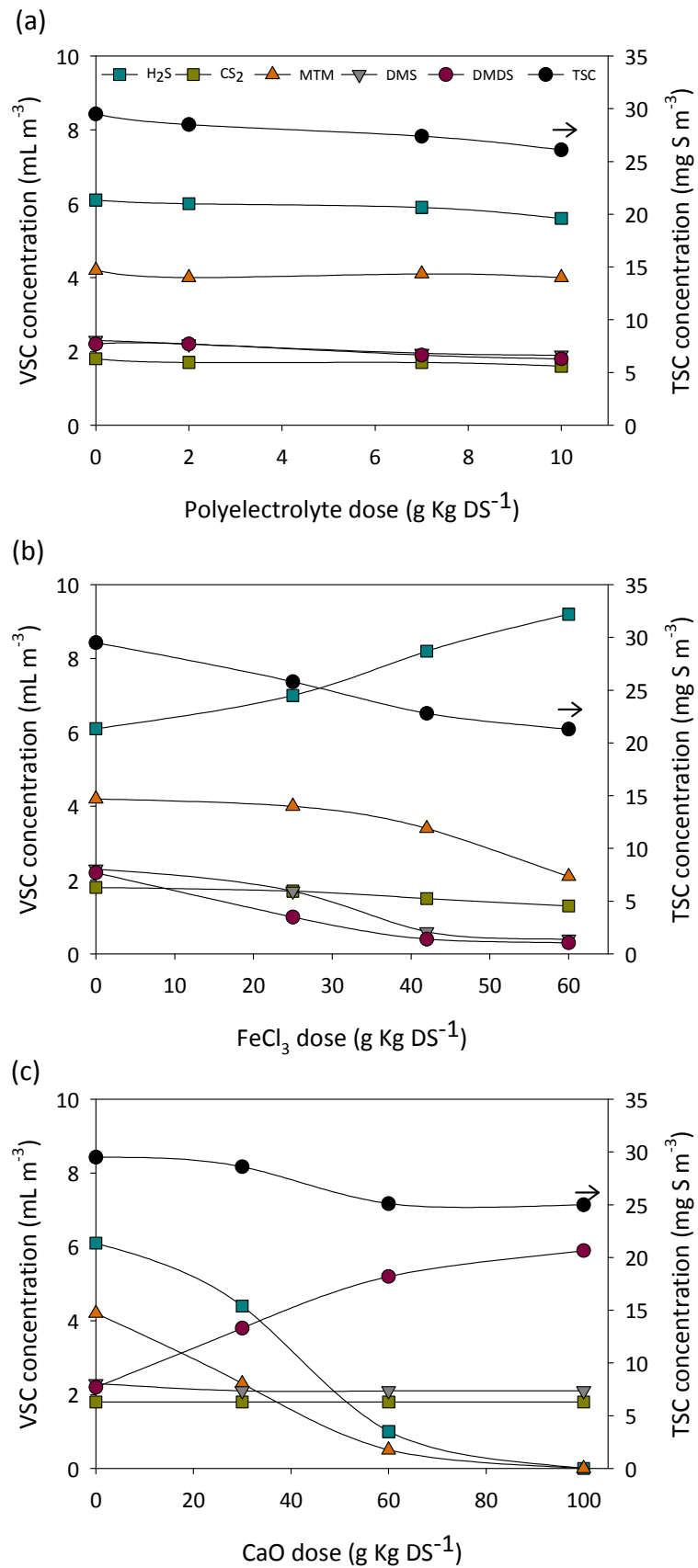


Figure 5.3 Influence of the individual dosage of chemical conditioners on VSC and TSC emissions: (a) polyelectrolyte, (b) iron chloride and (c) calcium oxide.

It is observed that polyelectrolyte conditioning slightly decreased the TSC emission (Figure 5.3a). This trend was also observed by Liu et al. (2012) who used a cationic polyacrylamide as a representative organic polymer.

The conditioning process with iron chloride causes a significant reduction of TSC emission (Figure 5.3b). Nevertheless, a significant increase in the concentration of H₂S (51%) was observed during iron chloride conditioning process. The addition of iron salts is commonly employed for the removal of H₂S through the precipitation of ferrous sulphide in wastewaters. The precipitation of ferrous sulphide is believed to be fast process. However, Nielsen et al. (2005) found that iron sulphide precipitation could take a few hours. Moreover, the effectiveness of iron salts depends on the composition of wastewater where the complexation of iron can take place (Araújo et al., 2000; Nielsen et al., 2005). These facts could explain the inefficiency of iron chloride for the removal of H₂S at short time of conditioning. Furthermore, the increase of H₂S emissions was related to the acidic conditions generated during iron chloride conditioning (pH = 3.8) which keep the sulphides contained in the sludge in its non-ionised form (Gostelow et al., 2001).

On the other hand, the sharp increase in pH caused by the addition of calcium oxide (pH = 11.1) reduces the emissions of VSCs such as H₂S and MTM (Figure 5.4c). Under this pH condition, H₂S and MTM are in their ionised form and therefore are not volatilised from the samples. However, the alkaline conditions cause a significant increase of DMDS emission, achieving concentrations around 6 mL m⁻³ in agreement with the results obtained by Kim et al. (2002) and Kim et al. (2003).

In addition to VSCs, other odorous-causing compounds such as volatile amines, which were non-detectable by the GC method employed, were released during thermal drying of sewage sludge. In order to have a more complete vision of odour emission during the process, olfactometric analysis were carried out. During polyelectrolyte conditioning, the odour emission was not increased and it was kept between 1077-2695 OU_E m⁻³ (Range 3) despite several authors detected odorous compounds with a lower odour threshold such as trimethylamine (TMA) and DMDS (Dentel et al. 2002; Kim et al. 2003). These authors demonstrated that cationic polymers can be degraded through enzymatic hydrolysis, releasing TMA, DMDS or their precursors in short periods of time. When the sludge was conditioned with iron chloride or calcium oxide, a significant increase in the odour concentration (2695-9692 OU_E m⁻³) was measured although significant reductions in the emission of VSCs had been observed. The increase of H₂S measured during iron chloride conditioning leads to an increase of odour concentration due to the low odour threshold of H₂S (0.41 µL m⁻³) (Van Gemert, 2003). On the other hand, a strong fishy odour perceived by panel members caused an increase of odour concentration from conditioned samples with calcium oxide. The perceived fishy odour in these samples was attributed to the emission of nitrogenised

compounds such as ammonia or TMA according to the odour classification developed by Burlingame et al. (2004). This distinctive fishy odour was also perceived by Kim et al. (2002) and Kim et al. (2003) in post-liming process. The authors attributed the emission to alkaline conditions which exceeding the pKa for TMA (pKa = 9.8) and therefore, the deprotonated TMA volatilisation.

5.3.1.2. Optimisation of sludge chemical conditioning process using RSM

The combined effects of the three independent variables (polyelectrolyte, iron chloride and calcium oxide) on the sludge handling process (dewaterability and odour emission) were evaluated using response surface methodology (RSM). The experimental matrix design and results (predicted and observed) for the overall optimisation are presented in Table 5.2. The regression model equations are presented in Table 5.3

The statistical significance of the model equation was evaluated by the F-test of variance (ANOVA). The statistical parameters of models obtained are given in Table 5.4. The coefficients of R^2 and R^2 adjusted by the model obtained for CST and TSC emission are close to 1.0. Thus, these values ensured a satisfactory adjustment of the quadratic models to the experimental data for CST and the TSC emission. The low precision in the data acquisition by means of the olfactometer (range measurements) leads to a worse fit of the model in the case of odour emission ($R^2 = 0.817$ and R^2 adjusted = 0.652). Nevertheless, the regression and corresponding value of "Prob>F" less than 0.05 in the three studied response indicates that models are considered statistically significant.

Table 5.2 Experimental design and results for overall optimisation

Trial	Variable			Responses					
	Polyelectrolyte	FeCl ₃	CaO	TSC emission (mg S m ⁻³)		Odour emission range (OU _E m ⁻³) ^a		CST (s)	
				Observed	Predicted	Observed	Predicted	Observed	Predicted
1	5	30	50	23.94	24.38	3.00	3.05	47.00	46.00
2	10	60	100	15.20	15.40	2.00	2.09	15.10	18.96
3	5	30	50	23.71	24.35	3.00	3.05	45.70	46.60
4	5	30	0	25.22	24.35	3.00	3.40	81.20	69.63
5	0	60	0	21.21	21.32	4.00	3.80	54.20	58.32
6	5	30	100	19.32	19.40	4.00	3.62	30.10	35.59
7	0	0	0	29.50	30.00	3.00	2.89	190.20	186.76
8	5	60	50	18.72	18.80	3.00	2.61	28.70	37.35
9	10	60	0	20.43	20.60	3.00	3.10	19.60	15.81
10	5	30	50	25.12	24.35	3.00	3.05	47.20	46.60
11	0	0	100	25.00	25.09	4.00	3.91	117.00	121.50
12	5	30	50	23.01	24.35	3.00	3.05	44.20	46.60
13	5	30	50	23.41	24.35	3.00	3.05	46.10	46.60
14	10	0	0	26.34	26.70	3.00	2.71	61.40	75.74
15	5	30	50	24.73	24.35	3.00	3.05	45.60	46.60
16	0	30	50	27.33	27.20	3.00	3.01	60.40	68.23
17	5	0	50	27.10	26.48	3.00	3.21	120.40	107.80
18	10	0	100	22.11	22.25	4.00	4.20	35.00	31.56
19	0	60	100	15.93	15.69	2.00	2.31	54.50	40.40
20	10	30	50	26.10	25.44	3.00	2.81	23.00	25.00

^a OU_E range: (1) 208-450 OU_E m⁻³; (2) 450-1077 OU_E m⁻³; (3) 1077-2695 OU_E m⁻³; (4) 2695-9692 OU_E m⁻³; (5) >9692 OU_E m⁻³

Table 5.3 Coded regression model equations established by RSM

Response	Model fit equation ^a
CST (s)	$46.93 - 33.12x_1 - 35.19x_2 - 15.49x_3 - 11.66x_1^2 + 26.19x_2^2 + 7.29x_3^2 + 17.10x_1x_2 + 5.25x_1x_3 + 11.93x_2x_3$
TSC emission (mg S m ⁻³)	$24.35 - 0.86x_1 + 3.85x_2 - 2.5x_3 + 1.95x_1^2 - 1.72x_2^2 - 2.5x_3^2 + 0.6x_1x_2 + 0.078x_1x_3 - 0.21x_2x_3$
Odour emission range (OU _E m ⁻³)	$3.05 - 0.10x_1 - 0.30x_2 + 0.001x_3 - 0.14x_1^2 - 0.14x_2^2 + 0.36x_3^2 - 0.13x_1x_2 + 0.12x_1x_3 - 0.63x_2x_3$

^a (x_1 , x_2 and x_3 correspond to coded dose of polyelectrolyte, iron chloride and calcium oxide, respectively)

Table 5.4 Statistical parameters obtained from the ANOVA.

Variable	TSC emission	Odour emission range	CST
R ²	0.979	0.817	0.967
R ² adjusted	0.961	0.652	0.937
Prob > F	< 0.0001	0.009	< 0.0001
Std. Dev.	1.78 mg S m ⁻³	0.33	10.58 s
CV	8.1	10.0	18.0
Adequate precision	27.5	9.10	24.71

The coefficient of variance (CV), which is defined as the ratio of the standard error of estimation to the mean value of the observed response, is a measure of reproducibility of the model which can be considered reasonably reproducible provided if the CV is not greater than 10% (Liu et al., 2013). The obtained CV values for sulphur and odour emission (8.1 and 10.0, respectively) showed a good precision and reliability of the experiments. The adequate precision compares the range of the predicted values at the design points to the average prediction error. Ratios greater than 4 indicate adequate model discrimination. The higher values of adequate precision confirm that predicted models can be used to navigate the space defined by the CCD (Ghafari et al., 2009). Therefore, the statistical analysis reveals that the models are reliable to describe the effects of undigested sludge conditioning on dewaterability and odour emissions.

For the graphical interpretation of the interactions between variables, the use of three-dimensional plots of the predicted regression models is recommended. The three-dimensional response surface plots of CST, sulphur emissions and odour emission are plotted between two interacting variables, while the third variable is kept constant at its zero level in order to easily visualise the relationships between parameters (Montgomery, 1996).

Figure 5.4 shows the three-dimensional response surface plots of CST. The lowest values of CST, which means a higher dewaterability, were obtained by combining high doses of polyelectrolyte and iron chloride (Figure 5.4a). Despite the reduction of CST occurred at a broad range of polyelectrolyte and iron chloride dosages, the most

significant reduction was obtained when iron chloride and polyelectrolyte dosages were higher than 30 and 6 g Kg DS⁻¹, respectively. This behaviour was observed even more markedly by Chitikela and Dentel (1998) who stated that the dual-conditioning improves the dewaterability of the sewage sludge. This trend was expected given the model fit equation (Table 5.3) which showed the most negative values for the individual coefficients of polyelectrolyte and iron chloride (-33.12x₁ and -35.19x₂, respectively) compared with the interaction coefficients. On the other hand, the synergistic effect on CST reduction by the dual-conditioning between polyelectrolyte and calcium oxide and between iron chloride and calcium oxide are not remarkable in agreement with the results reported by Zhai et al. (2012).

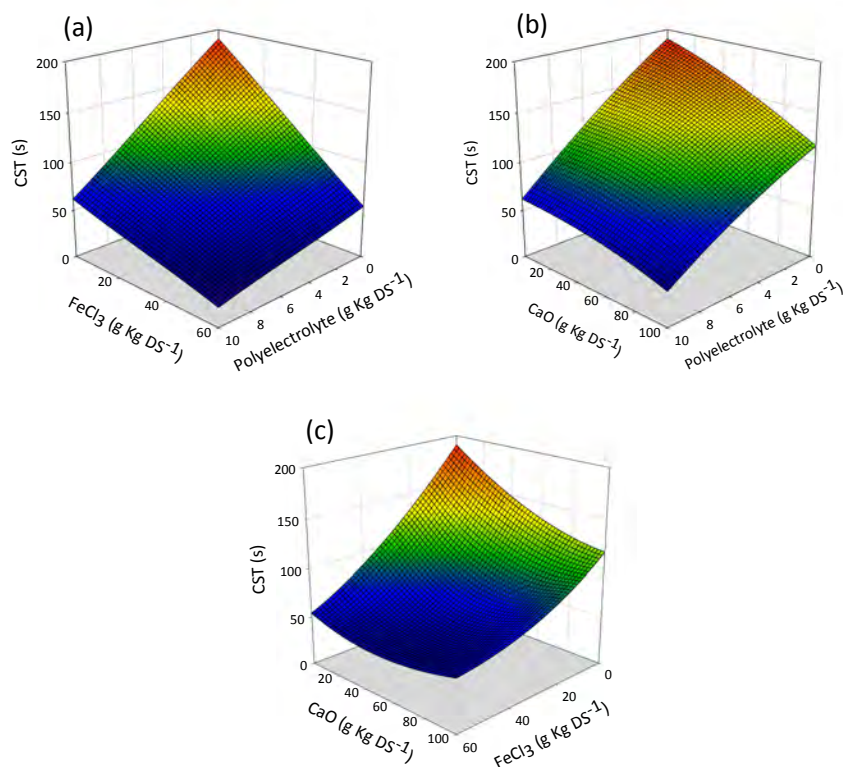


Figure 5.4 Three-dimensional response surface plots of CST showing the effect of variables: (a) FeCl₃ - polyelectrolyte dose, (b) CaO - polyelectrolyte dose, and (c) CaO - FeCl₃ dose

Figure 5.5 illustrated the three-dimensional response surface plots of the TSC emission. The effect of the combined use of iron chloride and polyelectrolyte on TSC emission is shown in Figure 5.5a. The response surface obtained is almost flat, suggesting that these conditioners do not affect significantly the emissions of the TSC during thermal drying. The same response was obtained by the addition of calcium oxide and polyelectrolyte together (Figure 5.5b). This fact confirms the results obtained in section 3.1.1, where both conditioners had a low influence on the reduction of sulphur compounds emission. Nevertheless, an important positive synergistic effect was observed by the addition of both inorganic conditioners at high doses (Figure 5.5c),

achieving percentage of TSC removal about 46%. This synergistic effect has been already observed in the model fit equation which showed that the interaction coefficient between calcium oxide and iron chloride ($-0.21x_2x_3$) had a greater influence on the TSC reduction compared with other interaction coefficients ($+0.61 x_1x_2$ and $+0.078 x_1x_3$).

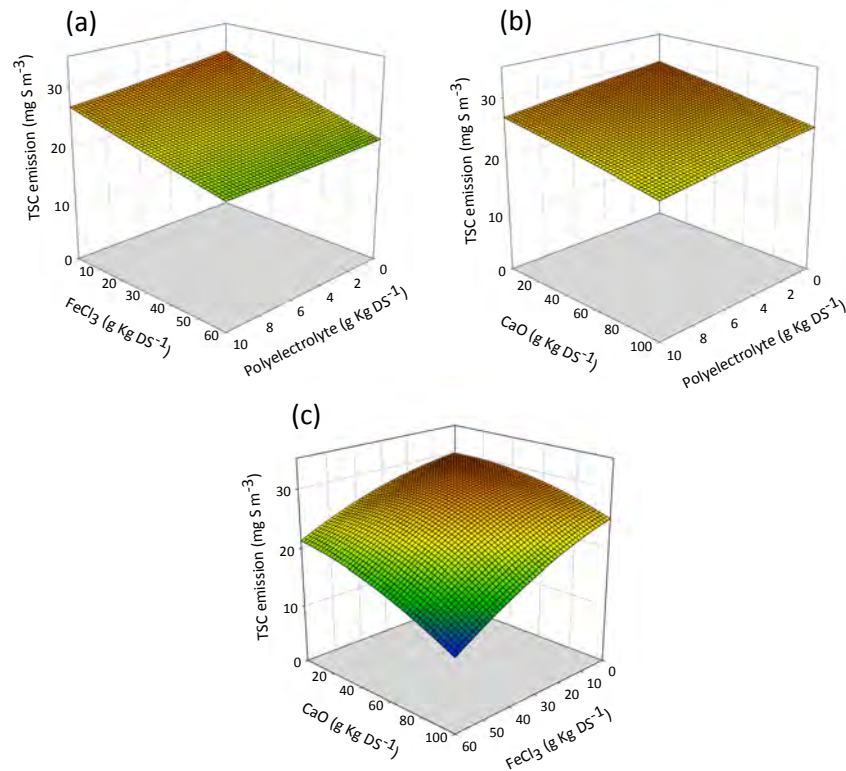


Figure 5.5 Three-dimensional response surface plots of TSC emission showing the effect of variables: (a) FeCl₃-polyelectrolyte dose, (b) CaO-polyelectrolyte dose, and (c) CaO - FeCl₃ dose

Several authors have correlated sulphur compounds emissions from digested sewage sludge to its protein content (Adams et al., 2008; Higgins et al., 2008). The authors have attributed the release of DMS, MTM, H₂S and DMDS to protein degradation by means of bio-transformations. In order to check this behaviour in undigested sewage sludge, the measurement of the bound extracellular polymeric substances (b-EPS) and soluble microbial products (SPM) were carried out. The relationship between TSC emissions and b-EPS and SPM are presented in Figure 5.6a and 5.6b, respectively. No correlation was found between the content of b-EPS in sludge and sulphur emissions, while the presence of SMP in undigested sewage sludge was directly correlated with the increasing emission of sulphur compounds during drying process.

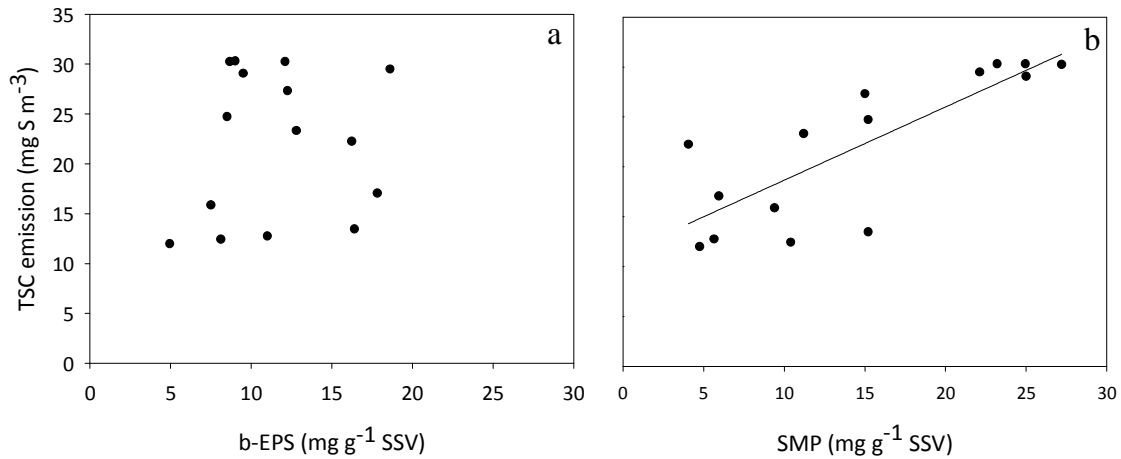


Figure 5.6 The effect of b-EPS (a) and SMP (b) on TSC emission from undigested sewage sludge.

The effects of chemical conditioners on odour emissions were also investigated (Figure 5.7). The results of the effect of iron chloride and polyelectrolyte dose (Figure 5.7a) reveals that the odour emission was negatively affected by the use of iron chloride, as observed on previous experiments. Nevertheless, this effect was slightly reduced by the increase of polyelectrolyte dose in the conditioned sample. A similar negative trend was observed combining calcium oxide with polyelectrolyte (Figure 5.7b).

The calcium oxide and iron chloride dose have a strong synergistic effect on the reduction of odour emissions (Figure 5.7c), as it was observed previously for TSC emissions (Figure 5.5c). This result corroborates the ones obtained in full-scale system where the correlation between olfactometric measurements and TSC concentration was established. Combining both conditioners (calcium oxide dose = 80-100 g Kg DS⁻¹; iron chloride dose = 40-60 g Kg DS⁻¹), a reduction of the odour emission from range 3 (1077-2695 OU_E m⁻³) to range 2 (450-1077 OU_E m⁻³) was achieved. The model fit equation showed the lowest negative values (-0.63x₂x₃) for the interaction coefficient between iron chloride and calcium oxide. The adjustment of pH by means of the calcium oxide addition kept the solution near neutral pH, thereby a reduction of odour emission was achieved (Adams et al., 2008).

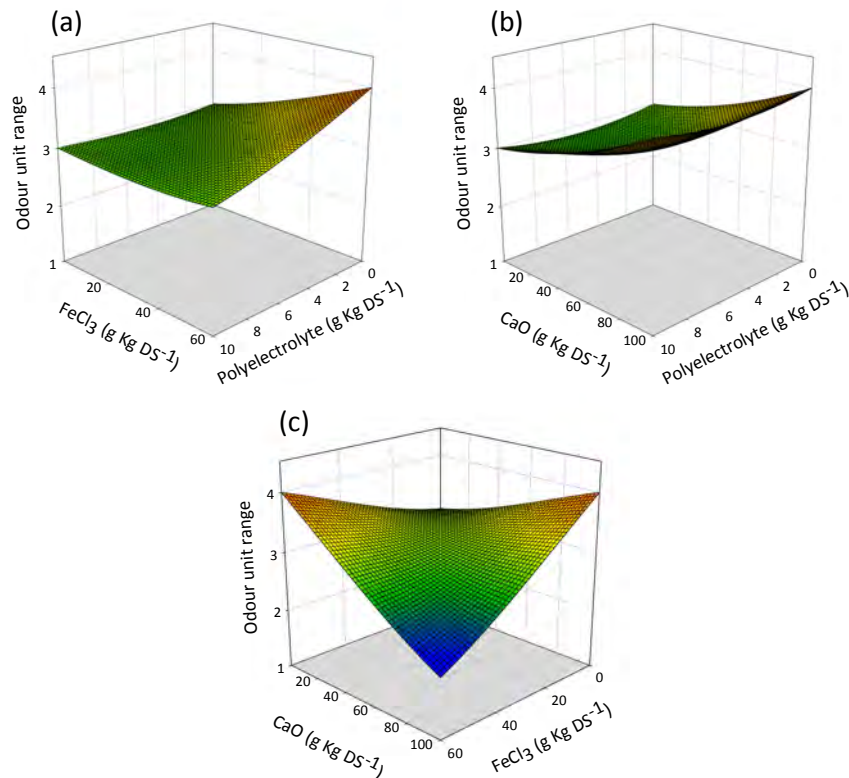


Figure 5.7 Three-dimensional response surface plots of odour emission showing the effect of variables: (a) FeCl₃-polyelectrolyte dose, (b) CaO-polyelectrolyte dose, and (c) CaO - FeCl₃ dose.

5.3.1.3. Model validation

A numerical optimization method employing desirability approach was used to optimise the response of the conditioning process (Amini et al., 2008). The numerical optimization found a point that maximises the desirability function. A minimum level of CST, TSC and odour emission, and the conditioners dosage within the tested ranges were set for maximum desirability criteria. Optimised conditions under specific constrains were obtained at 2.22 g Kg DS⁻¹ of polyelectrolyte, 60 g Kg DS⁻¹ of iron chloride and 100 g Kg DS⁻¹ of calcium oxide. The lowest dose of polyelectrolyte was chosen since the increase of this dose did not reduce further either sulphur compounds or odour emissions. Moreover, the use of low doses of polyelectrolyte avoids to increase cost of the process (Zhai et al., 2012) and the long-term risk to the surrounding environment associated with the its use (Yuan et al., 2011). Under the optimum conditions, the model predicts reduction percentages of 77% 54% and 50% for CST, TSC emission and odour emission, respectively. The obtained value of desirability (0.946) reveals that the estimated functions represent the experimental model and desired conditions. An additional experiment was carried out using the optimum conditions in order to verify the accuracy of the models proposed by RSM. The experimental results of CST, sulphur emissions and odour emissions under optimal

conditions were 29.3 s, 15.5 mg S m⁻³, 450-1077 OU_E m⁻³ (range 2), respectively. In these conditions, the measured concentration of H₂S, CS₂, MTM, DMS and DMDS in gas sample was 3.1, 1.2, 0.5, 1.6 and 1.8 mL m⁻³, respectively.

Table 5.5 shows the experimental response under optimal conditions compared with predicted response by the model. The close values obtained between experimental and predicted responses verify the model accuracy for the conditioning process.

Table 5.5 Verification experiment at optimal conditions

	Responses (% reduction)		
	Predicted	Experimental	Standard deviation
CST (s)	77.0	84.6	± 7.7
TSC emission (mg S m ⁻³)	54.1	48.0	± 6.4

5.3.2 Physical conditioning process

Figure 5.8 shows the effect of fly ash (FA) and activated carbon (AC) doses on the CST of the sewage sludge.

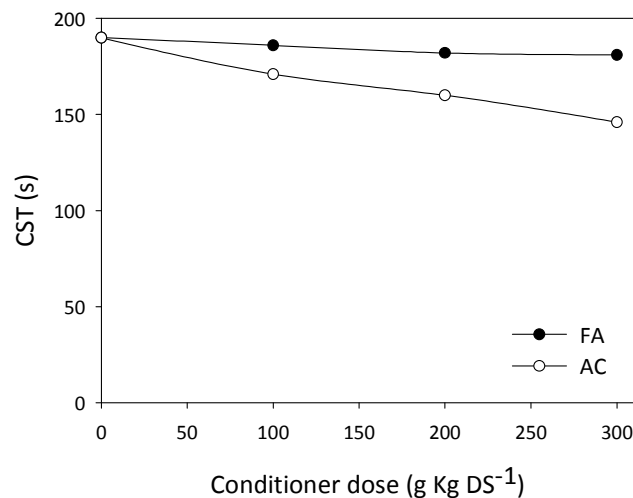


Figure 5.8 Effect of physical conditioners doses on the CST of the sludge

As mentioned above, the bounding of sludge particles to the surface of physical conditioners can act as draining media. This fact would favour the sludge dewaterability and therefore a reduction of CST value of the conditioned samples would be expected. Nevertheless, the addition of physical conditioners has an insignificant effect compared to the effect caused by chemical conditioners. A reduction of 5% and 25% on CST was obtained with the highest doses (300 g Kg DS⁻¹) of FA and AC, respectively. The same reductions on CST in oily sludge were achieved by Buyukkamaci and Kucukselek (2007) although a higher dose of fly ash was used for the same purpose (6% w/w of fly ash). However, the use of this last dose was more effective in the study conducted by Hwa and Jeyaseelan (1997) who obtained

reduction percentages around 80% in oily sludge. Although previous authors investigated the same typology of sewage sludge, the different characteristics of the sewage sludge determines the effectiveness of physical conditioners in the sewage sludge dewaterability.

The effect of physical conditioners addition on VSC emitted from conditioned sewage sludge is presented in Figure 5.9.

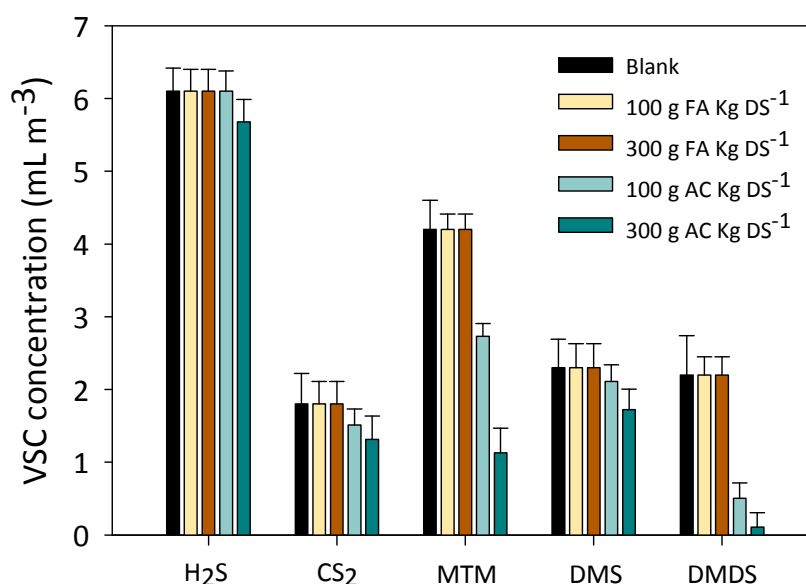


Figure 5.9 VSC concentration emitted from physical conditioned sludge during drying process.

VSC emissions have not been affected by the addition of FA into the sludge. Conversely, significant reductions on the release of VSC have been observed by means of the addition of AC as physical conditioner. All of VSCs, except H₂S, are reduced by the lowest dose of AC. These reductions were further notable using the highest dose of AC (300 g Kg DS⁻¹), especially for MTM and DMDS which were reduced about 73% and 89%, respectively.

Liu et al (2012) investigated the emission of odorous compounds during different chemical conditioning processes using coal fines as physical conditioners. The addition of coal fines together with iron chloride or calcium oxide slightly reduced the release of the odorous compounds such as ammonia or H₂S. One of the main differences between physical conditioners used in this conditioning process is the porosity of the materials. Fly ash has less surface area (30 m² g⁻¹) than the AC (875 m² g⁻¹). This textural property could explain the marked reduction of VSC emissions by the addition of AC onto sewage sludge. Thus, the VSC such as DMDS or MTM could be adsorbed onto AC from the liquid phase of sewage sludge during thermal drying process.

5.4 CONCLUSIONS

Chemical conditioning of sewage sludge using polyelectrolyte, iron chloride and calcium oxide was investigated in order to obtain higher dewaterability and low sulphur and odour emission. The individual assessment of the chemical conditioners reveals improvements on sludge dewaterability but an important increase of VSCs and odour emission during drying process. The pH conditions of conditioned samples play an important role on odour emissions, especially due to the formation of hydrogen sulphide and nitrogen compounds such as TMA. The combined optimisation of odour emissions and dewaterability was successfully achieved by using RSM. An additional experiment verified the model accuracy where the CST, TSC emission and odour emission were reduced 70%, 59%, 50% respectively, under optimal conditions.

Additionally, fly ash and activated carbon were used as physical conditioners. The enhancement of dewaterability by physical conditioners addition was not significant compared to chemical conditioners. Nevertheless, these conditioners had a marked effect on the reduction of VSC emissions, especially for DMDS and MTM.

INTEGRATION OF ADVANCED OXIDATION PROCESSES AT MILD CONDITIONS IN WET SCRUBBERS FOR ODOROUS SULPHUR COMPOUNDS TREATMENT

Adapted from:

Vega, E., Martin, M.J., Gonzalez-Olmos, R., 2014. *Integration of advanced oxidation processes at mild conditions in wet scrubbers for odorous sulphur compounds treatment. Chemosphere 109, 113-119*

6.1 BACKGROUND AND OBJECTIVES

The formation of chlorine by-products in wet scrubbers used for odour removal has led to the application of new oxidising agents such as hydroxyl radicals. These radicals are generated via advanced oxidation processes (AOP) and are used as oxidants in advanced oxidation scrubbers (AOS) instead of traditional oxidants. Thus, oxidants such as hydrogen peroxide or ozone, which can promote AOP have been recently investigated. AOS has been widely used for the removal of odorous compounds in the field of drinking water. However, a comparative study of different AOPs and their feasibility to be used in AOS has not been yet carried out.

Therefore, the main objective of the present chapter is to assess which is the optimal AOP that can be coupled into a wet scrubber for odour treatment. Thus, the advanced oxidation of an aqueous multicomponent mixture of VSC composed by ethyl mercaptan (ETM), dimethyl sulphide (DMS) and dimethyl disulphide (DMDS) is investigated. This study is focused on the use of UV/H₂O₂, H₂O₂/Fe²⁺, UV/H₂O₂/Fe²⁺ and O₃ at mild conditions (room temperature and pressure and pH around neutral). A comparative assessment regarding the oxidation efficiency and the total cost of each treatment is carried out.

6.2 METHODOLOGY

25 mL of a synthetic multicomponent solution containing 0.5 mg L⁻¹ of ETM, DMS and DMDS were treated by UV/H₂O₂, Fenton, photo-Fenton and ozone treatments using the same molar concentration of oxidants. The measurement of VSC concentration in headspace volume allowed the determination of oxidation degree in liquid phase as well as the mineralisation degree by the measurement of sulphate in liquid phase. Moreover, the oxidants consumption for each treatment was also measured. From all collected data, the total annual cost of each treatment for their implementation in a full-scale system was estimated. Figure 6.1 shows the diagram of the methodology used in this chapter. For further details about experimental and analytical procedures used, please refer to the materials and methods section indicated between brackets.



Figure 6.1 Diagram of methodology used in AOPs for VSC removal.

6.3 RESULTS AND DISCUSSION

6.3.1 Oxidation by UV/H₂O₂ treatment

Figure 6.2 shows the oxidation percentage of the ETM, DMS and DMDS during the UV/H₂O₂ treatment using 0.20 mM of hydrogen peroxide at neutral pH. The oxidation percentage was calculated as the % ratio between the concentration of the VSC at a given time and its initial concentration. The oxidation percentage of total sulphur compounds (TSC), which is defined as the sum of ETM, DMS plus DMDS (mg S L⁻¹) contained in water, is also plotted.

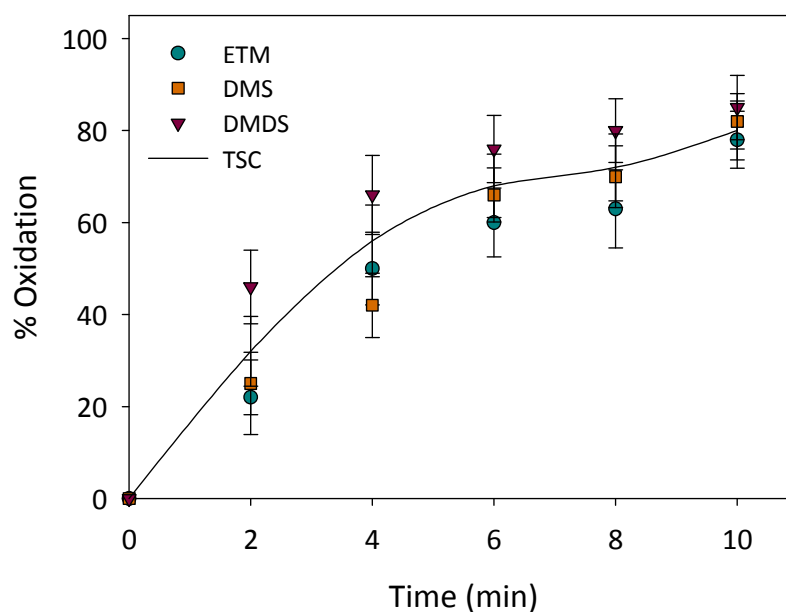


Figure 6.2 Oxidation percentages of ETM (circle), DMS (square), DMDS (triangle) and TSC (line) during UV/H₂O₂ treatment with $C_{0,H_2O_2} = 0.20$ mM;

At the end of the experiment (10 minutes) the oxidation percentage of the TSC was around 80%. Photolysis of H_2O_2 generates hydroxyl radicals by a direct process with a yield of two radicals formed per photon absorbed at 254 nm (Eq. 6.1) (Tuhkanen, 2004)



The reactivity of DMS and DMDS with hydroxyl radicals in liquid phase has been previously studied by several authors (Bonifačić et al., 1975a, Bonifačić et al., 1975b). As it is observed, the oxidation percentage of the mentioned compounds is similar, what is in agreement with the published reaction rate constants of DMS and DMDS with hydroxyl radicals ($K_{\text{DMS}/\cdot\text{OH}} = 1.9 \cdot 10^{10} \text{ M}^{-1} \text{ s}^{-1}$ and $K_{\text{DMDS}/\cdot\text{OH}} = 1.7 \cdot 10^{10} \text{ M}^{-1} \text{ s}^{-1}$). The hydrogen peroxide consumption was around 43% at the end of the reaction (0.086 mM) which is a concentration around 2 times lower than the stoichiometric amount needed for the complete oxidation of the multicomponent VSCs mixture.

On the other hand, different concentrations of hydrogen peroxide (0.20, 2.00 and 4.00 mM) were tested in order to study the influence of the oxidant concentration in the treatment (Figure 6.3).

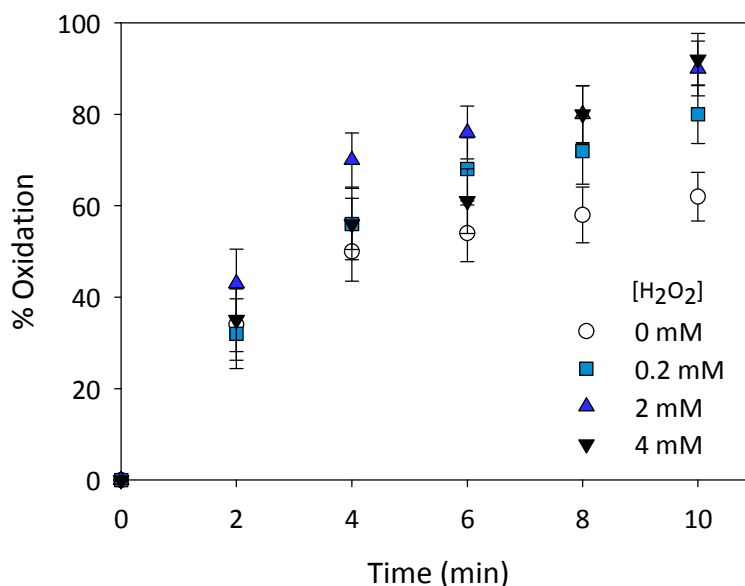


Figure 6.3 Effect of the H_2O_2 concentration in the oxidation of TSC during UV/ H_2O_2 treatment

$$C_{0,\text{TSC}} = 0.85 \text{ mg L}^{-1}$$

Higher oxidation percentages were obtained as the hydrogen peroxide concentration was increased up to 2 mM. The highest concentration of hydrogen peroxide (4 mM) did not cause significant improvement either in the oxidation rate or the oxidation percentages at the end of treatments. These results are explained by an excessive hydrogen peroxide concentration which scavenges the radicals according to the Eq. 6.2 (Tuhkanen, 2004).



It has to be highlighted that in the UV/H₂O₂ treatment both the UV photolysis and oxidation by a hydroxyl radical mechanisms take part. Thus, the UV-photolysis was carried out in order to ascertain the contribution of the sole presence of UV light in the UV/H₂O₂ treatment.

In UV treatment (Fig. 6.4a), the TSC oxidation was around 60% after 10 min of the reaction, while using H₂O₂ as a radical promoter (UV/H₂O₂), the oxidation was increased up to 80%. These results clearly point out that the effect of the UV photolysis is significant in the UV/H₂O₂. Furthermore, similar trends in the oxidation profiles were observed for ETM and DMDS achieving oxidation efficiencies around 70% and 80%, respectively, after 10 min. It was observed that ETM and DMDS were rapidly oxidised in the first minutes of the experiment. About 40% of DMS was oxidised in 10 min and the oxidation profile was more linear compared to the others compounds. The observed trends for each VSC are in agreement with their UV absorbance at 254 nm (Fig. 6.4b). The studied compounds absorb different amounts of radiation at 254 nm, being DMDS the compound which absorbs more radiation and DMS which absorbs less. So DMDS can absorb more photons at this wavelength with more energy to rise to excited electronic states which yields the S-S bond cleavage (Bookwalter et al., 1995).

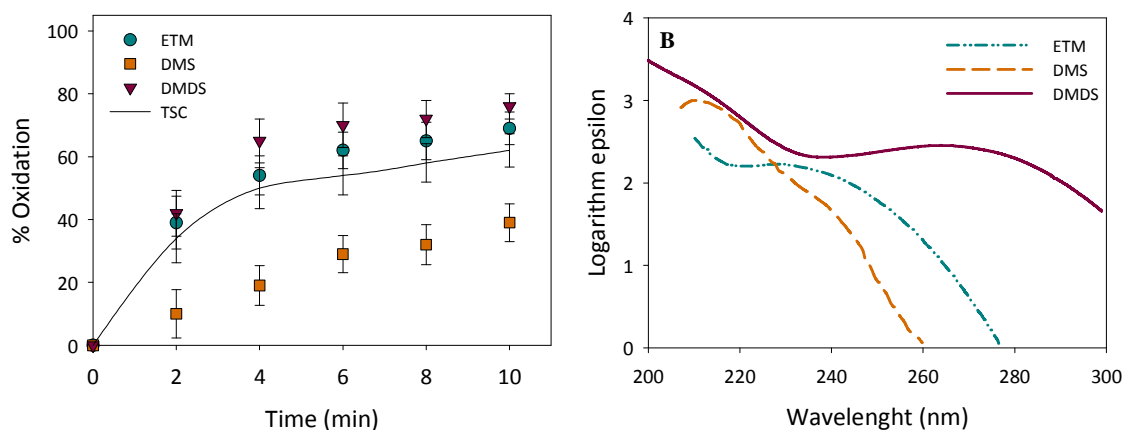


Figure 6.4 UV treatments: (A) oxidation percentages of ETM (circle), DMS (square), DMDS (triangle) and TSC (line) and (B) UV/VIS spectrum of the studied VSCs.

6.3.2 Oxidation by H₂O₂/Fe²⁺ and UV/H₂O₂/Fe²⁺ treatments

Figure 6.5 shows the oxidation percentage of the studied VSCs during the Fenton treatment using 0.20 mM of hydrogen peroxide, 0.018 mM of iron and neutral pH.

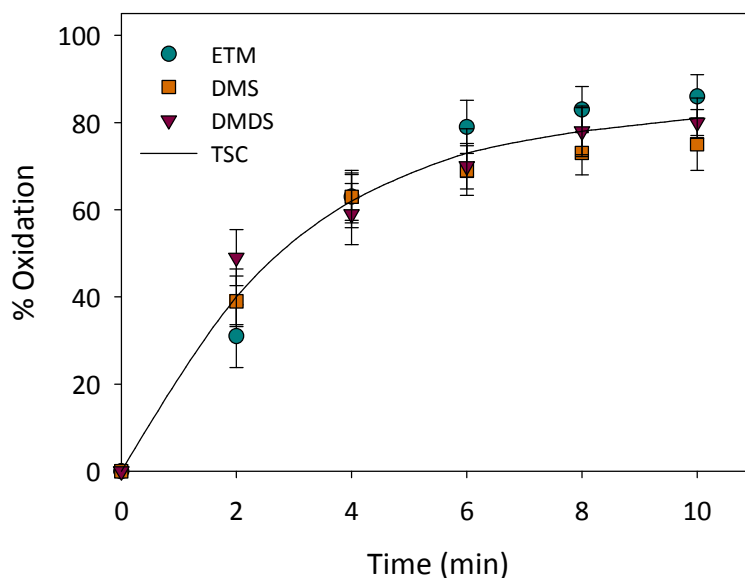


Figure 6.5 Oxidation percentages of ETM (circle), DMS (square), DMDS (triangle) and TSC (line) during Fenton reaction with $C_{0,H_2O_2} = 0.20$ mM and $C_{0,Fe^{2+}} = 0.018$ mM

At the end of the experiment, the oxidation percentage of the TSC was around 81% and the hydrogen peroxide consumption was 72% (0.14 mM). This consumption is higher than in UV/H₂O₂ treatment and closer to the theoretical amount needed for a total mineralisation of the VSCs. During the Fenton treatment hydroxyl radicals are generated through a well-known mechanism (Pignatello et al., 2006) which is summarised with the Eqs. 6.3 and 6.4.



It has to be highlighted that the difference in oxidation efficiencies among the three compounds is lower for Fenton treatment compared with UV/H₂O₂. This fact points out a significant effect of the UV photolysis on VSC removal. Thus, the VSCs are oxidised to the same extent in those treatments where the effect of light is reduced.

As it has been mentioned previously, the Fenton treatment is much more efficient at acid pH since iron remains in solution. If the amount of iron used is low and/or organic matter is present, as in the case of this experiment, it is possible that iron could form complexes and remains partially in solution. In order to check this, the precipitated iron fraction in this experiment before adding the hydrogen peroxide was analysed. The measurement of the dissolved iron concentration was carried out after filtering at 0.2 μ m the synthetic multicomponent solution with 0.018 mM of Fe²⁺ at neutral pH. The obtained results revealed that more than 95% of the initial iron content was in solution before the addition of hydrogen peroxide.

On the other hand, different Fe^{2+} concentrations (0.004, 0.009 and 0.018 mM) were tested in order to study their influence in the Fenton treatment at neutral pH (Figure 6.6).

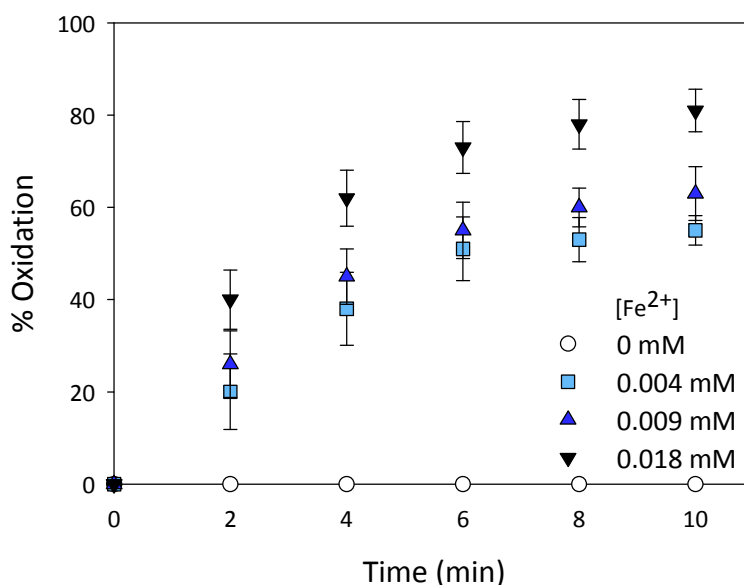


Figure 6.6 Effect of the Fe^{2+} concentration in the oxidation of TSC during Fenton treatment with $C_{0,\text{H}_2\text{O}_2} = 0.20 \text{ mM}$, $C_{0,\text{TSC}} = 0.85 \text{ mg L}^{-1}$

As it was expected, the increase in the dosage of Fe^{2+} caused a higher oxidation percentage of the VSCs. Blanks experiments were carried out in order to determine the effect of the sole presence of H_2O_2 (0.20 mM) or Fe^{2+} (0.018 mM) on the VSC oxidation. In both cases, the contribution to the VSCs oxidation was negligible in agreement with the results reported by Couvert et al. (2006).

In order to evaluate the oxidation of VSC with the photo-Fenton treatment, the established doses of H_2O_2 (0.20 mM) and Fe^{2+} (0.018 mM) were used. The oxidation percentages of TSC during photo-Fenton treatment are also shown in Fig. 6.7. The oxidation of TSC after 2 min of reaction was above 40% in the case of the Fenton treatment while it was higher than 75% by the simultaneous presence of the UV light and Fenton's reagents. The consumption of the hydrogen peroxide at 10 min of the photo-Fenton reaction was complete (0.2 mM). The important improvement observed in VSC oxidation in photo-Fenton reaction is due to the photocatalytic reduction of the Fe^{3+} generated back to Fe^{2+} , resulting in an overall increase in the production of hydroxyl radicals (Eqs. 5.3 and 5.5) as compared to Fenton treatment (Eqs. 5.3 and 5.4).



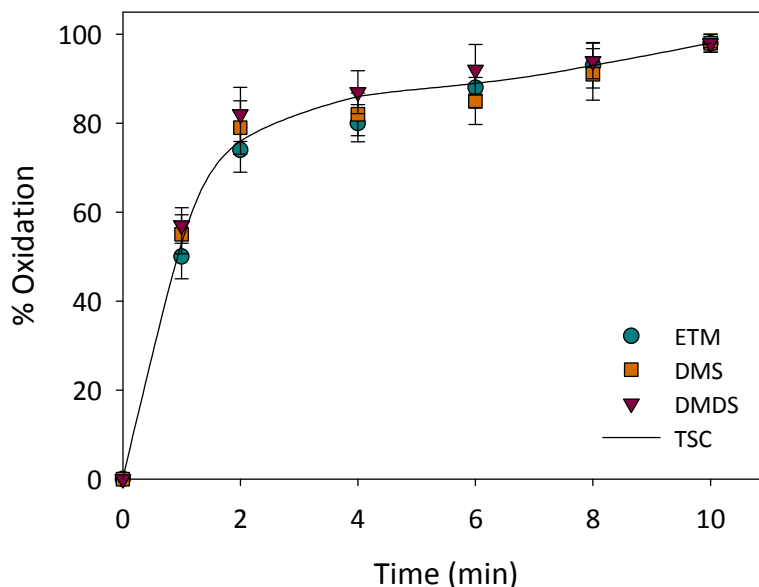


Figure 6.7 Oxidation percentages of ETM (circle), DMS (square), DMDS (triangle) and TSC (line) during photo-Fenton reaction with $C_{O_2} = 0.20$ mM and $C_{Fe^{2+}} = 0.018$ Mm

6.3.3 Oxidation by ozone treatment

Ozone can react through two pathways with organic substrates in water: direct oxidation with molecular ozone which is slow compared to hydroxyl radical oxidation and oxidation through hydroxyl radicals formed by ozone decomposition. In the case of VSCs the differences between both oxidation mechanisms can be important. As an example, for DMS the rate constant in aqueous phase with hydroxyl radical is higher by two orders of magnitude than that with ozone ($K_{DMS/\cdot OH} = 1.9 \cdot 10^{10} \text{ M}^{-1} \text{ s}^{-1}$ and $K_{DMS/O_3} = 4.0 \cdot 10^8 \text{ M}^{-1} \text{ s}^{-1}$) (Bonifačić et al., 1975a) (Lee and Zhou, 1994). Under acidic conditions the ozone pathway is of primary importance while under conditions such as high pH, exposure to UV or addition of hydrogen peroxide, the hydroxyl radical oxidation dominates. The oxidation percentages obtained by the ozone treatment using 0.20 mM of ozone are shown in Fig. 6.8.

The results show a complete oxidation of sulphur compounds from the fourth minute of the treatment and the consumption of ozone was complete at the end of the reaction. The fast oxidation percentages achieved with ozone, similar or even higher than those observed in other oxidation treatments with well-known radical mechanisms such as Fenton and photo-Fenton experiments, could indicate that the reaction was mainly driven by a radical mechanism instead of oxidation by molecular ozone.

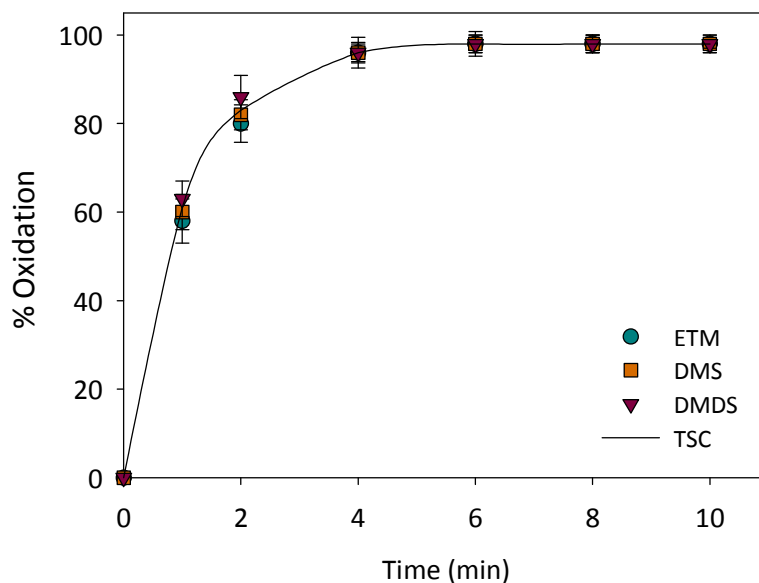


Figure 6.8 Oxidation percentages of ETM (circle), DMS (square), DMDS (triangle) and TSC (line) during ozone treatment with $C_{0,O_3} = 0.20$ mM

The effect of ozone concentration in the oxidation of TSC during ozone treatment was also studied (Figure 6.9). The increase of the ozone dosage to 0.4 mM yielded the complete oxidation of VSCs at the beginning of the experiment while the TSC were not oxidised by the lowest concentration of ozone (0.02 mM). It is also interesting to note that the plateau reached in the TSC oxidation percentage using 0.1 mM which is explained by the absence of ozone at this time due to the complete decomposition/consumption of ozone in water solution.

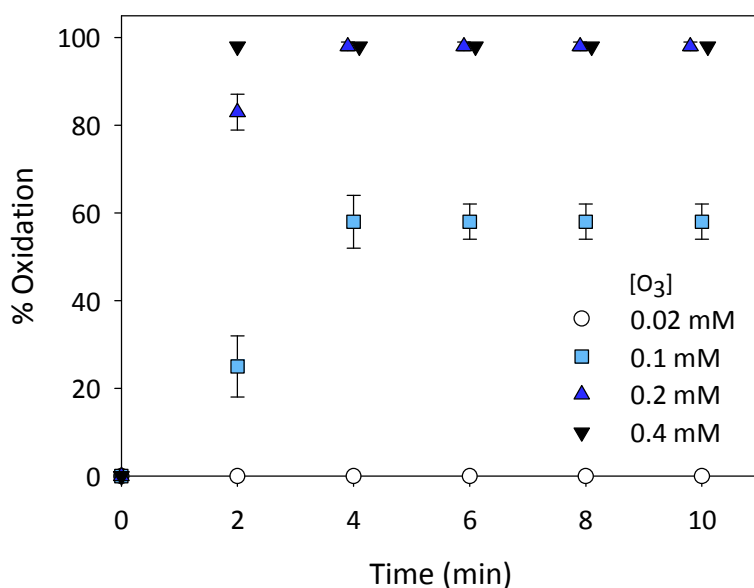


Figure 6.9 Effect of the O_3 concentration in the oxidation of TSC during ozone treatment $C_{0,TSC} = 0.85$ mg L⁻¹

6.3.4 Treatment comparison

All the processes were evaluated and compared by means of the efficiencies observed and the estimated total cost of each treatment. Table 6.1 shows the oxidation percentages of ETM, DMS, DMDS and the TSC, the mineralisation degree achieved and the oxidant consumption percentage for the tested treatments at 10 minutes.

Despite the different oxidation efficiencies among the studied compounds in the early stages of treatments, these differences were reduced at 10 min, achieving oxidation percentages above 75% for all tested treatments. Certainly, the photo-Fenton and the ozone were the treatments which achieved the highest oxidation percentage at 10 min. The degradation of the TSC is also evaluated and similar results were observed. The sulphur content as sulphate (SO_4^{2-} -S) of the aqueous phase at the end of each experiment was analysed to determine the mineralisation degree under the experimental conditions tested. Taking into account the initial total amount of sulphur compounds contained in water (0.85 mg S L^{-1}) and the amount of sulphur as sulphate obtained at the end of the treatments, the sulphur mass balance was calculated.

The results indicated that around 70% and 60% of the initial sulphur content was mineralised and was found as SO_4^{2-} in the solution by means of the photo-Fenton and ozone treatments, respectively. These results are in agreement with the study of Ma et al. (2013) who revealed that the oxidation of ETM by hydroxyl radicals yields the production of sulphate ions. Contrarily, these results are not in concordance with Krüger et al. (2009) who stated that most of SO_2 produced in the DMDS oxidation by means of Fenton process was volatilised, while a small amount was solubilised as SO_4^{2-} . The formation of the sulphate ions points to the cleavage of the C-S, S-S and S-H bonds in the studied oxidation processes. During the different treatments, neither elemental sulphur nor peaks associated to other sulphur compounds were detected. This is explained either by the possible formation of soluble non-volatile sulphur compounds which would not be transferred to the headspace and/or the low concentration of the generated sulphur compounds which could be below the detection limits of GC/PFPD as well as the IC. In the case of UV/ H_2O_2 and Fenton treatments, the mineralization degrees (54% and 58% respectively) were similar despite having different hydrogen peroxide consumptions (43% and 72%). This fact is explained by the competition for hydroxyl radical between Fe^{2+} and organic sulphur compounds in solution, leading to the non-productive decomposition of hydrogen peroxide and thereby consuming more amount of it (Neyens and Baeyens, 2003).

On the other hand, during the different AOPs the pHs were reduced among 0.2-0.5 pH units at the end of the reaction. This could be caused mainly by the generation of SO_4^{2-} or the formation of short chain organic acids. Ma et al. (2013) detected the formation of acetic acid during the first stages of the oxidation of ETM with hydroxyl radicals.

The application of AOPs in a full-scale system depends on the economic viability. Although the costs in full-scale systems are related to the nature and concentration of pollutant, the effluent flow rate and the configuration of the reactor (Andreozi et al., 1999), the costs estimation in lab-scale systems can be considered exclusively for comparative purpose. A cost estimation of different AOPs was calculated taking into account both capital cost (amortised annual capital cost) and operating cost (reagents and electrical cost) according to the methodology proposed by (Mahamuni and Adewuyi, 2010). The reagents and electricity consumptions were estimated based on a design flow of $0.05 \text{ m}^3 \text{ s}^{-1}$ of treated water (flow rate in wet scrubber installed in a wastewater treatment plant in Barcelona, which treats $11.6 \text{ m}^3 \text{ s}^{-1}$ of gas). The pseudo-first order rate constants (k, min^{-1}) were estimating using the half-life ($t_{0.5}, \text{min}$) of the TSC during each reaction.

For the economical assessment, a 90% of VSC removal efficiency was considered. Table 6.2 shows the design parameters such as k , the required time for 90% oxidation of TSC (t_{90}) and reactor volume, used to calculate the water treatment cost. Moreover, the amortised costs of the investment and the operational costs of each treatment are also presented. Specific details about the economic analysis are presented in Table 6.3.

Larger reactor volumes are required for UV/H₂O₂ and Fenton (40.2 and 33.5 m^3 , respectively) as compared with photo-Fenton (8.9 m^3) and ozone (7.8 m^3) according to the kinetic rates obtained in these treatments. The UV/H₂O₂ treatment shows the highest cost (0.384 € m^{-3}) because of the large reactor volume required and the high energy consumption. On the other hand, Fenton treatment has the lowest cost (0.058 € m^{-3}) since low power is required for this treatment. The energy consumption of photo-Fenton and ozone treatments involves a higher water treatment cost (0.120 and 0.133 € m^{-3} , respectively). It has to be highlighted that the reactor volume plays an important role in the full-scale design. Although the cost of these treatments are twice that of Fenton cost, photo-Fenton and ozone could be the most interesting option when in the engineering design there are space constraints or retrofitting complexities.

Table 6.1 Oxidation percentages of VSC (ETM, DMS, DMDS and TSC), the mineralisation degree achieved and the oxidant consumption percentage of the studied AOPs at 10 minutes

	VSC				mineralisation	Oxidant consumption
	ETM	DMS	DMDS	TSC		
UV/H ₂ O ₂ ^a	78 ± 5	82 ± 6	85 ± 7	80 ± 6	54 ± 7	43 ± 6
H ₂ O ₂ / Fe ²⁺ ^b	86 ± 5	75 ± 8	80 ± 5	81 ± 6	58 ± 11	72 ± 5
UV/H ₂ O ₂ / Fe ²⁺ ^b	98 ± 2	98 ± 2	98 ± 1	98 ± 2	70 ± 10	99 ± 1
O ₃ ^c	98 ± 2	98 ± 2	98 ± 1	98 ± 2	62 ± 14	99 ± 1

^a C_{0,H2O2} = 0.20 mM ;^b C_{0,H2O2} = 0.20 mM and C_{0,Fe²⁺} = 0.018 mM^c C_{0,O3} = 0.20 mM.**Table 6.2** Design parameters (pseudo-first order kinetics (k), the required time for 90% oxidation of TSC (t₉₀) and reactor volume (V_{reactor})) and the total costs of the studied AOPs.

	k (min ⁻¹)	t ₉₀ (min)	V _{reactor} (m ³)	Total cost (€ m ⁻³)		
				Amortised	Operational	Water treatment
UV/H ₂ O ₂ ^a	0.17	13.39	40.17	0.141	0.241	0.384
H ₂ O ₂ / Fe ²⁺ ^b	0.20	11.18	33.54	0.048	0.009	0.058
UV/H ₂ O ₂ / Fe ²⁺ ^b	0.77	2.98	8.94	0.058	0.061	0.120
O ₃ ^c	0.88	2.60	7.80	0.041	0.091	0.133

^a C_{0,H2O2} = 0.20 mM ;^b C_{0,H2O2} = 0.20 mM and C_{0,Fe²⁺} = 0.018 mM^c C_{0,O3} = 0.20 mM.

Table 6.3 Total annual cost of water treatment by the studied AOPs

CAPITAL COSTS										
	t_{90} (min)	Volume AOP reactor (m ³)	Energy (KW) ^a	n device ^b	Capital cost (€)					
					AOP reactor ^c	Piping + site work	Contractor O&P	Engineering	Total capital	Amortised capital cost ^d
UV/H ₂ O ₂	13.39	40.17	602.5	3012	1065868	1492216	1716048	1973456	2368147	223536
Fenton	11.18	33.54	0	1	367000	513800	590870	679500	815400	76968
Photo-Fenton	2.98	8.94	134.1	670	439862	615807	708178	814405	977286	92248
Ozone	2.6	7.80	234.0	1	314000	439600	505540	581371	697645	65852

^a The required energy was estimated based on a flow rate of 3000 l min⁻¹, the UV power density of 15 W/L and the O₃ density power of 30 W/L.

^b The energy supplied by a single unit of UV is 200W.

^c Cost of AOP based on the cost established by Mahamuni et al. 2010. The reactor material cost calculated using SuperPro Designer 8 has also been considered.

^d The total capital cost was amortised at a rate of 7% over a period of 20 years.

OPERATING COSTS						
	t_{90} (min)	Volume AOP reactor (m ³)	Energy (KW)	Annual electrical cost (€) ^e	Annual chemical cost (€) ^f	Operating cost (€)
UV/H ₂ O ₂	13.39	40.17	602.5	369483	11814	381297
Fenton	11.18	33.54	0	0	15163	15163
Photo-Fenton	2.98	8.94	134.1	82230	15163	97393
Ozone	2.6	7.80	234.0	143488	0	143488

^e Estimated taking into account the plant is running 8760 h year⁻¹ and electricity price in Spain (0.07 € kWh⁻¹)

^f Estimated taking into account the price of the hydrogen peroxide and iron chloride, 0.45 € Kg⁻¹ and 0.72 € Kg⁻¹, respectively.

TOTAL ANNUAL COSTS		
	Total annual cost (€)	Water treatment cost (€ m ⁻³) ^g
UV/H ₂ O ₂	604834	0.384
Fenton	92131	0.058
Photo-Fenton	189642	0.120
Ozone	209341	0.133

^g Water treatment cost based on the total amount of water treated in a year of 1576800 m³

6.4 CONCLUSIONS

The effectiveness of different AOPs on the oxidation of a multicomponent aqueous solution containing ETM, DMS and DMDS was investigated with the objective to assess which is the most suitable treatment to be coupled in a wet scrubber used in odour treatment facilities. UV/H₂O₂, Fenton, photo-Fenton and ozone were tested at mild conditions and the oxidation efficiencies obtained in each treatment were compared. The studied AOPs at mild conditions demonstrated to be suitable for removal of the studied VSCs. Photo-Fenton and ozone were the more efficient treatments, achieving up to a 95% of sulphur compounds oxidation in 10 minutes. Moreover, these mentioned treatments yielded a higher degree of mineralization (70%) than the other studied AOPs. The high conversion of sulphur atom in VSCs to SO₄²⁻ implies that high deodorization performance can be achieved via the coupling of wet scrubbers with these treatments.

Regarding the economic analysis, the Fenton treatment is the most economical option for the VSCs removal if there are no space constraints to install the required reactor volume. In the case of reactor volume limitations or retrofitting complexities, the ozone and photo-Fenton treatments should be considered as viable alternatives.

**ADSORPTION OF VOLATILE SULPHUR
COMPOUNDS ONTO MODIFIED ACTIVATED
CARBONS:
EFFECT OF OXYGEN FUNCTIONAL GROUPS**

Adapted from:

Vega, E., Lemus, J., Anfruns, A., Gonzalez-Olmos, R., Palomar, J., Martin, M.J., 2013. Adsorption of volatile sulphur compounds onto modified activated carbons: effect of oxygen functional groups. *Journal of Hazardous Materials* 258-259, 77-83.

7.1 BACKGROUND AND OBJECTIVES

The adsorption capacity of an activated carbon (AC) is well known to be highly influenced by its physical or porous structure but also by its chemical nature. The use of oxidising agents is the most commonly used technique to modify the surface chemistry of AC for improving its performance by means of the fixation of a high number of oxygen functional groups onto AC surface. Despite the application of AC has been further investigated for the removal of odour-causing compounds, few studies report about volatile sulphur compounds (VSC) adsorption at low concentration. Moreover, the role of oxygen functional groups onto AC in VSC adsorption process has not been deeply investigated.

Thus, the main objective is to investigate the effect of surface chemistry modifications in a commercial AC, by means of nitric acid and ozone oxidations, in the adsorption of ethyl mercaptan (ETM), dimethyl sulphide (DMS) and dimethyl disulphide (DMDS) at low concentration (below 4 ppm v/v). Finally, the predictive model quantum-chemical COSMO-RS (Conductor-like Screening Model for Real Solvents) model developed by Klamt et al. (2000) which is applied to predict thermodynamic data of adsorption (Mehler et al., 2002; Palomar et al., 2009; Lemus et al., 2012a; Lemus et al., 2012b) and absorption (Gonzalez-Miquel et al., 2011; Palomar et al., 2011a; Palomar et al., 2011b), was used to simulate the studied adsorption phenomena. The COSMO-RS model is useful tool to establish the role of oxygen containing surface functional groups for a future design of tailor-made adsorbents.

7.2 METHODOLOGY

Different ACs were tested for ETM, DMS and DMDS adsorption by means of dynamic adsorption tests. A commercial activated carbon (AC-R) was modified by nitric acid (AC-N) and ozone (AC-O30 and AC-O60) and their chemical and textural properties were characterised by TPD, XPS and $\text{pH}_{\text{slurry}}$ analysis. The adsorption tests were conducted in a fix-bed reactor at low inlet concentration of target compounds (4 ppmv) and the adsorption capacities were determined by the obtained breakthrough curves using GC/PFPD. Furthermore, the computational analysis was used to simulate the studied adsorption phenomena between VSC and oxygen functional groups in AC surface. Figure 7.1 shows the diagram of the methodology used in this chapter. For further details about experimental and analytical procedures used, please refer to the materials and methods section indicated between brackets.

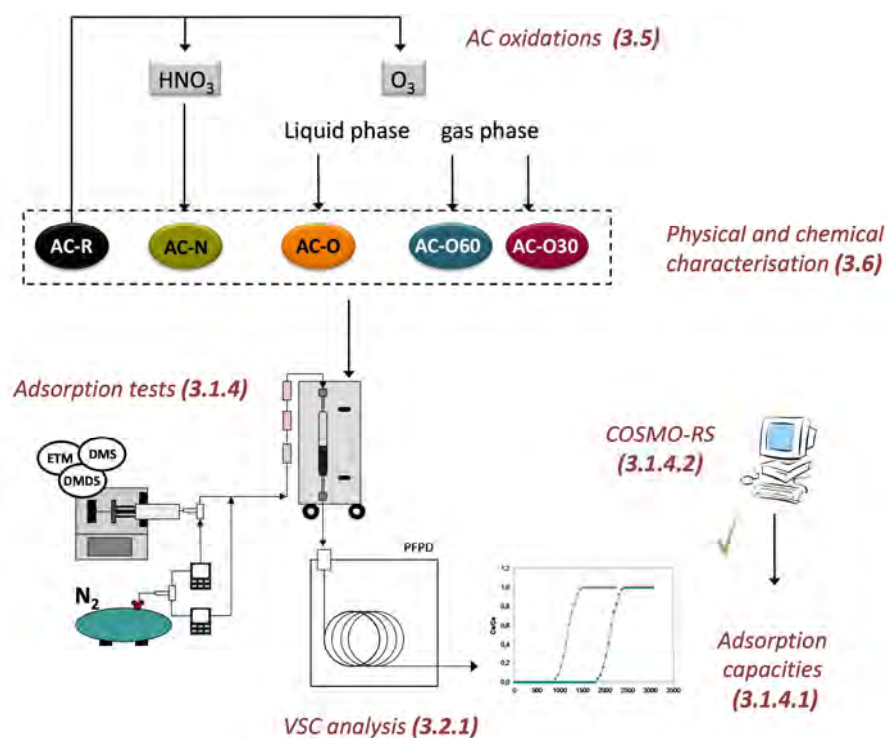


Figure 7.1 Diagram of methodology used in dynamic adsorption tests.

7.3 RESULTS AND DISCUSSION

7.3.1 As-received AC adsorption tests

The adsorption capacities of the AC-R were studied using dynamic adsorption tests. All adsorption tests were performed in N₂ stream in order to avoid chemical transformations of the studied VSCs. The obtained breakthrough curves for ETM, DMS and DMDS on AC-R are shown in Figure 7.2. The BT for DMDS is two-fold and five-fold to ETM and DMS respectively.

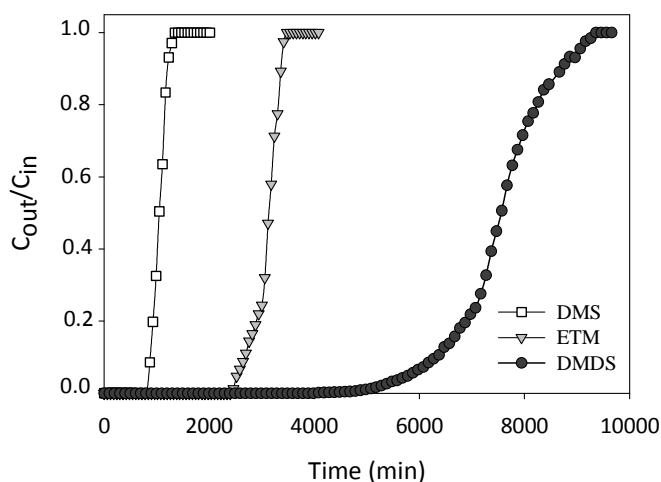


Figure 7.2 Breakthrough curves for ETM, DMS and DMDS on AC-R.

The COSMO-RS model was used to predict the Henry's constants (K_H) (partition coefficient between gas phase and AC) of the studied VSCs (ETM, DMS and DMDS). Table 7.1 shows the Henry's constant values for the studied VSCs and the functionalization AC models obtained by COSMO-RS.

Table 7.1 Henry's constant (bar) for different volatile sulphur compounds (ETM, DMS and DMDS) and the AC models (Scheme 1) predicted by COSMO-RS at 25 °C.

Model scheme	Functionalization	ETM	DMS	DMDS
AC	none	0.410	0.488	0.021
AC-COOCO	carboxylic anhydride	0.364	0.464	0.020
AC-OH	hydroxyl	0.159	0.149	0.020
AC-COOH	carboxylic acid	0.370	0.410	0.029
AC-CO	carbonyl	0.372	0.493	0.021

According to these results, the adsorption capacities followed the order DMDS \gg ETM $>$ DMS for AC model (not functionalised). The expected behaviour predicted by molecular model was experimentally confirmed by AC-R adsorption tests (Figure 7.2).

7.3.2 Surface characterization of oxidised ACs

According to the literature, the oxygen functional groups enrichment on the AC surface can improve the interaction between VSCs and AC, resulting in higher adsorption capacities (Bashkova et al., 2003, 2005; Cui and Turn, 2009; Cui et al., 2009; Lee et al., 2010). Therefore, the possible interactions between the different incorporated oxygen functionalities in the surface and sulphur compounds were also evaluated with COSMO-RS. This assessment was carried out using different molecular models of AC with a wide variety of functional groups. The predicted K_H indicated that the adsorption capacity can be modified depending on the nature of organic oxygen species of the AC surface (Table 7.1). Thus, the presence of HB-acceptor fragments, as hydroxyl groups (AC-OH model), can enhance the solute-AC interactions, and, consequently, increase the adsorption uptake in some extent, being this effect more significant with ETM and DMS. Furthermore, the model predicted that the DMDS adsorption was not affected by the presence of oxygen functional groups in the surface of ACs.

As mentioned before, the oxidation of AC leads to an increase in the concentration of oxygen functional groups in the AC surface. In order to study the surface chemistry of the studied ACs, the oxygen functional groups content was determined by TPD. The TPD profiles of the modified ACs indicated significant surface changes caused by the different oxidation treatments. The CO and CO₂ spectra (Figure 7.3a and Figure 7.3b, respectively) showed an important increase in the amount of CO and CO₂ evolved for all the oxidised ACs samples, especially for AC-N.

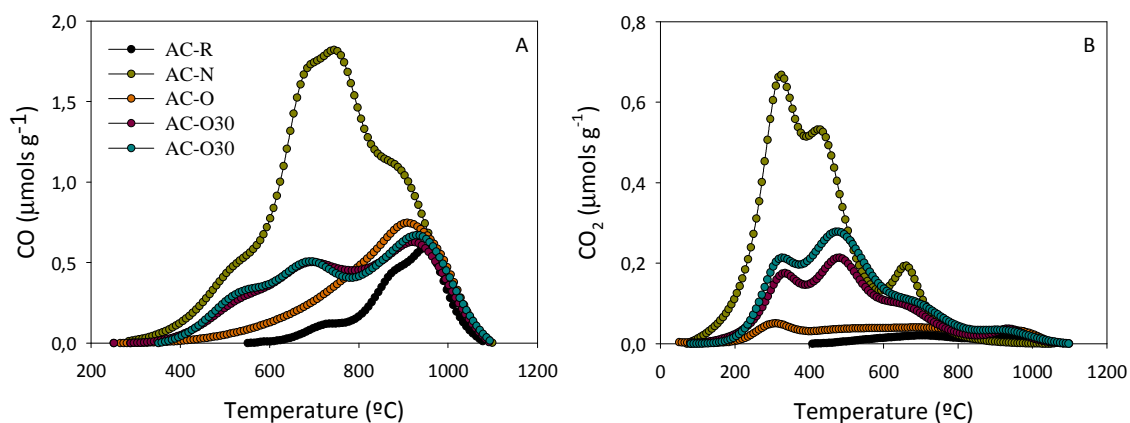


Figure 7.3 TPD spectra profiles for AC samples: (A) CO evolution; (B) CO₂ evolution.

In order to analyse which type of oxygen groups are responsible for CO and CO₂ emission, TPD spectra profiles were deconvoluted according to the literature (Figueiredo et al., 1999, 2007; Figueiredo and Pereira, 2010). The corresponding assessment of the different oxygen surface groups is shown in Table 7.2 and confirmed that the treatment with nitric acid leads to a high concentration of surface oxygen groups on AC surface. It is noteworthy that groups with donor character such as hydroxyl and carboxyl, were majority in the chemical composition of AC-N.

On the other hand, ozonised ACs presented a lower amount of incorporated groups. Unlike the AC-N, ozonised ACs had a significant enrichment in anhydric and carbonyl groups. The ozonisation in gas phase (AC-O30 and AC-O60) incorporated more oxygen functional groups than the ozonisation in water phase (AC-O). The samples AC-O30 and AC-O60 did not exhibit significant differences between them despite extending the ozonisation time. The significant increase of carboxylic groups which evolved CO₂ in a greater proportion than the groups which decompose in CO, leads to a decrease of CO/CO₂ ratio in the oxidised materials. Moreover, the incorporation of carboxylic groups with a higher acidic character, cause a decrease in the pH_{slurry} of oxidised samples. Thus, lower values of pH slurry could be related to lower CO/CO₂ ratio.

Table 7.2 Assessment of oxygen surface groups obtained by TPD, CO/CO₂ ratio and pH_{slurry} for the as-received and oxidised ACs.

	AC-R	AC-N	AC-O	AC-O30	AC-O60
CO ₂ total (μmol g ⁻¹)	53	1282	210	491	625
Carboxylic	4	662	25	152	147
Anhydric	7	481	63	212	300
Lactonic	42	139	122	127	136
CO total (μmol g ⁻¹)	456	3459	913	1349	1459
Anhydric	0	185	103	191	233
Phenolic	64	1849	344	514	519
Carbonylic	392	1425	467	644	706
CO/CO ₂ ratio	6.2	2.7	3.7	2.6	2.3
pH _{slurry}	7.6	3.4	5.8	4.7	4.0

In addition, the chemical composition of the few uppermost layers of the ACs was determined by XPS technique. The XPS spectra in C (1s) and O (1s) spectral regions were obtained for all studied samples and are shown in Figure 7.4.

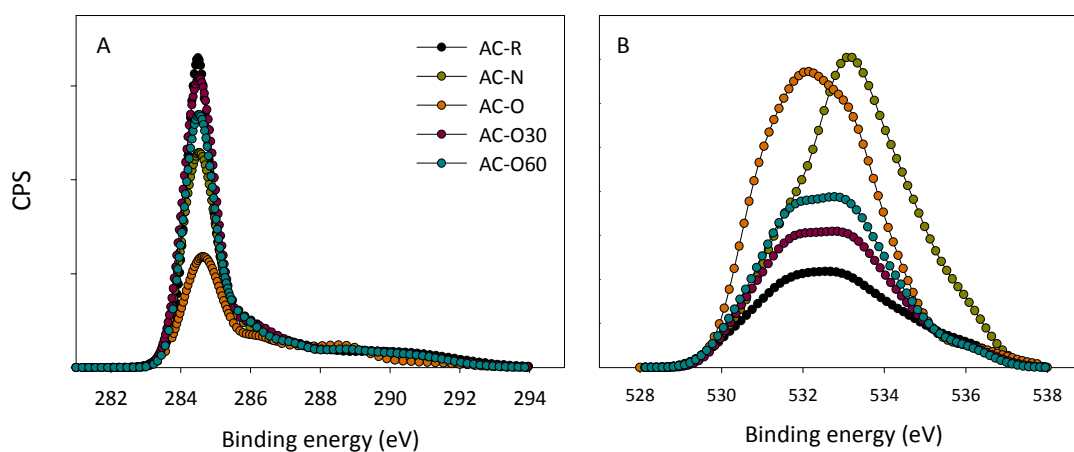


Figure 7.4 XPS spectra profiles for carbon samples: (A) C (1s) spectral region; (B) O (1s) spectral region.

In C (1s) spectra no significant differences was observed between all the studied ACs (Figure 7.4a). On the contrary, in O (1s) region, higher peaks were observed for all modified materials, especially in the case of AC-O and AC-N (Figure 7.4b). This means that these materials had a higher incorporation of oxygen groups in the external surface. The XPS curves were deconvoluted according to literature criteria (Moreno-Castilla et al., 2000; Rey et al., 2008; Figueiredo and Pereira, 2010) in order to study which are the most significant oxygen groups in the external surface. Table 7.3 shows the surface groups distribution (%) obtained by deconvolution of XPS curves. The nitric acid oxidation causes an important incorporation of oxygen functional groups, mainly carboxylic and anhydrides, in the most external AC surface. The low percentage of

hydroxyls groups in AC-N determined by XPS analysis meant that most of hydroxyls groups had been fixed in the internal surface of the carbon particles.

Table 7.3 Surface group distribution (%) obtained XPS of ACs.

eV	Assignment	Peak Contribution (%)				
		AC-R	AC-N	AC-O	AC-O30	AC-O60
C (1s)						
284.4	C=C	52.9	44.4	45.7	52.9	52.6
285.2	C (aliphatic "defects")	21.4	27.9	15	22.3	18.2
286.0	C-OH; C-O-C	5.0	4.3	12.9	3.3	7.1
287.1	C=O	4.3	4.3	3.2	2.6	3.9
288.5	COOH; COOC	9	12.6	18.3	10.2	11.5
291.0	$\pi \rightarrow \pi^*$	7.4	6.5	5	6.9	6.6
O (1s)						
531.1	C=O	22.1	13.7	11.6	14.2	23.6
532.2	C-OH, C-O-C	31.5	17.2	51.2	40.1	27.7
533.3	COOCO	9.8	23.1	20.1	15.1	22.4
534.2	COOH	23.3	34.5	11.1	19	16.1
535.9	Adsorbed H ₂ O	13.3	11.5	6.0	11.6	10.2

The changes in textural properties due to the oxidation of the ACs were also studied by N₂ adsorption-desorption isotherms at -196 °C. The obtained isotherms are shown in Figure 7.5.

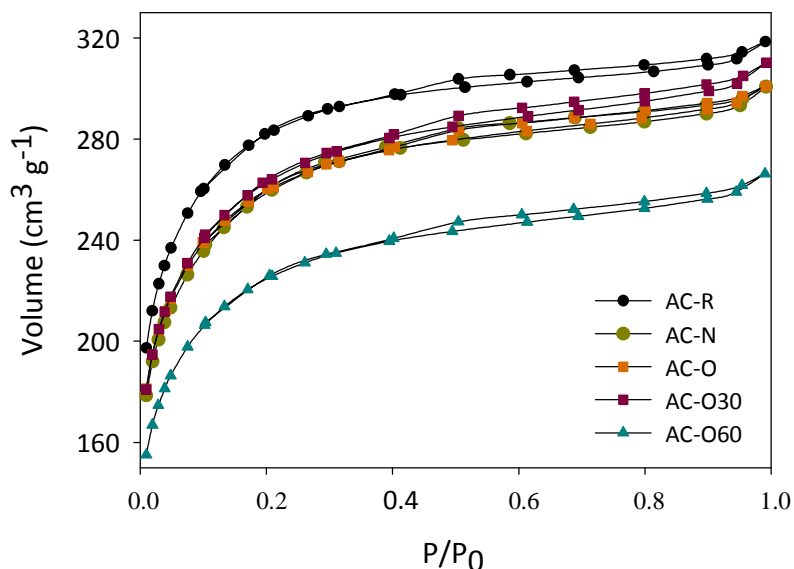


Figure 7.5 N₂ adsorption/desorption isotherms at -196°C of AC samples

It was observed a decrease in the adsorbed N₂ volume at low relative pressures ($P/P_0 < 0.2$) (attributable to the microporosity) with the oxidative treatments. The isotherms of the ACs samples were in all cases of type I (Brunauer et al., 1938; Brunauer et al., 1940), corresponding to microporous solids. The oxidative treatments decreased the amount of adsorbed nitrogen being AC-O60 the material which adsorbed the lowest

amount. Despite of this, the isotherms shape was similar for all ACs. From these adsorption isotherms, the results of surface area and pore volumes were obtained (Table 7.4). The decrease of the surface area (A_{BET}) and the micropore volume can be related to the destruction of the pore walls by strong oxidations with nitric acid and ozone. Furthermore, the incorporation of oxygen surface groups at the entrance of the pores may obstruct de N_2 access to the micropores, also causing a reduction of surface area (Rivera-Utrilla and Sánchez-Polo, 2011). This effect was more obvious in AC-N, which has a lower increase of mesoporosity.

Table 7.4 Textural properties of the as-received and oxidised ACs.

	$A_{\text{BET}}^{\text{a}}$ ($\text{m}^2 \text{g}^{-1}$)	$A_{\text{ext}}^{\text{b}}$ ($\text{m}^2 \text{g}^{-1}$)	$V_{\text{microp.}}^{\text{c}}$ ($\text{cm}^3 \text{g}^{-1}$)	$V_{\text{mesop.}}^{\text{d}}$ ($\text{cm}^3 \text{g}^{-1}$)	V_{t}^{e} ($\text{cm}^3 \text{g}^{-1}$)
AC-R	927	51	0.429	0.049	0.478
AC-N	861	55	0.394	0.054	0.448
AC-O	858	62	0.390	0.061	0.451
AC-O30	876	73	0.391	0.071	0.462
AC-O60	748	65	0.332	0.063	0.395

^a BET surface area determined from N_2 adsorption data.

^b External surface area determined from N_2 adsorption data

^c Micropore volume obtained by applying the Dubinin-Raduskevich equation to the N_2 adsorption data.

^d Mesoporus volume = $V_{\text{t}} - V_{\text{microp}}$

^e Total N_2 pore volumen at $P/P_0 = 0.95$

7.3.3 Oxidised ACs adsorption tests

The adsorption capacities of the oxidised ACs for VSCs were also determined by dynamic adsorption tests. The breakthrough curves obtained are shown in Figure 7.6. Different breakthrough curves profiles were observed in ETM and DMS with the oxidised materials while in the case of DMDS they were similar. The x/M and ST calculated for the as-received and oxidised AC samples are reported in Table 7.5.

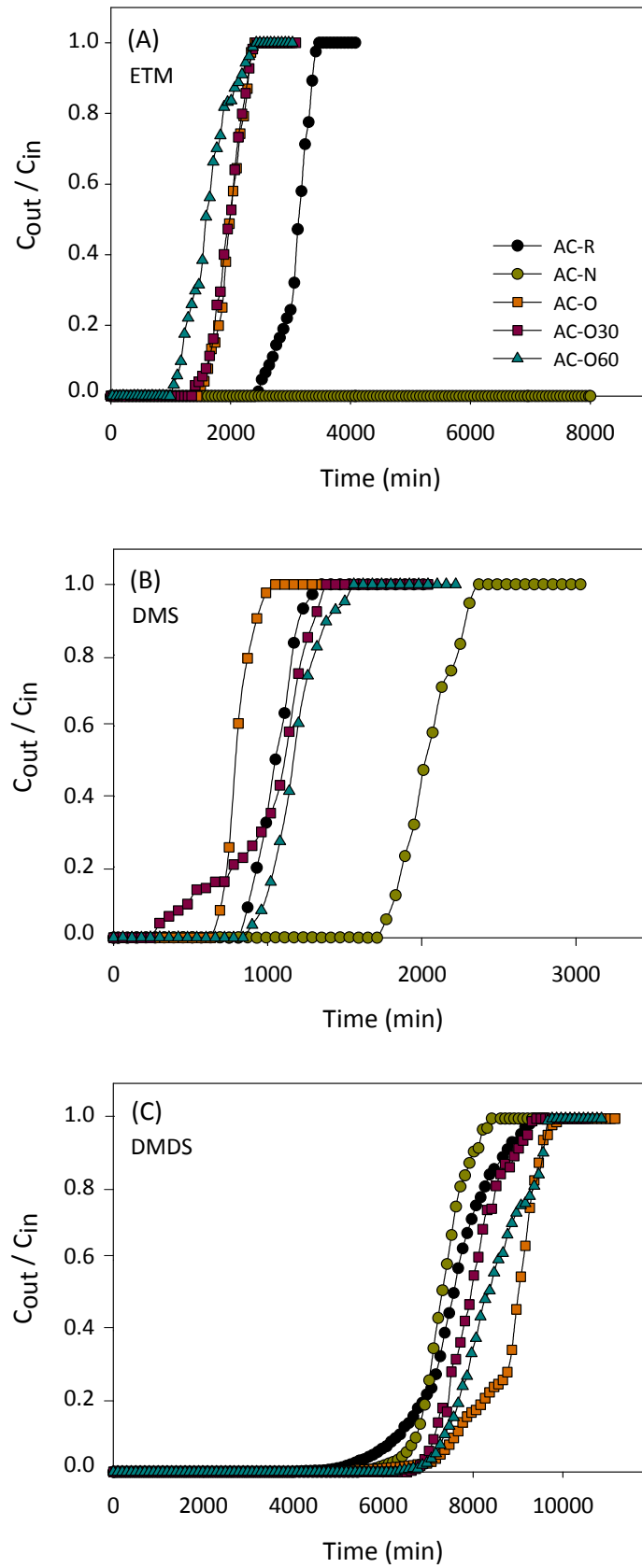


Figure 7.6 Breakthrough curves for ETM (A), DMS (B) and DMDS (C) on as-received and oxidised ACs.

Table 7.5 Saturation times (ST) and adsorption capacities in (x/M) of the as-received and oxidised ACs.

	ETM		DMS		DMDS	
	ST (min)	x/M _{ST} (mg g ⁻¹)	ST (min)	x/M _{ST} (mg g ⁻¹)	ST (min)	x/M _{ST} (mg g ⁻¹)
AC-R	3480	30	1350	8	8340	108
AC-N	>10080	>103	2370	21	8460	115
AC-O	2400	20	1050	8	9540	135
AC-O30	2430	21	1380	10	9960	142
AC-O60	2030	16	1560	12	9420	122

The adsorption capacities of ozonised materials for ETM were lower than those obtained with AC-R. AC-N presented higher adsorption capacities for ETM than any other material ($> 103 \text{ mg g}^{-1}$). ETM adsorption capacity could not be completely determined at low concentration because after 7 days of dynamic adsorption tests, breakthrough of AC-N for ETM was not observed. To discard the hypothesis of a possible catalytic process on the AC surface and speed up the exhaustion time, adsorption tests with AC-N and ETM were carried out at high concentration (100 ppm v/v). The resulting adsorption capacity of AC-N for ETM was 129 mg g^{-1} and no catalytic process was observed. A similar observation was reported by Cui et al. (2009) who studied the multicomponent adsorption of synthetic natural gas containing VSCs at low concentration (below 1 ppm) onto modified ACs and showed that the use of a carbonaceous material treated with nitric acid conducted to higher adsorption capacities of ETM.

The enhancement of adsorption capacity of AC-N was also evidenced in the adsorption of DMS. The adsorption capacity of AC-N was 2.6 times higher than AC-R and ozonised materials. On the other hand, ozone treatments did not let an increase in the adsorption capacity for DMS. These results are in agreement with Goyal et al. (2008) who concluded that the adsorption of DMS was enhanced by means of the nitric acid oxidation and that the adsorption involved hydrogen bonding between the carbon-oxygen surface groups and the sulphur atom of DMS without clarifying which is the main group responsible for this improvement. From our results, the significant increase in phenolic and carboxylic groups on AC-N indicated the presence of these groups could be the cause of the improvement in the adsorption capacities of VSCs.

On the contrary, the ozonised materials presented slightly higher adsorption capacities than AC-R and AC-N in the case of DMDS adsorption. However, these improvements are not significant if the typical error (10%) is considered. DMDS adsorption is not influenced by the incorporation of oxygen functional groups with both nitric and ozone oxidations. These results are in concordance with the study of Lee et al. (2010) who found that DMDS adsorption was unaffected by nitric acid oxidation of the adsorbents.

The molecular model predicts that any functionalization slightly improves the interactions compared to AC-R in the case of DMS as it was checked experimentally, This behaviour was only observed in our experimental results in the case of ETM on AC-N, but the rest of treated ACs obtained lower adsorption capacities than the untreated one, that can be attributed to the loss of porosity. Finally, in the case of DMDS, the similar and low K_H values confirmed that the great affinity for the ACs and the adsorption capacities remained practically constant with different AC models. As the functional enrichment was not selective, the repulsive and attractive interactions must be taken into account. For that reason, the simulation of the adsorption process on the studied ACs, considering the percentage of each oxygen functional groups was carried out. The obtained Henry's constants for the studied ACs are shown in Table 7.6.

Table 7.6 Henry's constant (bar) for different volatile sulphur compounds (ETM, DMS and DMDS) and the studied ACs predicted by COSMO-RS at 25 °C.

Model scheme	ETM	DMS	DMDS
AC-R	0.386	0.467	0.023
AC-N	0.314	0.338	0.024
AC-O	0.346	0.389	0.024
AC-O30	0.340	0.379	0.024
AC-O60	0.345	0.387	0.024

AC-N had the lowest K_H values in the case of ETM and DMS and these results were corroborated by improved adsorption capacities for AC-N compared to the other studied materials. These improvements can be explained by the great incorporation of HB-donor groups, especially hydroxyl group, on AC-N surface which facilitated the interaction of these groups towards the polar groups by means of hydrogen-bond (Tamai et al., 2006; Cui and Turn, 2009). Despite of these results, the model could not predict the significant improvement in the adsorption of ETM on AC-N due to the COSMO-RS does not take into account either the textural properties of ACs or the distribution of oxygen functional groups in AC particles. The massive incorporation of oxygen functional groups and the enrichment of hydroxyls in the internal surface of the carbon particles compensate the loss of porosity increasing the adsorption capacity of ETM.

7.4 CONCLUSIONS

The modification of AC with nitric acid and ozone oxidation caused changes on their textural properties, as well as enrichment of oxygen-containing groups onto carbonaceous matrix. The incorporation of oxygen surface groups was higher with nitric acid than with ozone oxidation. Only a massive incorporation of oxygen functional groups on the AC surface by means of nitric acid compensates the loss of porosity increasing the adsorption capacity for ETM and DMS. On the contrary, the studied oxidation treatments did not produce any increase in the DMDS adsorption. The predictive model COSMO-RS confirmed the higher affinity of DMDS with ACs obtaining lower values of K_H . Furthermore, the simulation established, in agreement with experimental results, that the incorporation HB-donor groups, especially hydroxyl groups, onto the carbonaceous matrix, provided a greater affinity between AC surface and VSCs, such as ETM and DMS. The results point out that a selective enrichment of the activated carbon surface would be an excellent tool for a future design of tailor-made adsorbents.

REMOVAL OF ODOROUS SULPHUR COMPOUNDS ONTO ACTIVATED CARBONS UNDER WET CONDITIONS

Adapted from:

Vega, E., Gonzalez-Olmos, R., Sánchez-Polo, M., Martin, M.J., 2014. *Adsorption of odorous sulphur compounds onto modified activated carbons by gamma irradiation. Submitted to Separation and Purification Technology*

8.1 BACKGROUND AND OBJECTIVES

The adsorption processes are added in sewage sludge treatment facilities at the end-of-pipe as polishing step. In most cases, this fact forces the adsorption beds to work under wet conditions because of the high humidity in the outflow of chemical scrubbers or biofiltration units.

For this reason, the main objective of this chapter is to investigate the effectiveness of activated carbons for ETM, DMS and DMDS removal under wet conditions and with the presence of oxygen in order to understand the adsorption behavior in operational conditions similar than those applied at industrial-scale. Furthermore, the modification of AC by gamma irradiation, which implies the modification of AC chemical properties without modifying textural properties, is also assessed.

8.2 METHODOLOGY

Different ACs were tested for ethyl mercaptan (ETM), dimethyl sulphide (DMS) and dimethyl disulphide (DMDS) adsorption by means of dynamic adsorption tests. A commercial activated carbon (AC-R) was modified by gamma irradiation under five experimental conditions and their chemical properties were characterised by elemental analysis, TPD, XPS and $\text{pH}_{\text{slurry}}$ analysis. The adsorption tests were conducted in a fix-bed reactor under wet conditions (70% RH) and with the presence of oxygen (21%) at low inlet concentration of target compounds (4 ppmv). The removal capacities were determined from the obtained breakthrough curves using a GC/PFPD analysis. Figure 8.1 shows the diagram of the methodology used in this chapter. For further details about experimental and analytical procedures used, please refer to the materials and methods section indicated between brackets.

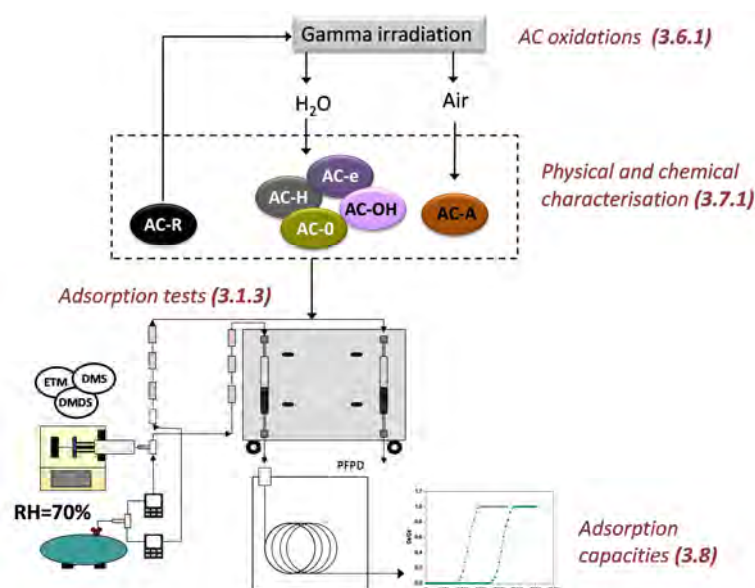


Figure 8.1 Diagram of methodology used in dynamic adsorption tests under wet conditions

8.3 RESULTS AND DISCUSSION

8.3.1 Surface chemical characterisation of ACs

The elemental analyses of the as-received and irradiated ACs are presented in Table 8.1. The results show changes in the chemical composition of irradiated materials. The increase in the oxygen content of irradiated ACs clearly indicates a modification of the oxygen functional groups in the ACs surface, more markedly in AC-OH and AC-O.

Table 8.1. Elemental analysis of as-received and irradiated ACs (%w/w)

	AC-R	AC-H	AC-e	AC-HO	AC-O	AC-A
% C	85.97	83.86	84.2	82.9	82.3	83.58
% H	0.80	0.95	1.14	0.9	1.05	0.86
% N	0.33	0.34	0.33	0.35	0.38	0.35
% O	12.9	14.85	14.33	15.85	16.27	15.21

For a deeper analysis of the chemical composition, the oxygen functional groups content of each AC was determined using TPD which provides information about the thermal stability and the amount and nature of the oxygen functional groups. Figure 8.2 shows the CO and CO₂ evolution profiles during the TPD experiments.

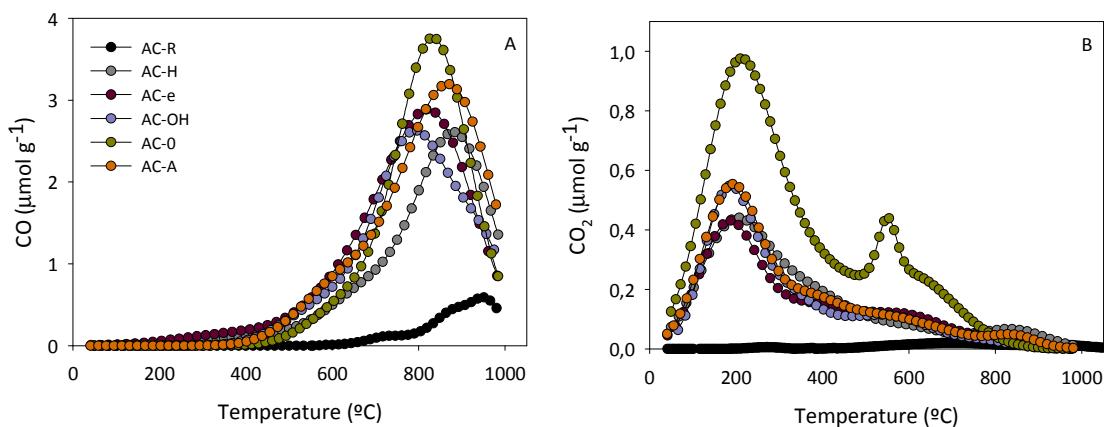


Figure 8.2 TPD spectra profiles for AC samples: (A) CO evolution; (B) CO₂ evolution

The TPD profiles indicated significant chemical surface changes of the irradiated ACs compared with AC-R. All irradiated samples showed an important increase in the amount of CO and CO₂ evolved, especially for the AC irradiated in the presence of all radicals (AC-O). In order to analyse the nature of the oxygen functional groups, TPD spectra profiles were deconvoluted according to the literature (Figueiredo et al., 1999, 2007; Figueiredo and Pereira, 2010). The corresponding assessment of different functionalities is shown in Table 8.2. As expected, a larger amount of oxygen functional groups on irradiated ACs was incorporated compared to AC-R according to the higher

values obtained in O/C_{TPD} ratios. It is important to point out the enrichment of functionalities with donor character such as carboxylic and phenolic in all irradiated ACs as well as anhydride groups. The incorporation of these oxygen functional groups was also observed by means of chemical modification (nitric acid and ozone). However, the amount of oxygen functional groups incorporated in AC surface was lower than those obtained using nitric acid or ozone. The distribution of oxygen functional groups on AC surface was different than those observed by Velo-Gala et al (2014) because of the authors reported that the nature of ACs is a decisive factor for the selective incorporation of oxygen functional groups in the AC surface.

Table 8.2 Assessment of oxygen surface groups obtained by TPD, O/C_{TPD} and $\text{pH}_{\text{slurry}}$ for the as-received and irradiated AC.

	AC-R	AC-H	AC-e	AC-HO	AC-O	AC-A
CO ₂ total ($\mu\text{mol g}^{-1}$)	53	129	106	125	260	121
Carboxylic	4	61	51	56	130	67
Anhydrides	7	43	34	39	67	11
Lactones	42	15	19	28	8	40
Pyrones	0	10	2	2	54	3
CO total ($\mu\text{mol g}^{-1}$)	456	707	749	734	808	760
Anhydride	0	86	61	71	130	136
Phenolic	64	156	330	501	510	372
Carbonyl	392	456	358	162	164	243
O/C_{TPD}	0.007	0.013	0.013	0.014	0.019	0.014
$\text{pH}_{\text{slurry}}$	7.2	8.3	3.8	6.8	10.1	9.7

As expected, the modification of the oxygen content of ACs and the nature and concentration of their groups yielded changes on the $\text{pH}_{\text{slurry}}$ of the modified ACs, covering a wide range of $\text{pH}_{\text{slurry}}$ (3.8-10.1). The irradiation of ACs in air (AC-A) and, especially in presence of all radicals (AC-O), caused an increase of alkalinity in the materials ($\text{pH} = 9.7$ and 10.1 , respectively). On the contrary, acid character was obtained by irradiation in the presence of e_{aq}^- (AC-e) ($\text{pH} = 3.8$).

In addition, the chemical composition of the few uppermost layers of the ACs was determined by XPS technique. The obtained XPS spectra in C (1s) and O (1s) spectral regions are shown in Figure 8.3. In C (1s) spectra no significant differences were observed between the studied ACs, while slight variations in O (1s) region profiles were observed in the irradiated ACs, especially with the presence of all radicals (AC-O).

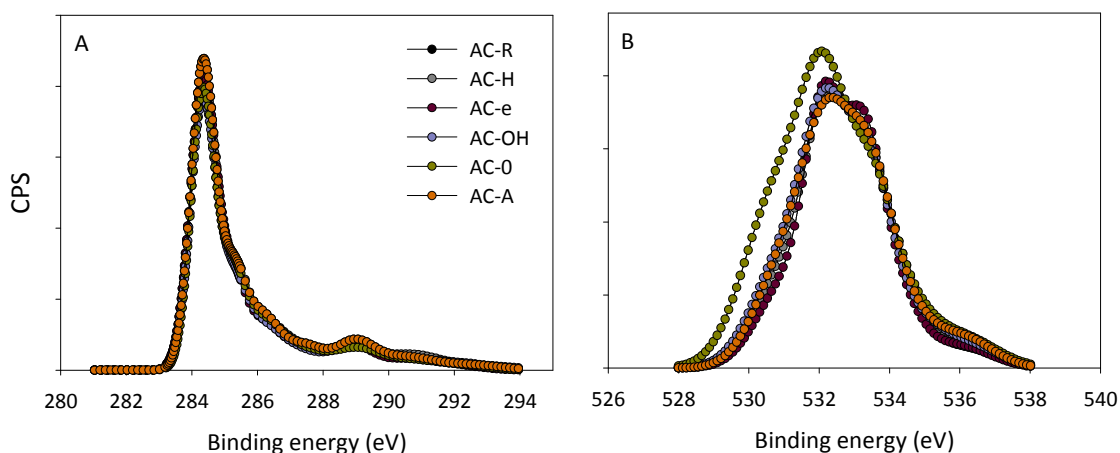


Figure 8.3 XPS spectra profiles for ACs: (a) C (1s) spectral region; (b) O (1s) spectral region

The peaks were deconvoluted according to the binding energies established by Moreno-Castilla et al (2000) and Figueiredo et al (2010). The corresponding assessment of different functionalities is shown in Table 8.3.

Table 8.3 Surface groups distribution (%) obtained in XPS and O/C_{XPS} ratio for the AC samples.

eV	Assignment	Peak contribution (%)					
		AC-R	AC-H	AC-e	AC-OH	AC-O	AC-A
C(1s)							
284.4	C=C (graphitic)	52.9	53.5	56.3	50.8	49.5	54.4
285.2	C (aliphatic "defects")	21.4	13.2	12.5	15.1	15.8	12.5
286.0	C-OH; C-O-C	5.0	12.9	13.0	15.6	15.7	12.1
287.1	C=O	4.3	5.2	5.4	2.7	6.1	4.9
288.5	COOH; COOC	9.0	6.7	6.4	8.9	6.8	8.4
291.0	$\pi \rightarrow \pi^*$	7.4	8.5	6.4	6.9	6.1	7.7
O (1s)							
531.1	C=O	22.1	23.6	19.7	21.4	32.8	22.2
532.2	C-OH, C-O-C	31.5	32.5	30.2	37.4	33.6	35.6
533.3	COOCO	9.8	22.8	32.7	23.3	15.1	19.9
534.2	COOH	23.3	16.4	11.5	12.2	12.8	16.0
535.9	Adsorbed H ₂ O	13.3	4.7	5.9	5.8	5.7	6.3
O/C_{XPS}		0.046	0.077	0.083	0.083	0.089	0.070

An increase in the oxygen functional groups in the uppermost layers of ACs was observed according with the results obtained from O/C_{XPS} ratio. In all irradiated ACs, the peak contribution of oxygen functional groups changed slightly compared with AC-R. In all treatments, the irradiation reduced the percentage of carbon atoms with sp^3 hybridization associated to the aliphatic defects in agreement with Velo-Gala et al. (2014). Moreover, an important increase of hydroxyl and anhydride groups were observed in the majority of AC samples, while carboxylic groups were significant

reduced in all irradiated ACs. Generally, the percentage contribution of other oxygen-containing functional groups remained constant in the majority of samples.

8.3.2 Adsorption tests

The adsorption capacities of the studied ACs for DMDS, DMS and ETM were determined by dynamic adsorption tests. The breakthrough curves obtained from the as-received and irradiated ACs are presented in Figure 8.3. The removal capacities were calculated until the olfactometric breakthrough time according to the odour threshold (OT) of each compound. The estimated breakthrough concentration (C_B) for each compound was also marked with dotted red lines in the Figure 8.3.

DMDS breakthrough curves (Figure 8.3a) show similar profiles for all samples and therefore their removal capacities calculated to the olfactometric breakthrough were equal for all AC samples ($\approx 2 \text{ mg g}^{-1}$). As expected, the breakthrough times of the ACs for DMDS under wet conditions (about 2000 min) were lower than those observed in the previous chapter under inert conditions (about 6000 min). Furthermore, these results corroborated both the results obtained by COSMO-RS and experimental data under inert conditions. In chapter 7, it was observed that the DMDS adsorption was not affected by the oxygen functional groups content in the ACs surface. The fact that only 2-3% of surface area is reduced by irradiation treatment (Velo-Gal et al., 2014) explains the similarity of the adsorption results. The importance of textural properties for DMDS adsorption was confirmed by means of an adsorption test using AC-N (AC modified with nitric acid used in adsorption tests of chapter 7) which has less surface area ($861 \text{ m}^2 \text{ g}^{-1}$) than AC-R ($927 \text{ m}^2 \text{ g}^{-1}$). The adsorption capacity obtained for AC-N was lower (0.8 mg g^{-1}) than those achieved by the irradiated ACs.

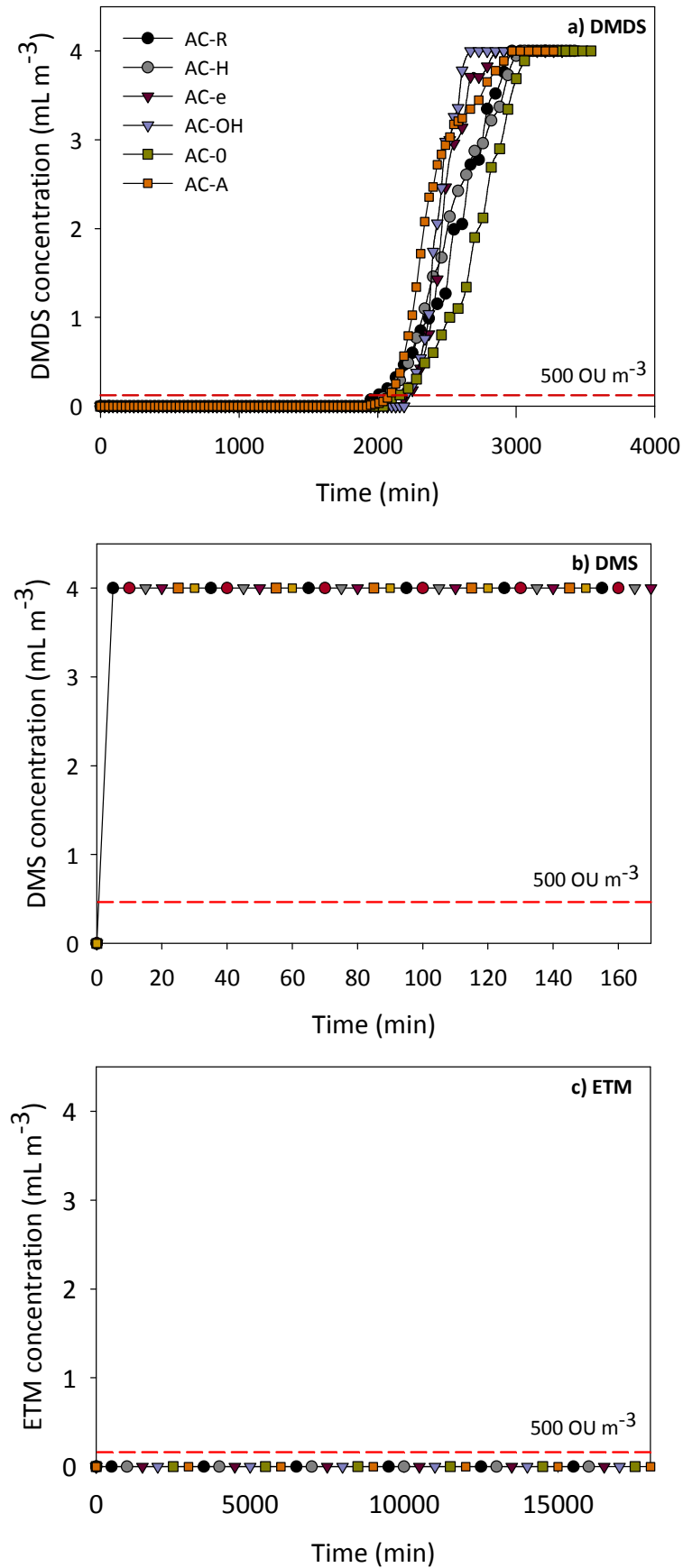


Figure 8.3 Breakthrough curves for DMDS (a), DMS (b) and ETM (c) on the ACs

The breakthrough curves for DMS are presented in Figure 8.3b. The results indicate that both the as received and irradiated ACs are not able to adsorb this compound under wet conditions. The presence of water and/or the presence of oxygen in the air stream lead to significant differences than those observed under inert conditions in chapter 7. In order to understand this unexpected behaviour, preliminary experiments for this research, which were carried out under the same conditions (concentration, temperature, flow) that the present research, were used. These experiments describe the adsorption process of a multi-component stream (H_2S , CS_2 , MTM, ETM, DMS and DMDS) at low concentration (4 ppmv) onto AC-R under two different conditions: i) inert conditions and ii) with air. Table 8.4 shows the results of adsorption capacities with different operational conditions.

Table 8.4 Adsorption capacities for DMS with different operational conditions

Adsorption	Operational Conditions	x/M_{BT} (mg g^{-1})
Single-component	Air and HR=70%	0.0
Single-component	N_2	8.0
Multi-component	N_2	3.2
Multi-component	Air	3.8

The results obtained from adsorption experiments of multi-component stream are similar despite the differences in the operational conditions. Therefore, the results reveal that the oxygen did not affect the adsorption capacities of AC-R for DMS. Under inert conditions, lower adsorption capacities were obtained in multi-component adsorption (3.2 mg g^{-1}) compared with the single-component adsorption (8.0 mg g^{-1}) in agreement with the results reported by Sidheswaran et al. (2011).

Thus, the results demonstrated that the competition between the DMS and water for the adsorption site on the AC is the main responsible for the difficult removal of DMS by AC, as occurs in the removal of some VOCs (Cal et al., 1996; Gironi and Piemonte, 2011).

In ETM adsorption tests, this compound was not detected at the outlet of the adsorption column (Figure 8.3c). However, diethyl disulphide (DEDS) was measured during the experiment. The breakthrough curves obtained for DEDS with the different ACs studied in this chapter are presented in Figure 8.5 and the estimated breakthrough concentration (C_{B}) for DEDS was also marked with dotted red lines.

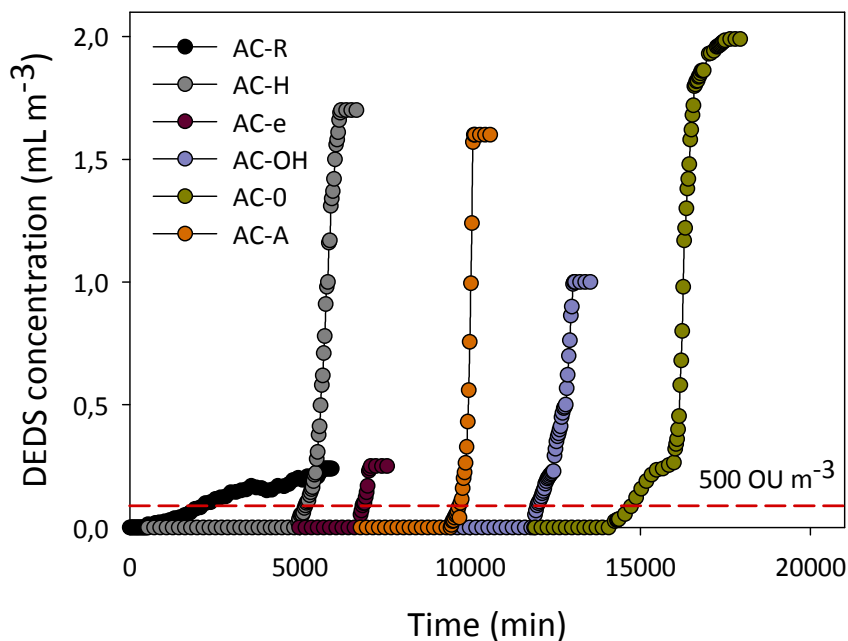


Figure 8.5 Breakthrough curves for DEDS on the ACs

This catalytic process from ETM has already been observed by Boulinguez and Le Cloirec (2010) who detected the formation of DEDS during desorption process with air of a AC used for ETM adsorption.

Given the catalytic process, the adsorption capacities of ETM were calculated taking into account that one mole of DEDS is formed from two moles of ETM. A detailed oxidation mechanism is explained below. Thus, the adsorption capacities were calculated as the amount of ETM removed using the breakthrough curves of DEDS. Table 8.5 shows the olfactometric breakthrough times (BT) and adsorption capacities of ACs samples for ETM.

Table 8.5 Olfactometric breakthrough times (BT) of DEDS and adsorption capacities for ETM of ACs samples

	BT (min)	x/M_{BT} (mg g⁻¹)
AC-R	2370	23
AC-H	5190	53
AC-e	6900	70
AC-OH	12030	122
AC-0	14790	152
AC-A	9720	100

The removal capacities of the irradiated ACs for ETM were higher than those obtained with the as-received AC (AC-R). The ACs irradiated in the presence of all radicals and in the presence of HO^\bullet (AC-0 and AC-OH, respectively), presented the highest breakthrough times and adsorption capacities for ETM (Table 8.5). Unlike the results

obtained with DMDS, the wet conditions and the presence of oxygen improve the performance of the irradiated ACs for the removal of ETM compared to the inert conditions.

As noted in the previous chapter, the chemical properties played an important role in the ETM removal process. Thus, the influence of oxygen functional groups in AC surface on ETM adsorption was also investigated. The effect of different functionalities calculated from TPD onto AC on the removal of ETM is presented in Figure 8.6.

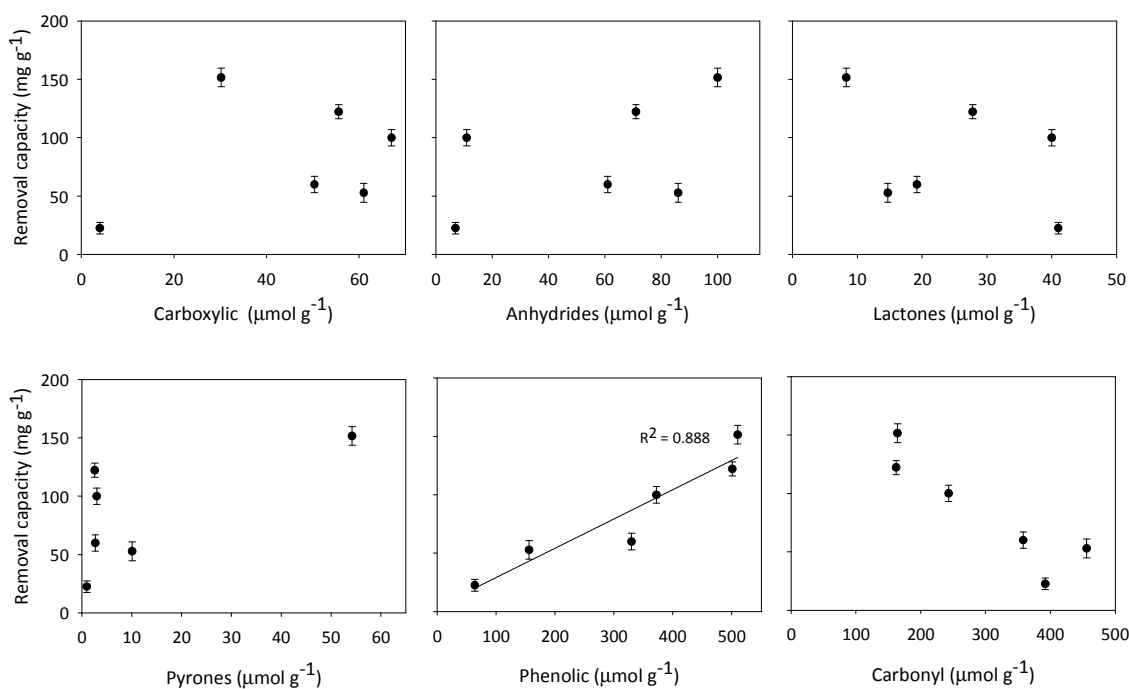
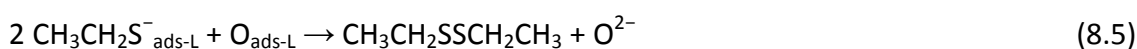
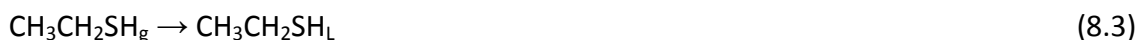


Figure 8.6 Effect of oxygen functional groups content from TPD analysis onto ACs samples on the removal capacity for ETM

Clearly, a greater amount of phenolic groups in the AC surface was directly correlated with the removal capacity of ETM. As observed in the previous chapter, the hydroxyl groups facilitate the adsorption of ETM because of the formation of hydrogen bonds interactions.

Bagreev et al. (2002) and Bashkova et al. (2002a) investigated in detail the adsorption process of methyl mercaptan onto ACs under wet conditions and in the presence of oxygen. The authors detected the DMDS formation, as oxidation by-product, during the adsorption process of methyl mercaptan. Moreover, the authors stated that the mercaptan adsorption process under wet conditions either may occur on the dry carbon surface or on the water clusters which are formed by the adsorbed water. Thus, the physico-chemical adsorption process takes place in the dry AC surface, while the catalytic process occurs mainly on water clusters. On this basis, Bashkova et al. (2002a) proposed the methyl mercaptan oxidation pathways which let assume similar oxidation pathways for ETM. Under wet conditions, adsorbed water in AC surface is

able to create water clusters where oxygen and mercaptan are dissolved in molecular form (Eq. 8.1 - 8.3). Then, depending on the pH, ethyl mercaptan is dissociated to thiolate ion (Eq. 8.4) which reacts with adsorbed oxygen leading the formation of DEDS (Eq. 8.5). The subscripts g, L and ads-L are species in gas phase, liquid phase and adsorbed in liquid phase, respectively.



On the other hand, the breakthrough curves of ACs for ETM reach different pseudo steady-state. According to the oxidation mechanism described in Eq. (8.5), the complete oxidation of ETM would be obtained at DEDS concentration of 2 mL m^{-3} . Thus, values below this concentration reveal the partial oxidation of ETM. The breakthrough curves obtained for ETM removal shows different degrees of oxidation of ETM to DEDS. As mentioned above, the pH is an important parameter for ethyl mercaptan dissociation takes place. The effect of the samples $\text{pH}_{\text{slurry}}$ on oxidation percentage of ETM is shown in Figure 8.7.

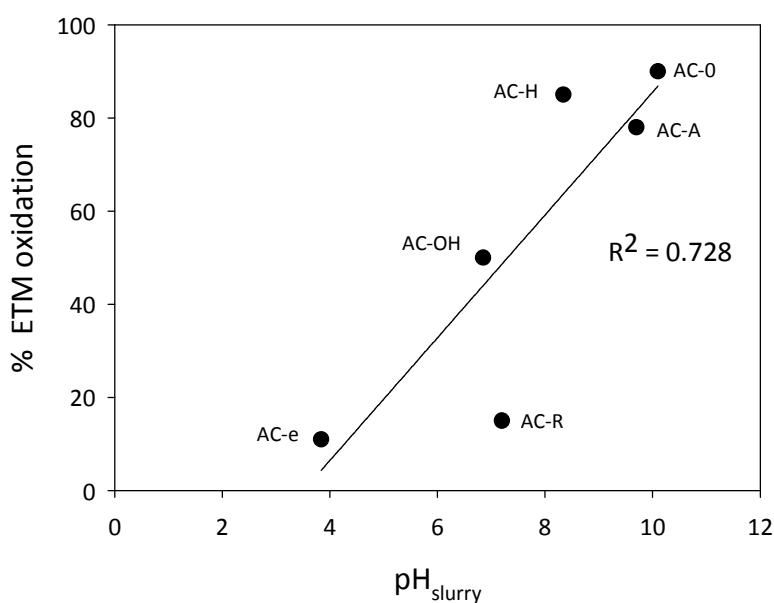


Figure 8.7 Effect of ACs samples $\text{pH}_{\text{slurry}}$ on the ETM oxidation

The result indicates that the alkaline ACs yielded higher oxidation percentages of ETM in agreement with the results reported by Bashkova et al., 2002b who noted the pH dependence in the proposed reaction pathways for methyl mercaptan. Thus, the authors stated that when the AC pH is higher than mercaptan pK_a , the thiolate ions concentration is much greater than the concentration of the mercaptan. According to this statement, the formation of thiolate ions from ETM would be favoured under alkaline conditions due to the ETM pK_a (10.6). The ETM dissociation to form DEDS has been observed despite the studied ACs do not exceed the ETM pK_a . This fact can be attributed to the wall effect on adsorption sites alters equilibrium and reaction and thereby shifts the equilibrium dissociation at lower pH than pK_a (Boulinguez and Le Cloirec, 2010).

8.4 CONCLUSIONS

Gamma irradiation yield changes in chemical properties in the uppermost layers as well as in the internal matrix of ACs. The most important incorporation of oxygen functional groups, especially carboxylic and phenolic, is observed in AC irradiated with ultrapure water in presence of all radicals.

Under wet conditions, lower adsorption capacities for DMS and DMDS were achieved than those obtained under inert conditions. DMS is not adsorbed on irradiated ACs under the studied conditions because of water prevents the adsorption process. On the other hand, the majority of irradiated AC improves the adsorption capacity for ETM compared to AC-R. A catalytic process was observed during ETM adsorption. The results obtained for ETM removal reveal that the enrichment with phenolic groups in AC surface increases the adsorption capacities for ETM. Furthermore, the results points out that the chemical properties of ACs play an important role in the DEDS formation as by-product during the ETM oxidation process on the AC surface.

GENERAL DISCUSSION

This chapter seeks to provide an overview of the most relevant aspects of this research in order to discuss them from a general point of view than those presented above.

The problems associated with the emission of odorous compounds from different steps in wastewater treatment plants (WWTPs), especially in sewage sludge processing, have been demonstrated by several authors (Frechen, 1988, Islam et al., 1998; Dincer and Muezzinoglu, 2008). Thus, this thesis aims to contribute to extending the knowledge on the minimisation and abatement of volatile sulphur compounds (VSC) in sewage sludge processing.

The first approach was to identify the main odour-compounds emitted from sewage sludge drying processes, both in lab and full scale (Chapter 4). Despite the complexity of the odorous samples from the drying processes, the estimation of the odour index allowed to demonstrate the separate influence between the concentration and the odour threshold of different odorous compounds. This fact revealed the importance of the volatile sulphur compounds (VSC) in the odour perception despite their low abundance compared with other volatile organic compounds (VOCs) in agreement with Adams et al (2008). In this study, an overview of the odorous compounds emitted during sewage sludge drying process was obtained by a GC-MS analytical method. However, these results provided poor information about all volatile sulphur compounds released from sewage sludge. For this reason, a selective analytical method for VSC, based in GC-PFPD, was used. Moreover, an olfactometric method was used as a complementary analysis to characterise gas samples.

Any facility design would have to consider the minimisation of pollutants emissions at source. In several cases, a simple modification on process can reduce the load of odorous compounds and therefore to benefit the end-of-pipe technologies (Lebrero et al., 2011). Based on the fact that the conditioners have been mainly used for improving the sludge dewaterability, this investigation focused on the optimisation of this process to reduce the emissions of VSC and odour. The present proposal demonstrated that the optimisation of conventional conditioning process can improve other responses such as the reduction of VSC and odour emission without leaving the main purpose of the process. The influence of the individual dosage of conditioners on the dewaterability and odour emissions was investigated in chapter 5 and the results revealed that chemical conditioners were more effectiveness in the reduction of CST and VSC emissions compared with physical conditioners. Nevertheless, the reduction of sulphur compounds using chemical conditioners individually had not led to a reduction in odour emissions. This fact reinforced the importance of the olfactometry as complementary technique, given the gaps in the analytical method, which can not establish the synergistic and antagonistic effects.

Given the amount of variables that could influence the response (dewaterability and odour emission) and the need to successfully optimise the conditioning process in

order to obtain the maximum sludge dewaterability and the minimum odour emission, response surface methodology was applied in this process. The optimal conditions for the mentioned purpose were achieved using the highest dose of inorganic chemical conditioners together (Table 5.5, chapter 5), improving the efficiencies than those observed individually. Nevertheless, this research has not considered the significant increase of sewage sludge volume which would imply an increase in the sewage sludge treatment cost (Turovskiy and Mathai, 2006). Hence, a detailed economic assessment of the conditioning process would be required for a better optimisation. Furthermore, the optimisation of conditioning process, which combines chemical and physical conditioners, could be an interesting alternative to be investigated in terms of effectiveness and cost reduction (Nelson and Brattlof, 1979).

The odour minimisation from the sewage sludge drying process was successfully achieved by the chemical conditioning process. However, the effect of minimisation was not sufficient to mitigate the odour nuisance during this process. For this reason, an effort to find more efficient technologies than those observed in full-scale was required. The effectiveness of chemical scrubber and biofilter for VSC removal at full-scale was investigated in chapter 4. Although their removal efficiencies were very low in some cases, the VSC removal followed different trends depending on the applied technology. For instance, mercaptans were successfully removed through chemical scrubbers, while DMDS was better removed by the biofilters. However, both technologies agreed on the removal difficulties of DMS. The significant variability in the removal efficiency of VSC led the study to search for more robust and versatile technologies. Thus, advanced oxidation processes (AOPs) and adsorption were investigated as alternative or/and complement to chemical scrubbers and biofilters.

The feasibility of coupling AOPs with scrubbers for VSC removal was demonstrated in chapter 6. The high conversion of sulphur to sulphate implies a high deodorisation capability of AOPs. Although all tested AOPs (UV/H₂O₂, Fenton, photo-Fenton and ozone) achieved high percentage removal for VSC, photo-Fenton and ozone reached the best short-term performance. It has to be highlighted that the accumulation of sulphate (mineralisation by-product) could interfere in the effectiveness of AOPs. Thus, the effect of sulphate as well as other VOCs, which could be absorbed into liquid solution, has to be investigated. When the economic analysis of AOPs was carried out, the time parameter played an important role in the dimensioning of the full-scale reactor which had a significant weight in the water treatment cost (Table 6.3, chapter 6). It has to be highlighted that the economic analysis revealed that the reactor volume limitations or retrofitting complexities play a key role in the decision of the most appropriate option to be implemented in a full-scale system.

Finally, the adsorption process as polishing treatment was assessed. In order to improve the adsorption capacities of AC for VSC, it was necessary to study in depth the

physicochemical interactions between AC and VSC. The oxidation of the AC using nitric acid and ozone allowed to modify markedly the chemical properties of the as-received AC by the introduction of oxygen functional groups. However, the oxidations also caused changes in the textural properties in agreement with the results reported by Pereira et al. 2003 and Valdés et al. 2002 who stated that the destruction of pore walls during the oxidation processes. The oxidative treatment of ACs allowed to obtain samples with different chemical and textural properties and thus to find a possible correlation between the oxygen functional groups and adsorption capacities. The adsorption test revealed that the presence of hydroxyl groups in AC surface improves the adsorption capacities of ETM and DMS. So far, several authors have attributed the improved adsorption capacities for mercaptans to the presence of oxygen functional groups which could form hydrogen bonds with the polar group of mercaptans (Tamai et al. 2006, Cui et al, 2009). More specifically, Goyal et al (2008) attributed this interaction to the presence of carboxyl groups. In order to know the interactions between VSC and the presence of oxygen functional groups and to corroborate the experimental results, the interactions were simulated by predictive model COSMO-RS.

COSMO-RS predicted the Henry constants (K_H) between each VSC and the main functionalities in the AC surface. Thus, the lower values of K_H mean higher affinity of the adsorbent for VSC (Palomar et al. 2009). According with the results obtained by the model, the hydroxyls groups seems to be mainly responsible for the improvement because of the lowest obtained values of K_H (Table 7.1, chapter 7). Thus, the predictive model confirmed the experimental results obtained in adsorption tests. Furthermore, the DMDS adsorption process followed the expected trend by COSMO-RS which predicted that this compound is not affected by the presence of oxygen functional groups on ACs. Therefore, the predictive model COSMO-RS confirmed all the experimental results and demonstrated to be an excellent tool for the design of tailor-made adsorbents.

A modification of AC, which allows the selective incorporation of hydroxyl groups without modifying textural properties, was sought according with the results obtained in adsorption experiments under inert conditions. For this reason, it was decided to modify the AC by gamma irradiation (Chapter 8). In order to assess the real effectiveness of irradiated ACs, the adsorption tests were carried out under wet conditions and with the presence of oxygen, simulating the real conditions of the adsorbents. The characterisation of irradiated ACs revealed that the incorporation of hydroxyl groups was lower than expected. Velo-Gala et al (2014) noted that the nature of AC, which undergoes irradiation, is critical for obtaining successfully results in the enrichment with oxygen functional groups.

The adsorption tests under wet conditions and with the presence of oxygen showed different trends than those obtained under inert conditions. DMS was not adsorbed on

any irradiated ACs because of the presence of water seems to displace DMS (Cal et al., 1996). Moreover, a catalytic process was observed in ETM adsorption process leading to the formation of DEDS as by-product. In terms of odour removal, this fact would not be beneficial because of DEDS has a lower odour threshold than ETM (Van Gemert, 2003), i.e., the ofactometric breakthrough concentration would be lower than those would be obtained for ETM.

In addition to the foregoing, a comparative assessment of the efficiency of all procedures applied in this thesis for VSC removal has been carried out in this chapter. For this purpose, the most significant contributions have been summarised in Table 9.1.

Table 9.1 Summary of the effectiveness of technologies assessed for VSC removal

	MINIMISATION		END-OF-PIPE TECHNOLOGIES				
	Conditioning ^a		Scrubber ^b	Biofilter ^b	AOPs ^c	AC	
	Chemical	Physical				Inert ^d	wet ^e
H ₂ S	+	+	-	+	NI	NI	NI
MTM	+	+	+	+	NI	NI	NI
ETM	NI	NI	++	-	+++	++	+++
DMS	+	+	-	-	+++	++	-
DMDS	+	+++	-	++	+++	+++	++

NI: not investigated in this thesis

^a Chapter 5; ^b chapter 4; ^c Chapter 6; ^d Chapter 7; ^e Chapter 8

The efficiency for H₂S and MTM removal could only be assessed in the conditioning process as well as the current technologies at full-scale. These compounds were significantly reduced through chemical conditioning process but not enough to not consider the end-of-pipe technologies. Although this thesis has not been focused on the removal of these compounds, several authors demonstrated the effectiveness of the adsorption process for the successfully removal of H₂S (Bandosz, 2002; Le Leuch et al., 2003; Bouzaza et al., 2004) and MTM (Bashkova et al., 2002; Kim and Yie, 2005).

The comparison between target compounds (ETM, DMS and DMDS) has shown divergent results. Given that ETM was not found in the conditioning process, the evaluation is limited to the end-of-pipe technologies. Generally, ETM is able to be removed with high efficiencies by the studied technologies, being the application of AOPs the most successful technology. On the other hand, the most difficult compound to be removed is DMS. Except for AOPs, the tested technologies achieved low removal percentages. The inability of ACs for removing DMS under real conditions, it considers the need to dehumidify the gas outflow in order to improve the efficiency of the adsorbers.

Finally, the highest removal efficiencies were obtained for DMDS. The high affinity of this compound towards AC caused higher efficiencies in the adsorption process as well as in the physical conditioning process where the AC was used as conditioner. Moreover, this compound was also successfully removed either with AOPs or biofilters.

In general terms, the results point to the need of optimising and combining each of studied technologies for optimal volatile sulphur compounds removal in the sewage sludge processing.

GENERAL CONCLUSIONS

This thesis comprises the research of minimisation of volatile sulphur compounds and odour emission in sewage sludge drying process through the optimisation of the conditioning process, as well as the effectiveness of advanced oxidation and adsorption processes as sulphur compounds abatement technologies at the end-of-pipe.

The first approach was to identify the main odour-causing compounds during the drying process, both in lab and full-scale. From this study, it was concluded that:

- The odorous matrix is highly complex, composed by a large amount of volatile sulphur compounds.
- The odour index estimation demonstrated the separate influence of the odour-causing compound concentration and the olfactory threshold. DMDS was the main odour contributor in the samples because of its low odour threshold in spite of being less abundant than others VOCs.
- The analysis of VSC removal efficiencies of current end-of-pipe technologies demonstrated the difficulty in removing VSC within complex matrices.

Once the scope of the problem related to VSC was identified, the minimisation of the VSC and odour emission during drying process was investigated. From this study, it was concluded that:

- A significant minimisation of VSC volatile sulphur compounds and odour emissions from drying process was achieved using chemical conditioners.
- The olfactometry is a reliable technique to complement the analytical methods. Furthermore, the olfactometric analysis allows identifying synergistic and antagonistic effects which can not be determined by analytical methods.
- Response surface methodology was successfully applied to improve the sludge dewaterability and odour emission simultaneously.
- The minimisation of VSC and odour emissions was also noted by means of activated carbon as physical conditioner. However, the specific role of this physical conditioner in the reduction of odorous emissions has to be studied in depth. Moreover, the response surface methodology could be used to optimise a combined conditioning process using chemical and physical conditioners.

The implementation of the latter methodology in the conditioning process would reduce the release of odour-causing compounds in sewage sludge processing. Nevertheless, the minimisation obtained by optimizing the conditioning process is not sufficient to mitigate the odour nuisance. Therefore, the research of end-of-pipe technologies has been required.

In this sense, the feasibility of coupling advanced oxidation process with scrubbers for volatile sulphur compounds removal was demonstrated. From this study, it was concluded that:

- The advanced oxidation processes are suitable for the removal of volatile sulphur compounds in liquid phase.
- Fenton and photo-Fenton were the most efficient treatments which yielded the highest efficiency removal as well as the mineralisation degree.
- The high conversion of sulphur atoms to sulphate implies the high deodourisation capability of advanced oxidation processes. However, the accumulation of sulphate in the liquid phase could interfere in the effectiveness of advanced oxidation process. Thus, the effect of sulphate as well as other VOCs would have to be investigated.
- The economic analysis revealed that the reactor volume limitations or retrofitting complexities play a key role in the decision of the most appropriate option to be implemented in a full-scale system.

An adsorption process onto modified AC was proposed for VSC removal at low concentration. From this research, it was concluded that:

- The oxidation of AC using nitric acid or ozone caused changes on their textural properties, as well as an important enrichment of oxygen functional groups onto the carbonaceous matrix.
- The adsorption capacities of the activated carbons for the removal of ETM and DMS were improved by introducing hydroxyl groups in the activated carbon surface via the formation of hydrogen bonds. However, the adsorption process of DMDS was not affected by the chemical properties of the AC.
- An adsorption process to treat a multicomponent effluent has to be investigated in order to discard a roll-up phenomenon between target compounds.
- The predictive model COSMO-RS confirmed the experimental results and demonstrated to be an excellent tool for the design of tailor-made adsorbents.
- Although the performance was improved by the chemical modification of the activated carbon, better results would be expected based on the results provided by the predictive model.

Finally, the effectiveness of ACs for VSC removal under wet conditions and with the presence of oxygen was investigated. From this study, it was concluded that:

- The wet conditions prevented the adsorption of DMS onto irradiated activated carbons. This fact gains relevance when considering the location of the adsorption process, as typically they are downstream of a biofiltration process.

- The incorporation of hydroxyl groups on the activated carbon surface improved the removal capacities for the ETM. Moreover, the results pointed out that the chemical properties of ACs played an important role in the DEDS formation as by-product of ETM oxidation process on the carbon surface.

An overview of the results points to the need of optimising and combining each of studied technologies for optimal volatile sulphur compounds removal in the sewage sludge processing.



REFERENCES

REFERENCES

A

Adams, G.A, Witherspoon, J., Card, T., Geselbracht, J., Glindermann, D., Hagreaves, R., Hentz, L., Higgins, M., Murthy, S., 2003. Identifying and Controlling odours in the Municipal Wastewater Environment Phase 2: Impacts of in-plant parameters on biosolids odor quality. Water Environment Research Foundation, Alexandria, VA, USA

Adams, G.A., Witherspoon, J., Erdal, Z., Forbes, B., McEwen, D., Hagreaves, R., Higgins, M.J., Novak, J., 2008. Identifying and Controlling odours in the Municipal Wastewater Environment Phase 3: Biosolids processing Modifications for Cake Odour Reduction. Water Environment Research Foundation, Alexandria, VA, USA.

Albertson, O.E., Kopper, M., 1983. Fine-coal-aided centrifugal dewatering of waste activated sludge. *J. Water Pollut. Control Fed.* 55, 145-156.

Aldin, S., Tu, F., Nakhla, G., Ray, M.B., 2011. Simulating the degradation of odor precursors in primary and waste-activated sludge during anaerobic digestion. *Appl. Biochem. Biotechnol.* 164, 1292-1304.

Andreozzi, R., Caprio, V., Insola, A., Marotta, R., 1999. Advanced oxidation processes (AOP) for water purification and recovery. *Catal. Today* 53, 51-59.

Anfruns, A., Martin, M.J., Montes-Morán, M.A., 2011. Removal of odourous VOCs using sludge-based adsorbents. *Chem. Eng. J.* 166, 1022-1031.

APHA, 2005. American Public Health Association, Standard Methods for the Examination of Waste and Wastewater, Washington, DC, USA.

Appels, L., Baeyens, J., Degrève, J., Dewil, R., 2008. Principles and potential of the anaerobic digestion of waste-activated sludge. *Prog. Energy Combust. Sci.* 34, 755-781.

Araújo, A.L.C., De Oliveira, R., Mara, D.D., Pearson, H.W., Silva, S.A., 2000. Sulphur and phosphorus transformations in wastewater storage and treatment reservoirs in northeast Brazil. *Water Sci. Technol.* 42 (10), 203-210.

Atinault, E., De Waele, V., Schmidhammer, U., Fattahi, M., Mostafavi, M., 2008. Scavenging of e_s^- and OH^\bullet radicals in concentrated HCl and NaCl aqueous solutions. *Chem. Phys. Lett.* 460, 461-465.

B

Bader, H., Hoigne, J., 1981. Determination of ozone in water by the indigo method. *Water Res.* 15, 449-456.

Bagreev, A., Bashkova, S., Bandosz, T.J., 2002. Dual role of water in the process of methyl mercaptan adsorption on activated carbons. *Langmuir* 18, 8553-8559.

Bandosz, T.J., 2002. On the adsorption/oxidation of hydrogen sulfide on activated carbons at ambient temperatures. *J. Colloid Interface Sci.* 246, 1-20.

Bashkova, S., Bandosz, T.J., 2009. The effects of urea modification and heat treatment on the process of NO₂ removal by wood-based activated carbon. *J. Colloid Interf. Sci.* 333, 97-103.

Bashkova, S., Bagreev, A., Bandosz, T.J., 2005. Catalytic properties of activated carbon surface in the process of adsorption/oxidation of methyl mercaptan. *Catal. Today* 99, 323-328.

Bashkova, S., Bagreev, A., Bandosz, T.J., 2003. Adsorption/oxidation of CH₃SH on activated carbons containing nitrogen. *Langmuir* 19, 6115-6121.

Bashkova, S., Bagreev, A., Bandosz, T.J., 2002a. Adsorption of methyl mercaptan on activated carbons. *Environ. Sci. Technol.* 36, 2777-2782.

Bashkova, S., Bagreev, A., Bandosz, T.J., 2002b. Effect of surface characteristics on adsorption of methyl mercaptan on activated carbons. *Ind. Eng. Chem. Res.* 41, 4346-4352.

Benítez, J., Rodríguez, A., Suárez, A., 1994. Optimization technique for sewage sludge conditioning with polymer and skeleton builders. *Water Res.* 28, 2067-2073.

Berenguer, R., Marco-Lozar, J.P., Quijada, C., Cazorla-Amorós, D., Morallón, E., 2012. A comparison between oxidation of activated carbon by electrochemical and chemical treatments. *Carbon* 50, 1123-1134.

Biard, P.F., Couvert, A., Renner, C., Levasseur, J.P., 2011. Intensification of volatile organic compounds mass transfer in a compact scrubber using the O₃/H₂O₂ advanced oxidation process: Kinetic study and hydroxyl radical tracking. *Chemosphere* 85, 1122-1129.

Biard, P.F., Couvert, A., Renner, C., Levasseur, J.P., 2009. Assessment and optimisation of VOC mass transfer enhancement by advanced oxidation process in a compact wet scrubber. *Chemosphere* 77, 182-187.

Bonifačić, M., Möckel, H., Bahnemann, D., Asmus, K.D., 1975a. Formation of positive ions and other primary species in the oxidation of sulphides by hydroxyl radicals. *J. Chem. Soc. Perkin Trans. 2*, 675-685.

- Bonifačić, M., Schäfer, K., Möckel, H., Asmus, K.D., 1975b. Primary steps in the reactions of organic disulfides with hydroxyl radicals in aqueous solution. *J. Phys. Chem.* 79, 1496-1502.
- Bonnin, C., Laborie, A., Paillard, H., 1990. Odor nuisances created by sludge treatment: Problems and solutions. *Water Sci. Technol.* 22, 65-74.
- Bookwalter, C.W., Zoller, D.L., Ross, P.L., Johnston, M.V., 1995. Bond-selective photodissociation of aliphatic disulfides. *J. Am. Soc. Mass. Spectrom.* 6, 872-876.
- Bordado, J.C.M., Gomes, J.F.P., 2003. Emission and odour control in Kraft pulp mills. *J. Cleaner Prod.* 11, 797-801.
- Bouchy, L., Senante, E., Dauthuille, P., Aupetitgendere, M., Harry, J.P., Venot, S., Rouge, P., 2009. Odour creation potential of sludge during composting and drying. IWA Sustainable Management & Technologies of Sludge Conference, Harbin (China).
- Boulinguez, B., Le Cloirec, P., 2010. Chemical transformations of sulfur compounds adsorbed onto activated carbon materials during thermal desorption. *Carbon* 48, 1558-1569.
- Bouzaza, A., Laplanche, A., Marsteau, S., 2004. Adsorption-oxidation of hydrogen sulfide on activated carbon fibers: Effect of the composition and the relative humidity of the gas phase. *Chemosphere* 54, 481-488.
- Brunauer, S., Deming, L.S., Deming, W.E., Teller, E., 1940. On a theory of the van der Waals adsorption of gases. *J. Am. Chem. Soc.* 62, 1723-1732.
- Brunauer, S., Emmett, P.H., Teller, E., 1938. Adsorption of gases in multimolecular layers. *J. Am. Chem. Soc.* 60, 309-319.
- Burke, G.M., Wurster, D.E., Berg, M.J., Veng-Pedersen, P., Schottelius, D.D., 1992. Surface characterization of activated charcoal by x-ray photoelectron spectroscopy (XPS): Correlation with phenobarbital adsorption data. *Pharm. Res.* 9, 126-130.
- Burlingame, G.A., Suffet, I.H., Khiari, D., Bruchet, A.L., 2004. Development of an odor wheel classification scheme for wastewater. *Water Sci. Technol.* 49 (9), 201-209.
- Buyukkamaci, N., Kucukselek, E., 2007. Improvement of dewatering capacity of a petrochemical sludge. *J. Hazard. Mater.* 144, 323-327.
- Buxton, G.V., Greenstock, C.L., Helman, W.P., Ross, A.B., 1988. Critical review of rate constants for reactions of hydrated electrons, hydrogen atoms and hydroxyl radicals ($^{\circ}\text{OH}/^{\circ}\text{O}^{-}$) in aqueous solution. *J. Phys. Chem.* 17, 513-886.

C

Cal, M.P., Rood, M.J., Larson, S.M., 1996. Removal of VOCs from humidified gas streams using activated carbon cloth. *Gas Sep. Purif.* 10, 117-121.

Cal, M.P., Rood, M.J., Larson, S.M., 1997. Gas phase adsorption of volatile organic compounds and water vapor on activated carbon cloth. *Energy Fuels* 11, 311-315.

Calvo, L., Gilarranz, M.A., Casas, J.A., Mohedano, A.F., Rodríguez, J.J., 2006. Hydrodechlorination of 4-chlorophenol in aqueous phase using Pd/AC catalysts prepared with modified active carbon supports. *Appl. Catal., B.* 67, 68-76.

Canals-Batlle, C., Ros, A., Lillo-Ródenas, M.A., Fuente, E., Montes-Morán, M.A., Martín, M.J., Linares-Solano, A., 2008. Carbonaceous adsorbents for NH₃ removal at room temperature. *Carbon* 46, 176-178.

Card, T., 2001. Chemical odour scrubbing systems. in: Stuetz, R., Frechen, F.-B. *Odours in Wastewater Treatment: Measurement, Modeling and Control.* IWA Publishing, London.

Cazorla-Amorós, D., Ribes-Pérez, D., Román-Martínez, M.C., Linares-Solano, A., 1996. Selective porosity development by calcium-catalyzed carbon gasification. *Carbon* 34, 869-878.

CEN, "European Standard EN 13725," in *Air Quality – Determination of odor concentration by dynamic olfactometry*, 2003. Brussels, Belgium.

Chang, J.S., Abu-Orf, M., Dentel, S.K., 2005. Alkylamine odors from degradation of flocculant polymers in sludges. *Water Res.* 39, 3369-3375.

Chang, I.S., Lee, C.H., 1998. Membrane filtration characteristics in membrane-coupled activated sludge system - The effect of physiological states of activated sludge on membrane fouling. *Desalination* 120, 221-233.

Charron, I., Féliers, C., Couvert, A., Laplanche, A., Patria, L., Requieme, B., 2004. Use of hydrogen peroxide in scrubbing towers for odor removal in wastewater treatment plants. *Water Sci. Technol.* 50(4), 267-274.

Chen, C., Zhang, P., Zeng, G., Deng, J., Zhou, Y., Lu, H., 2010. Sewage sludge conditioning with coal fly ash modified by sulfuric acid. *Chem. Eng. J.* 158, 616-622.

Chen, G.W., Lin, W.W., Lee, D.J., 1996. Capillary suction time (CST) as a measure of sludge dewaterability. *Water Sci. Technol.* 34 (3-4), 443-448.

Cheremisinoff, P.N., Ellerbusch, F., 1980. Carbon Adsorption Handbook. Ann Arbor Science Publishers, Michigan.

Chitikela, S., Dentel, S.K., 1998. Dual-chemical conditioning and dewatering of anaerobically digested biosolids: Laboratory evaluations. *Water Environ. Res.* 70, 1062-1069.

Cho, K.S., Hirai, M., Shoda, M., 1991. Degradation characteristics of hydrogen sulfide, methanethiol, dimethyl sulfide and dimethyl disulfide by *Thiobacillus thioparus* DW44 isolated from peat biofilter. *J. Ferment. Bioeng.* 71, 384-389.

Cordero, T., Rodriguez-Mirasol, J., Tancredi, N., Piriz, J., Vivo, G., Rodriguez, J.J., 2002. Influence of surface composition and pore structure on Cr(III) adsorption onto activated carbons. *Ind. Eng. Chem. Res.* 41, 6042-6048.

COSMOtherm C2.1, release 0.1.06. 2003. GmbH & Co KG, Leverkusen, Germany.

Couvert, A., Sanchez, C., Laplanche, A., Renner, C., 2008. Scrubbing intensification for sulphur and ammonia compounds removal. *Chemosphere* 70, 1510-1517.

Couvert, A., Charron, I., Laplanche, A., Renner, C., Patria, L., Requieme, B., 2006. Treatment of odorous sulphur compounds by chemical scrubbing with hydrogen peroxide-Application to a laboratory plant. *Chem. Eng. Sci.* 61, 7240-7248.

Cui, H., Turn, S.Q., 2009a. Adsorption/desorption of dimethylsulfide on activated carbon modified with iron chloride. *Appl. Catal., B.* 88, 25-31.

Cui, H., Turn, S.Q., Reese, M.A., 2009b. Removal of sulfur compounds from utility pipelined synthetic natural gas using modified activated carbons. *Catal. Today* 139, 274-279.

D

De la Cruz, N., Giménez, J., Esplugas, S., Grandjean, D., De Alencastro, L.F., Pulgarín, C., 2012. Degradation of 32 emergent contaminants by UV and neutral photo-fenton in domestic wastewater effluent previously treated by activated sludge. *Water Res.* 46, 1947-1957.

Defoer, N., De Bo, I., Van Langenhove, H., Dewulf, J., Van Elst, T., 2002. Gas chromatography-mass spectrometry as a tool for estimating odour concentrations of biofilter effluents at aerobic composting and rendering plants. *J. Chromatogr. A.* 970, 259-273.

Dentel, S.K., Griffin, G., Turkmen, M., 2002. Analysis of odors from flocculant polymer. WEFTEC 2002, Chicago, IL

Dentel, S.K., 2001. Conditioning, thickening, and dewatering: Research update/research needs. *Water Sci. Technol.* 44 (10), 9-18.

Devai, I., Delaune, R.D., 2002. Effectiveness of selected chemicals for controlling emission of malodorous sulfur gases in sewage sludge. *Environ. Technol.* 23, 319-329.

Devai, I., DeLaune, R.D., 1999. Emission of reduced malodorous sulfur gases from wastewater treatment plants. *Water Environ. Res.* 71, 203-207.

Dewulf, J., Van Langenhove, H., De Smedt, E., Geuens, S., 2001. Combination of advanced oxidation processes and gas absorption for the treatment of chlorinated solvents in waste gases. *Water Sci. Technol.* 44 (9), 173-180.

Dincer, F., Muezzinoglu, A., 2008. Odor-causing volatile organic compounds in wastewater treatment plant units and sludge management areas. *J. Environ. Sci. Heal. A* 43, 1569-1574.

Domingo-García, M., López Garzón, F.J., Pérez-Mendoza, M.J., 2002. On the characterization of chemical surface groups of carbon materials. *J. Colloid Interf. Sci.* 248, 116-122.

Domingo-García, M., López-Garzón, F.J., Pérez-Mendoza, M., 2000. Effect of some oxidation treatments on the textural characteristics and surface chemical nature of an activated carbon. *J. Colloid Interf. Sci.* 222, 233-240.

Dubinin, M.M., 1979. *Characterisation of porous solids* Society of chemical industries, London.

Ⓔ

Ershov, B.G., Kelm, M., Gordeev, A.V., Janata, E., 2002. A pulse radiolysis study of the oxidation of Br^- by Cl_2^- in aqueous solution: Formation and properties of ClBr^\cdot . *PCCP.* 4, 1872-1875.

Esplugas, S., Giménez, J., Contreras, S., Pascual, E., Rodríguez, M., 2002. Comparison of different advanced oxidation processes for phenol degradation. *Water Res.* 36, 1034-1042.

Estrada, J.M., Kraakman, N.J.R.B., Muñoz, R., Lebrero, R., 2011. A comparative analysis of odour treatment technologies in wastewater treatment plants. *Environ. Sci. Technol.* 45, 1100-1106.

Ⓕ

Feitz, A.J., Guan, J., Chattopadhyay, G., Waite, T.D., 2002. Photo-Fenton degradation of dichloromethane for gas phase treatment. *Chemosphere* 48, 401-406.

Feng, X., Deng, J., Lei, H., Bai, T., Fan, Q., Li, Z., 2009. Dewaterability of waste activated sludge with ultrasound conditioning. *Bioresour. Technol.* 100, 1074-1081.

Fenton, H.J.H., 1894. LXXIII. - Oxidation of tartaric acid in presence of iron. *J. Chem. Soc. Trans.* 65, 899-910.

Figueiredo, J.L., Pereira, M.F.R., 2010. The role of surface chemistry in catalysis with carbons. *Catal. Today* 150, 2-7.

Figueiredo, J.L., Pereira, M.F.R., Freitas, M.M.A., Órfão, J.J.M., 2007. Characterization of active sites on carbon catalysts. *Ind. Eng. Chem. Res.* 46, 4110-4115.

Figueiredo, J.L., Pereira, M.F.R., Freitas, M.M.A., Órfão, J.J.M., 1999. Modification of the surface chemistry of activated carbons. *Carbon* 37, 1379-1389.

Flemming, H.C., Wingender, J., 2001. Relevance of microbial extracellular polymeric substances (EPSs) - Part I: Structural and ecological aspects. *Wat. Sci. Technol.* 43(6), 1-8.

Forster, C.F., 1971. Activated sludge surfaces in relation to the sludge volume index. *Water Res.* 5, 861-870.

Frechen, F.B., 1994. Odour emissions of wastewater treatment plants - Recent German experiences. *Water Sci. Technol.* 30, 35-46.

Frechen, F.B., 1988. Odour emissions and odour control at wastewater treatment plants in west Germany. *Water Sci. Technol.* 20 (4-5), 264-266.

Freudenthal, K., Otterpohl, R., Behrendt, J., 2005. Absorption of odourous substances using selective gas-liquid separation processes. *Waste Manage.* 25, 975-984.

Frisch, M., Trucks, G., Schlegel, H., Robb, M., Cheeseman, J., et al. 2004. Gaussian 03, revision B.05.

Frølund, B., Palmgren, R., Keiding, K., Nielsen, P.H., 1996. Extraction of extracellular polymers from activated sludge using a cation exchange resin. *Water Res.* 30, 1749-1758.



Gabriel, D., Deshusses, M.A., 2003. Performance of a full-scale biotrickling filter treating H₂S at a gas contact time of 1.6 to 2.2 seconds. *Environ. Prog.* 22, 111-118.

Getoff, N., Lutz, W., 1985. Radiation induced decomposition of hydrocarbons in water resources. *Radiat. Phys. Chem.* 25, 21-26.

Ghafari, S., Aziz, H.A., Isa, M.H., Zinatizadeh, A.A., 2009. Application of response surface methodology (RSM) to optimize coagulation-flocculation treatment of leachate using poly-aluminum chloride (PAC) and alum. *J. Hazard. Mater.* 163, 650-656.

Gironi, F., Piemonte, V., 2011. VOCs removal from dilute vapour streams by adsorption onto activated carbon. *Chem. Eng. J.* 172, 671-677.

Gonçalves, M., Sánchez-García, L., Oliveira Jardim, E.D., Silvestre-Albero, J., Rodríguez-Reinoso, F., 2011. Ammonia removal using activated carbons: Effect of the surface chemistry in dry and moist conditions. *Environ. Sci. Technol.* 45, 10605-10610.

Gonzalez-Miquel, M., Palomar, J., Omar, S., Rodriguez, F., 2011. CO₂/N₂ selectivity prediction in supported ionic liquid membranes (SILMs) by COSMO-RS. *Ind. Eng. Chem. Res.* 50, 5739-5748.

Gonzalez-Olmos, R., Roland, U., Toufar, H., Kopinke, F.D., Georgi, A., 2009. Fe-zeolites as catalysts for chemical oxidation of MTBE in water with H₂O₂. *Appl. Catal., B.* 89, 356-364.

Gostelow, P., Parsons, S.A., Stuetz, R.M., 2001. Odour measurements for sewage treatment works. *Water Res.* 35, 579-597.

Goyal, M., Dhawan, R., Bhagat, M., 2008. Adsorption of dimethyl sulfide vapors by activated carbons. *Colloids Surf. A.* 322, 164-169.

Gu, L., Zhang, X., Lei, L., Zhang, Y., 2009. Enhanced degradation of nitrophenol in ozonation integrated plasma modified activated carbons. *Microporous Mesoporous Mater.* 119, 237-244.

H

Higgins, M.J., 2010. Evaluation of aluminium and iron addition during aconditioning and dewatering for odor control PHASE VI. Water Environment Research Foundation Alexandria, VA.

Higgins, M.J., Adams, G., Chen, Y.C., Erdal, Z., Forbes Jr, R.H., Glindemann, D., Hargreaves, J.R., McEwen, D., Murthy, S.N., Novak, J.T., Witherspoon, J., 2008. Role of protein, amino acids, and enzyme activity on odor production from anaerobically digested and dewatered biosolids. *Water Environ. Res.* 80, 127-135.

Ho, K.L., Chung, Y.C., Lin, Y.H., Tseng, C.P., 2008. Microbial populations analysis and field application of biofilter for the removal of volatile-sulfur compounds from swine wastewater treatment system. *J. Hazard. Mater.* 152, 580-588.

Hoygaard Bruus, J., Halkjaer Nielsen, P., Keiding, K., 1992. On the stability of activated sludge flocs with implications to dewatering. *Water Res.* 26, 1597-1604.

Hwa, T.J., Jeyaseelan, S., 1997. Comparison of lime and alum as oily sludge conditioners. *Water Sci. Technol.* 36, 117-124.

Hwa, T.J., Jeyaseelan, S., 1997. Conditioning of oily sludges with municipal solid wastes incinerator fly ash. *Water Sci. Technol.* 35 (8), 231-238.

Hwang, K.Y., Shin, E.B., Choi, H.B., 1997. A mechanical pretreatment of waste activated sludge for improvement of anaerobic digestion system. *Water Sci. Technol.* 36, 111-116.

Hwang, Y., Matsuo, T., Hanaki, K., Suzuki, N., 1994. Removal of odorous compounds in wastewater by using activated carbon, ozonation and aerated biofilter. *Water Res.* 28, 2309-2319.

⌋

Islam, A.K.M.N., Hanaki, K., Matsuo, T., 1998. Fate of dissolved odorous compounds in sewage treatment plants. *Water Sci. Technol.* 38, 337-344.

Israelson, G., 2004. Results of testing various natural gas desulfurization adsorbents. *J. Mater. Eng. Perform.* 13, 282-286.

⌋

Jankowska, J., A., S., Choma, J., 1991. *Active carbon*. Ellis Horwood, New York.

Jo, C.H., Dietrich, A.M., Tanko, J.M., 2011. Simultaneous degradation of disinfection byproducts and earthy-musty odorants by the UV/H₂O₂ advanced oxidation process. *Water Res.* 45, 2507-2516.

⌋

Karageorgos, P., Latos, M., Kotsifaki, C., Lazaridis, M., Kalogerakis, N., 2010. Treatment of unpleasant odors in municipal wastewater treatment plants. *Water Sci. Technol.* 61, 2635-2644.

Kastner, J.R., Das, K.C., Hu, C., McClendon, R., 2003. Effect of pH and temperature on the kinetics of odor oxidation using chlorine dioxide. *J. Air Waste Manage. Assoc.* 53, 1218-1224.

Kastner, J.R., Das, K.C., 2002. Wet scrubber analysis of volatile organic compound removal in the rendering industry. *J. Air Waste Manage. Assoc.* 52, 459-469.

Katoh, H., Kuniyoshi, I., Hirai, M., Shoda, M., 1995. Studies of the oxidation mechanism of sulphur-containing gases on wet activated carbon fibre. *Appl. Catal., B.* 6, 255-262.

Kawamoto, K., Ishimaru, K., Imamura, Y., 2005. Reactivity of wood charcoal with ozone. *J. Wood Sci.* 51, 66-72.

Kawasaki, N., Kinoshita, H., Oue, T., Nakamura, T., Tanada, S., 2004. Study on adsorption kinetic of aromatic hydrocarbons onto activated carbon in gaseous flow method. *J. Colloid Interface Sci.* 275, 40-43.

Kim, H., Murthy, S., Peot, C., Ramirez, M., Strawn, M., Park, C.H., McConnell, L.L., 2003. Examination of mechanisms for odor compound generation during lime stabilization. *Water Environ. Res.* 75, 121-125.

Kim, H., Murthy, S., McConnell, L.L., Peot, C., Ramirez, M., Strawn, M., 2002. Characterization of wastewater and solids odors using solid phase microextraction at a large wastewater treatment plant. *Water Sci. Technol.* 46 (10) 9-16.

Klamt, A., Eckert, F., 2000. COSMO-RS: a novel and efficient method for the a priori prediction of thermophysical data of liquids. *Fluid Phase Equilib.* 172, 43-72.

Koe, L.C.C., Tan, N.C., 1990. Odour generation potential of wastewaters. *Water Res.* 24, 1453-1458.

Kohl, S., Drochner, A., Vogel, H., 2010. Quantification of oxygen surface groups on carbon materials via diffuse reflectance FT-IR spectroscopy and temperature programmed desorption. *Catal. Today* 150, 67-70.

Kopp, J., Dichtl, N., 2001. Influence of the free water content on the dewaterability of sewage sludges. *Water Sci. Technol.* 44 (10) 177-183.

Krüger, R.L., Dallago, R.M., Di Luccio, M., 2009. Degradation of dimethyl disulfide using homogeneous Fenton's reaction. *J. Hazard. Mater.* 169, 443-447.

↳

Langlais, B., Reckhow, D.A., Brink, D.R., 1991. *Ozone in water treatment: Application and Engineering* Lewis Publishers INC, Chelsea.

Laor, Y., Naor, M., Ravid, U., Fine, P., Halachmi, I., Chen, Y., Baybikov, R., 2011. Odorants and malodors associated with land application of biosolids stabilized with lime and coal fly ash. *J. Environ. Qual.* 40, 1405-1415.

LaVerne, J.A., Ryan, M.R., Mu, T., 2009. Hydrogen production in the radiolysis of bromide solutions. *Radiat. Phys. Chem.* 78, 1148-1152.

- Le Leuch, L.M., Bandosz, T.J., 2007. The role of water and surface acidity on the reactive adsorption of ammonia on modified activated carbons. *Carbon* 45, 568-578.
- Le Leuch, L.M., Subrenat, A., Le Cloirec, P., 2003. Hydrogen sulfide adsorption and oxidation onto activated carbon cloths: Applications to odorous gaseous emission treatments. *Langmuir* 19, 10869-10877.
- Lebrero, R., Bouchy, L., Stuetz, R., Muñoz, R., 2011. Odor assessment and management in wastewater treatment plants: A review. *Crit. Rev. Environ. Sci. Technol.* 41, 915-950.
- Lebrero, R., Rodríguez, E., Martín, M., García-Encina, P.A., Muñoz, R., 2010. H₂S and VOCs abatement robustness in biofilters and air diffusion bioreactors: A comparative study. *Water Res.* 44, 3905-3914.
- Lee, S.W., Daud, W.M.A.W., Lee, M.G., 2010. Adsorption characteristics of methyl mercaptan, dimethyl disulfide, and trimethylamine on coconut-based activated carbons modified with acid and base. *J. Ind. Eng. Chem.* 16, 973-977.
- Lee, D.J., Tay, J.H., Huang, Y.T., He, P.J., 2005. Introduction to sludge treatment in: Wang, L.J., Huang, Y.T., Shammas, N.K. *Handbook of environmental engineering, physicochemical treatment processes* The Humana Press, Totowa, New Jersey.
- Lee, C.H., Liu, J.C., 2000. Enhanced sludge dewatering by dual polyelectrolytes conditioning. *Water Res.* 34, 4430-4436.
- Lee, Y.-N., Zhou, X., 1994. Aqueous reaction kinetics of ozone and dimethylsulfide and its atmospheric implications. *J. Geophys. Res. D: Atmos.* 99, 3597-3605.
- Lemus, J., Martín-Martínez, M., Palomar, J., Gómez-Sainero, L., Gilarranz, M.A., Rodríguez, J.J., 2012a. Removal of chlorinated organic volatile compounds by gas phase adsorption with activated carbon. *Chem. Eng. J.* 211-212, 246-254.
- Lemus, J., Palomar, J., Heras, F., Gilarranz, M.A., Rodríguez, J.J., 2012b. Developing criteria for the recovery of ionic liquids from aqueous phase by adsorption with activated carbon. *Sep. Purif. Technol.* 97, 11-19.
- Leonardos, G., Kendall, D., Bernard, N., 1969. Odor Threshold Determinations of 53 Odorant Chemicals. *J. Air Pollut. Control Assoc.* 19, 91-95.
- Li, N., Ma, X., Zha, Q., Kim, K., Chen, Y., Song, C., 2011. Maximizing the number of oxygen-containing functional groups on activated carbon by using ammonium persulfate and improving the temperature-programmed desorption characterization of carbon surface chemistry. *Carbon* 49, 5002-5013.

Li, L., Liu, S., Liu, J., 2011. Surface modification of coconut shell based activated carbon for the improvement of hydrophobic VOC removal. *J. Hazard. Mater.* 192, 683-690.

Li, Y.H., Lee, C.W., Gullett, B.K., 2003. Importance of activated carbon's oxygen surface functional groups on elemental mercury adsorption. *Fuel* 82, 451-457.

Lillo-Ródenas, M.A., Cazorla-Amorós, D., Linares-Solano, A., 2005. Behaviour of activated carbons with different pore size distributions and surface oxygen groups for benzene and toluene adsorption at low concentrations. *Carbon* 43, 1758-1767.

Lin, C.W., Chang, D.P.Y., 2005. Formation and emission of chlorinated byproducts from a bench-scale packed-bed odor scrubber. *Water Air Soil Pollut.* 162, 19-35.

Liu, H., Yang, J., Zhu, N., Zhang, H., Li, Y., He, S., Yang, C., Yao, H., 2013. A comprehensive insight into the combined effects of Fenton's reagent and skeleton builders on sludge deep dewatering performance. *J. Hazard. Mater.* 258-259, 144-150.

Liu, H., Luo, G.Q., Hu, H.Y., Zhang, Q., Yang, J.K., Yao, H., 2012. Emission characteristics of nitrogen- and sulfur-containing odorous compounds during different sewage sludge chemical conditioning processes. *J. Hazard. Mater.* 235-236, 298-306.

Liu, Y.X., Zhang, J., 2011. Photochemical oxidation removal of NO and SO₂ from simulated flue gas of coal-fired power plants by wet scrubbing using UV/H₂O₂ advanced oxidation process. *Ind. Eng. Chem. Res.* 50, 3836-3841.

Liu, T.X., Li, X.Z., Li, F.B., 2010. Development of a photocatalytic wet scrubbing process for gaseous odor treatment. *Ind. Eng. Chem. Res.* 49, 3617-3622.

López-González, J., Martínez-Vilchez, F., Rodríguez-Reinoso, F., 1980. Preparation and characterization of active carbons from olive stones. *Carbon* 18, 413-418. Lopez-Ramon, M.V., Stoekli, F., Moreno-Castilla, C., Carrasco-Marin, F., 1999. On the characterization of acidic and basic surface sites on carbons by various techniques. *Carbon* 37, 1215-1221.

Lovato, M.E., Martín, C.A., Cassano, A.E., 2009. A reaction kinetic model for ozone decomposition in aqueous media valid for neutral and acidic pH. *Chem. Eng. J.* 146, 486-497.

Lowry, O.H., Rosebrough, N.J., Farr, A.L., Randall, R.J., 1951. Protein measurement with the Folin phenol reagent. *J. Biol. Chem.* 193, 265-275.

Lu, N., Yu, H.T., Su, Y., Wu, Y., 2012. Water absorption and photocatalytic activity of TiO₂ in a scrubber system for odor control at varying pH. *Sep. Purif. Technol.* 90, 196-203.

M

- Ma, X., Wu, Z., Zhou, M., Ding, J., 2013. Electrochemical scission of C-S bond in ethanethiol on a modified β -PbO₂ anode in aqueous solution. *Sep. Purif. Technol.* 109, 72-76.
- Mahamuni, N.N., Adewuyi, Y.G., 2010. Advanced oxidation processes (AOPs) involving ultrasound for waste water treatment: A review with emphasis on cost estimation. *Ultrason. Sonochem.* 17, 990-1003.
- Marsh, H., Rodríguez-Reinoso, F., 2006. *Activated carbon*. Elsevier, Amsterdam.
- Matilainen, A., Sillanpää, M., 2010. Removal of natural organic matter from drinking water by advanced oxidation processes. *Chemosphere* 80, 351-365.
- Mawhinney, D.B., Yates Jr, J.T., 2001. FTIR study of the oxidation of amorphous carbon by ozone at 300 K - Direct COOH formation. *Carbon* 39, 1167-1173.
- Mehler, C., Klamt, A., Peukert, W., 2002. Use of COSMO-RS for the prediction of adsorption equilibria. *AIChE Journal* 48, 1093-1099.
- Mendham, J., Denney, R.C., Barnes, J.D., Thomas, M.J.K., 2000. *Vogel's Textbook of Quantitative Chemical Analysis*. Longman, London, UK.
- Metcalf. Eddy., 2003. *Wastewater engineering: treatment and reuse*. McGraw-Hill, New York.
- Mezyk, S.P., Bartels, D.M., 1997. Temperature dependence of hydrogen atom reaction with nitrate and nitrite species in aqueous solution. *J. Phys. Chem. A.* 101, 6233-6237.
- Mills, B., 1995, Review of methods of odour control. *Filtr. Separat.* 2, 147-152.
- Mohajeri, S., Aziz, H.A., Isa, M.H., Zahed, M.A., Adlan, M.N., 2010. Statistical optimization of process parameters for landfill leachate treatment using electro-Fenton technique. *J. Hazard. Mater.* 176, 749-758.
- Montgomery, D.C., 1996. *Design and analysis of experiments* fourth ed. John Wiley and Sons, USA.
- Moreno-Castilla, C., López-Ramón, M.V., Carrasco-Marín, F., 2000. Changes in surface chemistry of activated carbons by wet oxidation. *Carbon* 38, 1995-2001.
- Moreno-Castilla, C., Ferro-García, M.A., Joly, J.P., Bautista-Toledo, I., Carrasco-Marín, F., Rivera-Utrilla, J., 1995. Activated carbon surface modifications by nitric acid, hydrogen peroxide, and ammonium peroxydisulfate treatments. *Langmuir* 11, 4386-4392.

Moretti, E.C., 2002. Reduce VOC and HAP emissions. *Chem. Eng. Prog.* 98, 30-40.

Muller, C.D., Abu-Orf, M., Blumenschein, C.D., Novak, J.T., 2009. A comparative study of ultrasonic pretreatment and an internal recycle for the enhancement of mesophilic anaerobic digestion. *Water Environ. Res.* 81, 2398-2410.

Murthy, S., Kim, H., Peot, C., McConnell, L., Strawn, M., Sadick, T., Dolak, I., 2003. Evaluation of odor characteristics of heat-dried biosolids product. *Water Environ. Res.* 75, 523-531.

Myslinski, T., Basu, S., Rhode, S., Hunt, G., Shilinsky, K., 2000. Fate of air toxics and VOCs in the odor control scrubbers at the Deer Island Treatment Plant. *Environ. Prog.* 19, 229-237.

Myung Cha, J., Suk Cha, W., Lee, J.H., 1999. Removal of organo-sulphur odour compounds by *Thiobacillus novellus* SRM, sulphur-oxidizing microorganisms. *Process Biochem.* 34, 659-665.

N

Nelson, R.F., Brattlof, B.D., 1979. Sludge pressure filtration with fly ash addition. *J. Water Pollut. Control Fed.* 51, 1024-1031.

Neyens, E., Baeyens, J., 2003. A review of classic Fenton's peroxidation as an advanced oxidation technique. *J. Hazard. Mater.* 98, 33-50.

Nguyen-Thanh, D., Bandosz, T.J., 2005. Activated carbons with metal containing bentonite binders as adsorbents of hydrogen sulfide. *Carbon* 43, 359-367.

Nielsen, A.H., Lens, P., Vollertsen, J., Hvitved-Jacobsen, T., 2005. Sulfide-iron interactions in domestic wastewater from a gravity sewer. *Water Res.* 39, 2747-2755.

Novak, J.T., Verma, N., Muller, C.D., 2007. The role of iron and aluminium in digestion and odor formation. *Water Sci. Technol.* 56 (9), 59-65.

Novak, J.T., Adams, G., Chen, Y.C., Erdal, Z., Forbes Jr, R.H., Glindemann, D., Hargreaves, J.R., Hentz, L., Higgins, M.J., Murthy, S.N., Witherspoon, J., 2006. Generation pattern of sulfur containing gases from anaerobically digested sludge cakes. *Water Environ. Res.* 78, 821-827.

P

Pagans, E., Font, X., Sánchez, A., 2007. Coupling composting and biofiltration for ammonia and volatile organic compound removal. *Biosystems Eng.* 97, 491-500.

Palomar, J., Gonzalez-Miquel, M., Bedia, J., Rodriguez, F., Rodriguez, J.J., 2011a. Task-specific ionic liquids for efficient ammonia absorption. *Sep. Purif. Technol.* 82, 43-52.

Palomar, J., Gonzalez-Miquel, M., Polo, A., Rodriguez, F., 2011b. Understanding the physical absorption of CO₂ in ionic liquids using the COSMO-RS method. *Ind. Eng. Chem. Res.* 50, 3452-3463.

Palomar, J., Lemus, J., Gilarranz, M.A., Rodriguez, J.J., 2009. Adsorption of ionic liquids from aqueous effluents by activated carbon. *Carbon* 47, 1846-1856.

Parsons, S., 2004. *Advanced oxidation processes for water and wastewater treatment.* IWA Publishing, London.

Pereira, M.F.R., Soares, S.F., Órfão, J.J.M., Figueiredo, J.L., 2003. Adsorption of dyes on activated carbons: Influence of surface chemical groups. *Carbon* 41, 811-821.

Peter, A., Von Gunten, U., 2007. Oxidation kinetics of selected taste and odor compounds during ozonation of drinking water. *Environ. Sci. Technol.* 41, 626-631.

Peterson, G.L., 1977. A simplification of the protein assay method of Lowry et al. Which is more generally applicable. *Anal. Biochem.* 83, 346-356.

Pignatello, J.J., Oliveros, E., MacKay, A., 2006. Advanced oxidation processes for organic contaminant destruction based on the fenton reaction and related chemistry. *Crit. Rev. Env. Sci. Technol.* 36, 1-84.

Pradhan, B.K., Sandle, N.K., 1999. Effect of different oxidizing agent treatments on the surface properties of activated carbons. *Carbon* 37, 1323-1332.

Prados-Joya, G., 2010. Tratamiento de aguas para la eliminación de antibióticos - nitroimidazoles- mediante adsorción sobre carbón activado y tecnologías avanzadas de oxidación. Tesis doctoral. Department of inorganic chemistry. University of Granada, Granada.

Q

Qi, Y., Thapa, K.B., Hoadley, A.F.A., 2011a. Application of filtration aids for improving sludge dewatering properties - A review. *Chem. Eng. J.* 171, 373-384.

Qi, Y., Thapa, K.B., Hoadley, A.F.A., 2011b. Benefit of lignite as a filter aid for dewatering of digested sewage sludge demonstrated in pilot scale trials. *Chem. Eng. J.* 166, 504-510.

R

Ramírez, M., Gómez, J.M., Aroca, G., Cantero, D., 2009. Removal of hydrogen sulfide by immobilized *Thiobacillus thioautotrophicus* in a biotrickling filter packed with polyurethane foam. *Bioresour. Technol.* 100, 4989-4995.

Ras, M.R., Borrull, F., Marcé, R.M., 2008. Determination of volatile organic sulfur compounds in the air at sewage management areas by thermal desorption and gas chromatography-mass spectrometry. *Talanta* 74, 562-569.

Rey, A., Faraldos, M., Bahamonde, A., Casas, J.A., Zazo, J.A., Rodríguez, J.J., 2008. Role of the activated carbon surface on catalytic wet peroxide oxidation. *Ind. Eng. Chem. Res.* 47, 8166-8174.

Rivera-Utrilla, J., Sánchez-Polo, M., 2011. Adsorbent-adsorbate interactions in the adsorption of organic and inorganic species on ozonized activated carbons: A short review. *Adsorption* 17, 611-620.

Rodríguez-Reinoso, F., Linares-Solano, A., 1989. Microporous structures of activated carbon as revealed by adsorption methods. *Chemistry and Physics of Carbon*. Thromer PA, New York.

Rosenfeld, P.E., 2001. Effect of high carbon ash on biosolids odor emissions and microbial activity. *Water Air Soil Pollut.* 131, 245-260.

Roth, O., Laverne, J.A., 2011. Effect of pH on H₂O₂ production in the radiolysis of water. *J. Biol. Chem. A.* 115, 700-708.

Ruthven, D.M., 1984. Principles of adsorption and adsorption processes John Wiley & Sons, New York.

Rouquerol, F., Rouquerol, J., Sing, K.S.W., 1999. Adsorption of powders and porous solids. Academic press, London.

S

Sanchez, C., Couvert, A., Laplanche, A., Renner, C., 2006. New compact scrubber for odour removal in wastewater treatment plants. *Water Sci. Technol.* 54(9), 45-52.

Schlegelmilch, M., Streese, J., Stegmann, R., 2005. Odour management and treatment technologies: An overview. *Waste Manage.* 25, 928-939.

Sekyiamah, K., Kim, H., McConnell, L.L., Torrents, A., Ramirez, M., 2008. Identification of seasonal variations in volatile sulfur compound formation and release from the secondary treatment system at a large wastewater treatment plant. *Water Environ. Res.* 80, 2261-2267.

Shim, J.W., Park, S.J., Ryu, S.K., 2001. Effect of modification with HNO₃ and NaOH on metal adsorption by pitch-based activated carbon fibers. *Carbon* 39, 1635-1642.

Siegell, J.H., 1996. Feature Report: VOC control options. *Chem. Eng.* 103, 92-96.

Sidheswaran, M.A., Destailats, H., Sullivan, D.P., Cohn, S., Fisk, W.J., 2012. Energy efficient indoor VOC air cleaning with activated carbon fiber (ACF) filters. *Build. Environ.* 47, 357-367.

Sing, K.S.W., 1998. Adsorption methods for the characterization of porous materials. *Adv. Colloid Interface Sci.* 76-77, 3-11.

Singer, D.C., 2001. *A Laboratory Quality Handbook of the Best Practices and Relevant Regulations*. Quality Press, USA.

Socol, C.R., Woiciechowski, A.L., Vandenberghe, L.P.S., Soares, M., Neto, G.K., Thomaz-Socol, V., 2003. Biofiltration: An Emerging Technology. *Indian J. Biotechnol.* 2, 396-410.

Sotelo, J.L., Beltran, F.J., Benitez, F.J., Beltran-Heredia, J., 1987. Ozone decomposition in water: kinetic study. *Ind. Eng. Chem. Res.* 26, 39-43.

Staelin, J., Hoigne, J., 1985. Decomposition of ozone in water in the presence of organic solutes acting as promoters and inhibitors of radical chain reactions. *Environ. Sci. Technol.* 19, 1206-1213.

Subramanian, R., Novak, J.T., Murthy, S., Glinderman, D., North, J., 2005. Investigating the role of process conditions in wastewater sludge odour generation. *WEFTEC 2005*, Washington DC, USA, 6582-6604

Suffet, I.H., Burlingame, G.A., Rosenfeld, P.E., Bruchet, A., 2004. The value of an odor-quality-wheel classification scheme for wastewater treatment plants. *Water Sci. Technol.* 50(4), 25-32.

†

Tamai, H., Nagoya, H., Shiono, T., 2006. Adsorption of methyl mercaptan on surface modified activated carbon. *J. Colloid Interface Sci.* 300, 814-817.

Tambosi, J.L., Di Domenico, M., Schirmer, W.N., José, H.J., Moreira, R.d.F.P.M., 2006. Treatment of paper and pulp wastewater and removal of odorous compounds by a Fenton-like process at the pilot scale. *J. Chem. Technol. Biotechnol.* 81, 1426-1432.

Tang, S., Lu, N., Wang, J.K., Ryu, S.K., Choi, H.S., 2007. Novel effects of surface modification on activated carbon fibers using a low pressure plasma treatment. *J. Phys. Chem. C* 111, 1820-1829.

Tenney, M.W., Cole, T.G., 1968. The use of fly ash in conditioning biological sludges for vacuum filtration. *J. Water Pollut. Control Fed. Suppl.*:281-302.

Tokumura, M., Wada, Y., Usami, Y., Yamaki, T., Mizukoshi, A., Noguchi, M., Yanagisawa, Y., 2012. Method of removal of volatile organic compounds by using wet scrubber coupled with photo-Fenton reaction - Preventing emission of by-products. *Chemosphere* 89, 1238-1242.

Tony, M.A., Zhao, Y.Q., Fu, J.F., Tayeb, A.M., 2008. Conditioning of aluminium-based water treatment sludge with Fenton's reagent: Effectiveness and optimising study to improve dewaterability. *Chemosphere* 72, 673-677.

Tornes, O., Whipps, A., 2004. The influence of operating experiences in the design of the IVAR thermal drying plant expansion in Stavanger, Norway. *Water Sci. Technol.* 49(10), 179-184.

Tsang, K.R., Vesilind, P.A., 1990. Moisture distribution in sludges. *Water Sci. Technol.* 22, 135-142.

Tsunoda, R., Ozawa, T., Ando, J.I., 1998. Ozone treatment of coal- and coffee grounds-based active carbons: Water vapor adsorption and surface fractal micropores. *J. Colloid Interf. Sci.* 205, 265-270.

Tuhkanen, T., 2004. UV/H₂O₂ processes. in: Parsons, S. *Advanced Oxidation Processes for Waste and Wastewater Treatments*. IWA Publishing, London, UK.

Turovskiy, I.S., Mathai, P.K., 2006. *Wastewater sludge processing*. Wiley-Interscience. John Wiley & Sons, Hoboken, New Jersey.

V

Valdés, H., Sanchez-Polo, M., Zaror, C.A., 2003. Effect of ozonation on the activated carbon surface chemical properties and on 2-mercaptobenzothiazole adsorption. *Lat. Am. Appl. Res.* 33, 219-223.

Valdés, H., Sánchez-Polo, M., Rivera-Utrilla, J., Zaror, C.A., 2002. Effect of ozone treatment on surface properties of activated carbon. *Langmuir* 18, 2111-2116.

Van Durme, G.P., McNamara, B.F., McGinley, C.M., 1992. Bench-scale removal of odor and volatile organic compounds at a composting facility. *Water Environ. Res.* 64, 19-27.

Van Gemert, L.J., 2003. *Odour thresholds: Compilations of odour threshold values in air, water and other media*. Oliemans Punter & Partners, The Netherlands.

Van Groenestijn, J.W., Hesselink, P.G.M., 1993. Biotechniques for air pollution control. *Biodegradation* 4, 283-301.

Velo-Gala, I., López-Peñalver, J.J., Sánchez-Polo, M., Rivera-Utrilla, J., 2013. Surface modifications of activated carbon by gamma irradiation. *Carbon*. 67, 236-249.

Vermilyea, A.W., Voelker, B.M., 2009. Photo-fenton reaction at near neutral pH. *Environ. Sci. Technol.* 43, 6927-6933.

Vilmain, J.B., Courousse, V., Biard, P.F., Azizi, M., Couvert, A., 2013. Kinetic study of hydrogen sulfide absorption in aqueous chlorine solution. *Chem. Eng. Res. Des.* 92 (2), 191-204.

Vincent, A.J., 2001. Sources of odours in wastewater treatment. in: Stuetz, R., Frechen, F.B. *Odours in wastewater treatment: Measurement, modelling and control*. IWA, London, England.

Von Gunten, U., 2003. Ozonation of drinking water: Part I. Oxidation kinetics and product formation. *Water Research* 37, 1443-1467.

W

Walling, C., 1975. Fenton's reagent revisited. *Acc. Chem. Res.* 8, 125-131.

Wan, Z., Hameed, B.H., 2011. Transesterification of palm oil to methyl ester on activated carbon supported calcium oxide catalyst. *Bioresour. Technol.* 102, 2659-2664.

Wang, S., 2008. A Comparative study of Fenton and Fenton-like reaction kinetics in decolourisation of wastewater. *Dyes Pigm.* 76, 714-720.

Weiss, J., 1935. Investigations on the radical HO₂ in solution. *Trans. Faraday Soc.* 31, 668-681.

Werther, J., Ogada, T., 1999. Sewage sludge combustion. *Prog. Energy Combust. Sci.* 25, 55-116.

Witek-Krowiak, A., Chojnacka, K., Podstawczyk, D., Dawiec, A., Pokomeda, K., 2014. Application of response surface methodology and artificial neural network methods in modelling and optimization of biosorption process. *Bioresour. Technol.* In Press. <http://dx.doi.org/10.1016/j.biortech.2014.01.021>

Wu, C.C., Huang, C., Lee, D.J., 1997. Effects of polymer dosage on alum sludge dewatering characteristics and physical properties. *Colloids Surf., A.* 122, 89-96.

Y

Yuan, H.P., Cheng, X.B., Chen, S.P., Zhu, N.W., Zhou, Z.Y., 2011. New sludge pretreatment method to improve dewaterability of waste activated sludge. *Bioresour. Technol.* 102, 5659-5664.

Yuan, H., Zhu, N., Song, L., 2010. Conditioning of sewage sludge with electrolysis: Effectiveness and optimizing study to improve dewaterability. *Bioresour. Technol.* 101, 4285-4290.

Z

Zall, J., Galil, N., Rehbun, M., 1987. Skeleton builders for conditioning oily sludge. *J. Water Pollut. Control Fed.* 59, 699-706.

Zarra, T., Naddeo, V., Belgiorno, V., Reiser, M., Kranert, M., 2008. Odour monitoring of small wastewater treatment plant located in sensitive environment. *Water Sci. Technol.* 58(1), 89-94.

Zhai, L.F., Sun, M., Song, W., Wang, G., 2012. An integrated approach to optimize the conditioning chemicals for enhanced sludge conditioning in a pilot-scale sludge dewatering process. *Bioresour. Technol.* 121, 161-168.

Zhang, L., De Schryver, P., De Gusseme, B., De Muynck, W., Boon, N., Verstraete, W., 2008. Chemical and biological technologies for hydrogen sulfide emission control in sewer systems: A review. *Water Res.* 42, 1-12.

Zhao, Y.Q., 2002. Enhancement of alum sludge dewatering capacity by using gypsum as skeleton builder. *Colloids Surf., A* 211, 205-212.

ANNEX

The calibration curves of volatile sulphur compounds in gas (Figure A1) and liquid phase (Figure A2) and the standard calibration of protein (Figure A3), hydrogen peroxide (Figure A4) and iron (Figure A5) content are presented in this annex.

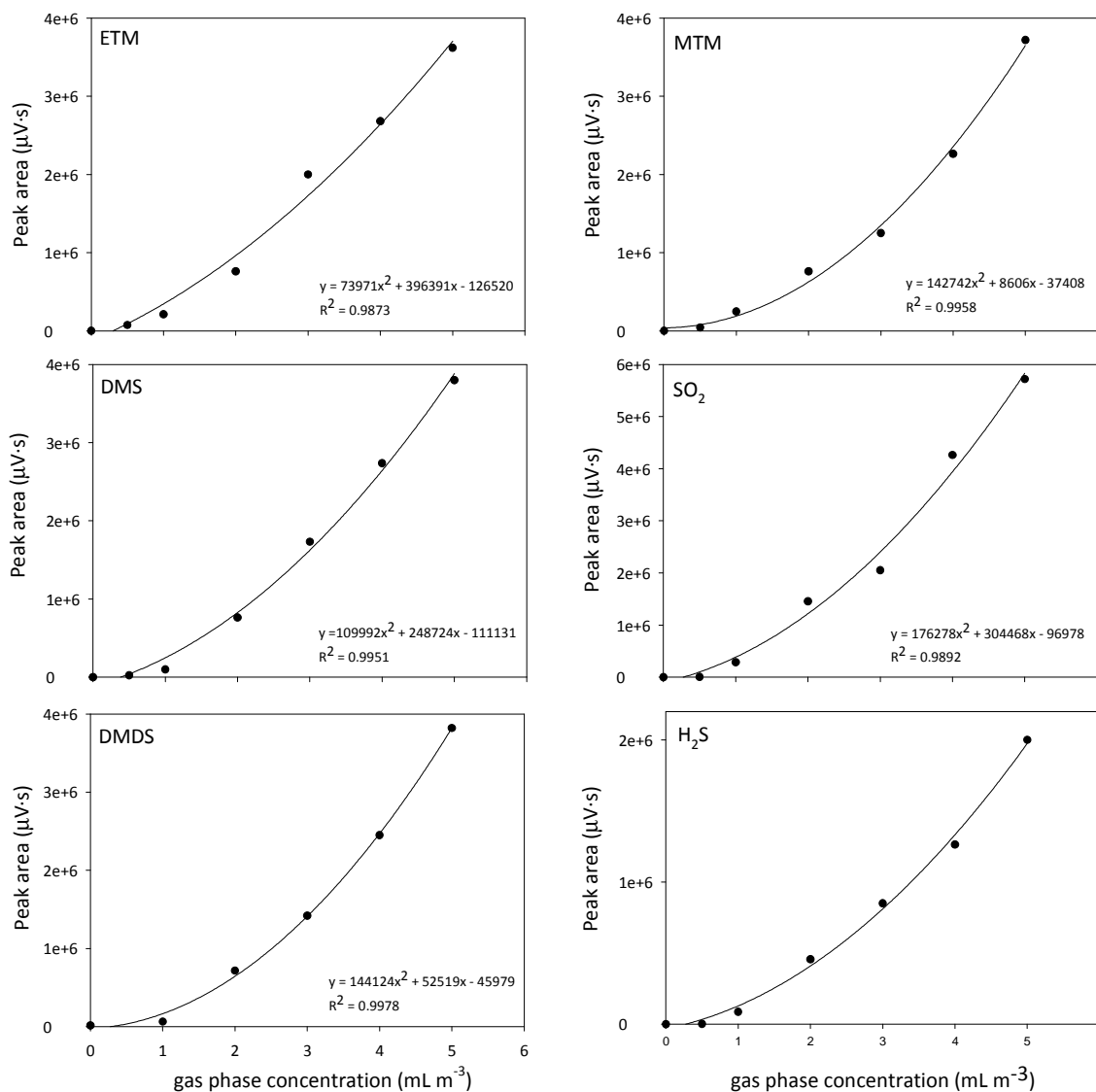


Figure A1. Calibration curves of volatile sulphur compounds in gas phase

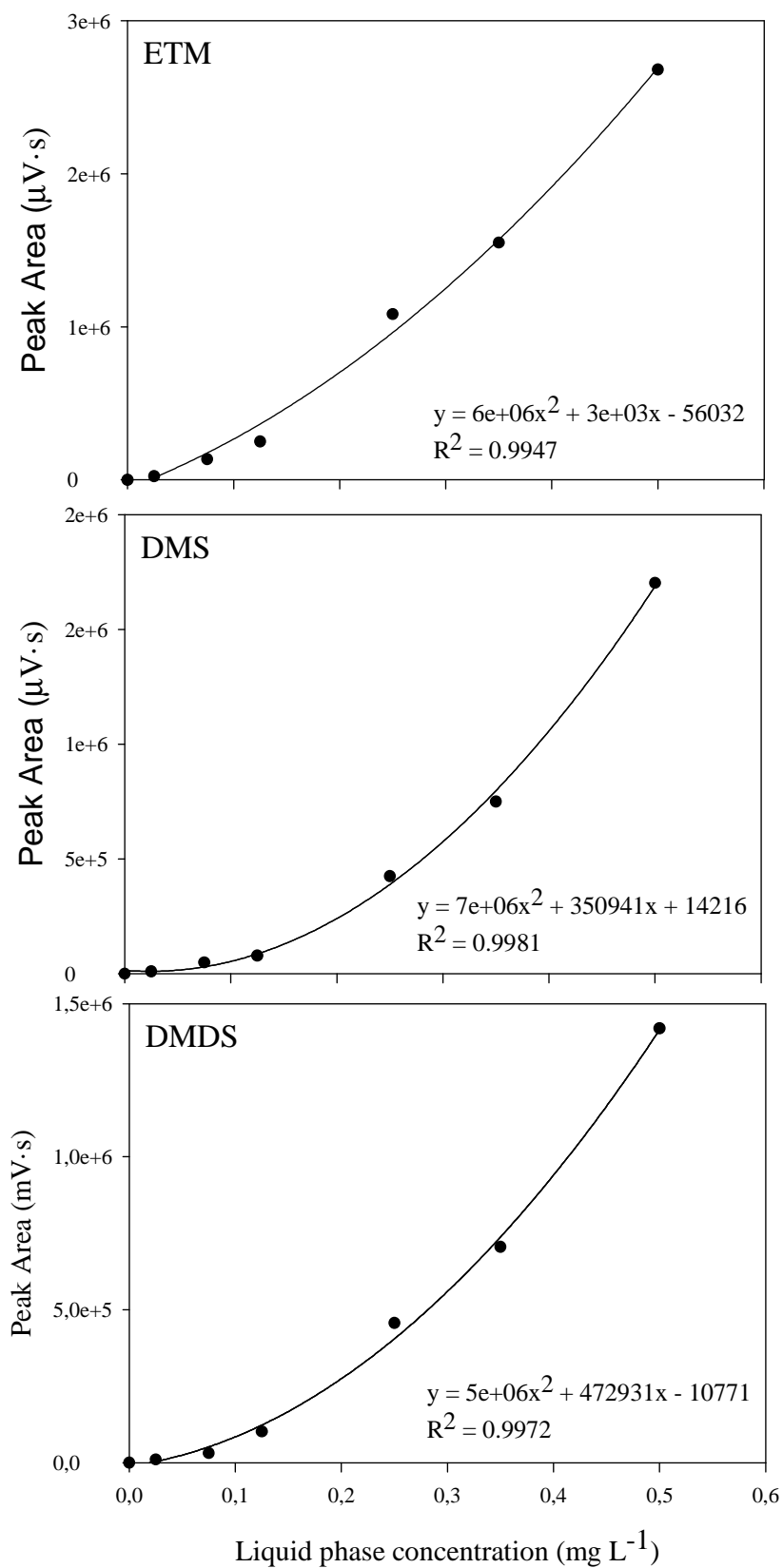


Figure A2 Calibration curves of volatile sulphur compounds in liquid phase

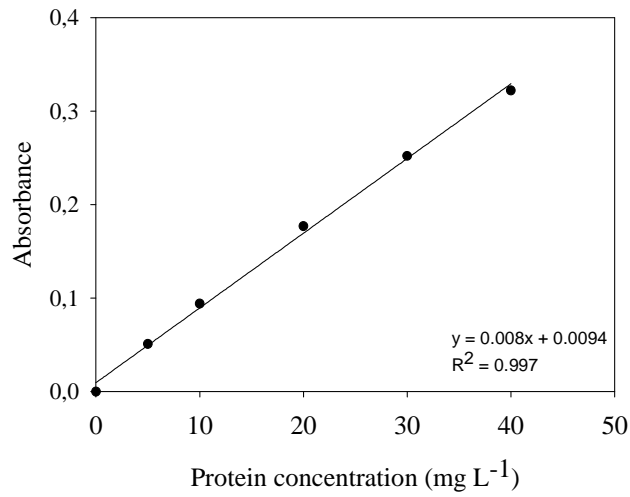


Figure A3 Standard calibration curve of protein content

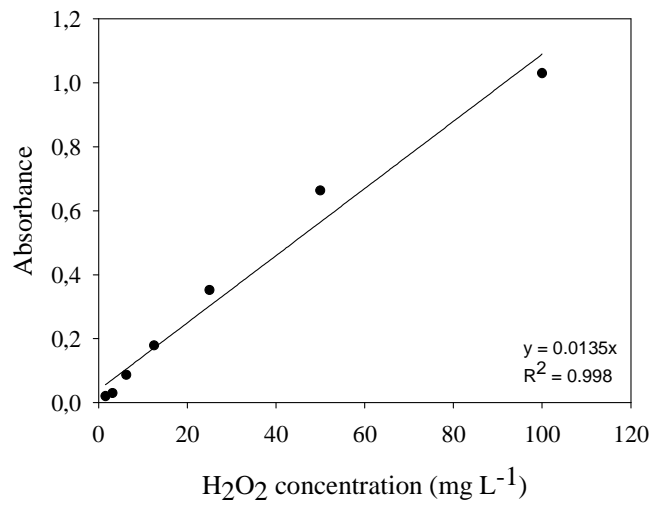


Figure A4 Standard calibration curve of hydrogen peroxide content

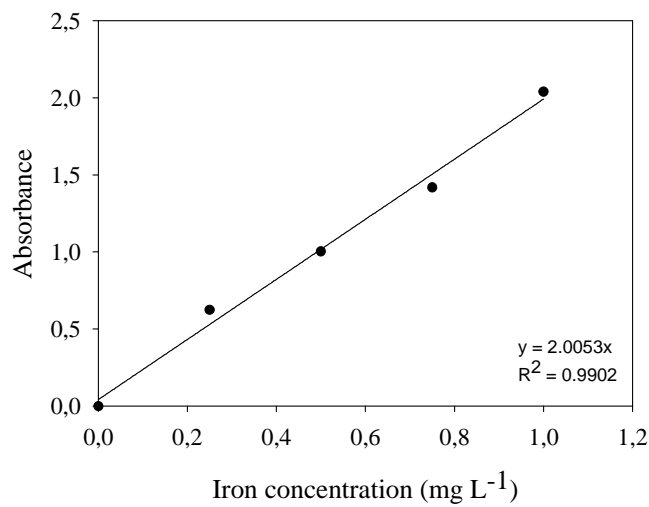


Figure A5 Standard calibration curve of dissolved iron content

